"Evaluating Anti-Cholera Toxin Activity of Pure Herbal Compounds from Traditional Medicinal Plants"

Thesis submitted to

KLE ACADEMY OF HIGHER EDUCATION AND RESEARCH

(Deemed -to -be -University)

[Declared as Deemed-to-be-University u/s 3 of the UGC Act, 1956 vide Govt. of India Notification No.F.9-19/2000-U.3 (A)]

Accredited 'A^{+}' Grade by NAAC (3rd Cycle)

Placed in Category 'A' by MHRD (GoI)

For the award of the degree of

Doctor of Philosophy

In the Faculty of Science-

Interdisciplinary Studies/Research

By

Mrs. RAJITHA CHARLA

(Registration No: KAHER/Ph.D./18-19/D01218021)

Under the Guidance of

Dr. Subarna Roy Msc., Ph.D

Scientist-G & Director

ICMR-National Institute of Traditional Medicine, Belagavi

JULY - 2023

UNDERTAKING

I, **Rajitha Charla,** hereby declare that the information and the data mentioned in my thesis entitled "**Evaluating Anti-Cholera Toxin Activity of Pure Herbal Compounds From Traditional Medicinal Plants**" belongs to me and is original.

I am aware of definition of plagiarism as detailed below:

- An act or instance of using or closely imitating the language and thoughts of another author without authorization and there presentation of that author's work as one's own, as by not crediting the original author.
- A piece of writing or other work reflecting such unauthorized use or imitation.
- The deliberate or reckless representation of another's words, thoughts or ideas as one's own without attribution in connection with submission of academic work, whether graded or otherwise.

I hereby declare that the thesis prepared by me is original-one and does not involve plagiarism anywhere. In case at a later stage it is found that I have indulged in plagiarism, then I am solely responsible for the same and the Institution is at liberty to take any disciplinary action against me including cancellation of dissertation or any other penalties imposed by the University.

Date: 26/09/2023
Place: Belagavi

Mrs. Rajitha Charla
Full time Ph. D. Research Scholar
Reg No - DO1218021
KAHER, Belagavi

PLAGIARISM REPORT

KLE ACADEMY OF HIGHER EDUCATION AND RESEARCH
(Formerly known as KLE University)
(Deemed-to-be-University established u/s 3 of the UGC Act, 1956)
Accredited A+ Grade by NAAC (3rd Cycle) Placed in Category 'A' by MHRD (GoI)
JNMC Campus, Nehru Nagar, Belagavi-590 010, Karnataka State, India
☎: 0831-2444444 Web: http://www.kledeemeduniversity.edu.in E-mail: info@kledeemeduniversity.edu.in

Ref. No. KAHER/AA/23-24/D- 150 4th July 2023

Madam,

The soft copy of Ph.D. research thesis of **Ms. Rajitha Charla, Faculty of Science-Interdisciplinary Studies/Research** of KAHER, Belagavi has been submitted for anti-plagiarism check at the office of the undersigned through "Turn-it-in" package. The scan has been carried out and the scanned output reveals a match percentage of **5%** which is within the acceptable limit of 10%.

To obtain the comprehensive report of the plagiarism test, research scholar can send a mail to **diracademic@kledeemeduniversity.edu.in** along with the Registration Number, Name of the Scholar, Name of Guide/Co-guide and title of the thesis.

DIRECTOR ACADEMIC AFFAIRS Deemed-to-be University

Dr.(Mrs.) Roopa M. Bellad
Director, Academic Affairs

To,

Ms. Rajitha Charla
Full-Time Ph.D. Scholar, 2018-19 Batch
Faculty of Science-Interdisciplinary Studies/Research, KAHER
Belagavi.

Cc to :
1. Dr. Subarna Roy, Director, ICMR-NIIM, Belagavi-Guide

KLE ACADEMY OF HIGHER EDUCATION AND RESEARCH

(Deemed-to-be-University)

(Declared as Deemed-to-be-University u/s 3of the UGC Act, 1956 vide Govt of India Notification No.F.9-19/2000-U.3(A))

Accredited 'A^{+}' Grade by NAAC (3rd Cycle)

Placed in Category 'A' by MHRD (Go I)

KLE
EMPOWERING PROFESSIONALS

Copyright Declaration

We hereby declare that **KLE ACADEMY OF HIGHER EDUCATION AND RESEARCH, BELAGAVI, KARNATAKA,** shall have the rights to preserve, use and disseminate this thesis in print or electronic format for academic/research purpose.

Rajitha Charla
Full time Ph.D Research Scholar
Reg no-D01218021
KAHER, Belagavi

Date: 26/07/2023

Place: Belagavi

Signature of the Guide
Dr. Subarna Roy Msc., Ph.D
Scientist-G & Director
ICMR-National Institute of Traditional Medicine, Belagavi-590010, India

ICMR-NATIONAL INSTITUTE OF TRADITIONAL MEDICINE BELAGAVI

KLE ACADEMY OF HIGHER EDUCATION AND RESEARCH

(Deemed-to-be-University)

(Declared as Deemed-to-be-University u/s 3of the UGC Act, 1956 vide Govt of India Notification No.F.9-19/2000-U.3(A))

Accredited 'A^{+}' Grade by NAAC (3rd Cycle)

Placed in Category 'A' by MHRD (Go I)

KLE
EMPOWERING PROFESSIONALS

Declaration

I hereby declare that the thesis entitled **"Evaluating Anti-Cholera Toxin Activity of Pure Herbal Compounds From Traditional Medicinal Plants"** is a bonafide and original research carried out by me under the guidance of **Dr. Subarna Roy**, Scientist-G & Director, ICMR-NITM Belagavi-590010. The thesis or any part thereof has not formed the basis for the award of any degree/fellowship or similar title to any candidate of any University.

Date: 26/09/2023
Place: Belagavi

Rajitha Charla
Full time Ph.D Research Scholar
Reg no-D01218021
KAHER, Belagavi

KLE ACADEMY OF HIGHER EDUCATION AND RESEARCH

(Deemed-to-be-University)

(Declared as Deemed-to-be-University u/s 3of the UGC Act, 1956 vide Govt of India Notification No.F.9-19/2000-U.3(A))

Accredited 'A^{+}' Grade by NAAC (3rd Cycle)

Placed in Category 'A' by MHRD (Go I)

KLE
EMPOWERING PROFESSIONALS

Certificate

This is to certify that the thesis entitled **"Evaluating Anti-Cholera Toxin Activity of Pure Herbal Compounds From Traditional Medicinal Plants"** is a bonafide record of original research carried out by **Mrs. Rajitha Charla** under the guidance **Dr. Subarna Roy,** Scientist-G & Director, ICMR-NITM, Belagavi-590010.

Date: 26/07/2023

Place: Belagavi

Signature

Dr. R. B. Nerli

Dean, Faculty of Interdisciplinary Science, KAHER, Belagavi

KLE ACADEMY OF HIGHER EDUCATION AND RESEARCH

(Deemed-to-be-University)

(Declared as Deemed-to-be-University u/s 3of the UGC Act, 1956 vide Govt of India Notification No.F.9-19/2000-U.3(A))

Accredited 'A^{+}' Grade by NAAC (3rd Cycle)

Placed in Category 'A' by MHRD (Go I)

KLE
EMPOWERING PROFESSIONALS

Certificate

This is to certify that the thesis entitled **"Evaluating Anti-Cholera Toxin Activity of Pure Herbal Compounds From Traditional Medicinal Plants"** is a bonafide record of original research carried out by **Mrs. Rajitha Charla** for the award of degree of **DOCTOR OF PHILOSOPHY IN FACULTY OF SCIENCE-INTERDISCIPLINARY STUDIES/RESEARCH** under my supervision and guidance.

Date: 26/09/2023

Place: Belagavi

Signature of the Guide

Dr. Subarna Roy M.Sc., Ph.D

Scientist-G & Director

ICMR- NITM, Belagavi

ACKNOWLEDGEMENT

I am truly delighted to extend my heartfelt appreciation and profound gratitude to ***Dr. Subarna Roy,*** *my esteemed mentor. I am incredibly fortunate to have had the opportunity to work under his invaluable guidance. His genuine interest in my development coupled with his overwhelming willingness to help and assist me, has been instrumental in completing my research work. His mentorship has not only enhanced my research skills but has also shaped me into a more organized and confident individual.*

I am immensely grateful to ***Dr. Harish DR,*** *Scientist-C, ICMR-NITM for his unwavering support and guidance in my research throughout its various stages. His invaluable insights, coupled with his kindness and dynamic approach have been crucial in overcoming the challenges and consistently propelled my work in the right direction. Without his scientific input and expertise, my research work would not have been possible*

I also thank ***Dr. R K. Joshi****, Scientist-D, ICMR-NITM, Belagavi, for helping with the analytical methods and* ***Dr. Harsha. Hegde****, Scientist-E, ICMR-NITM, Belagavi, for authenticating the plants.*

I am extremely thankful to the ***Division of Human Resource Planning and Development, Indian Council of Medical Research*** *for providing me with necessary financial funding/fellowship from the year 2017-2021 for a period of five years which supported my research studies. I also thank the* ***Department of Molecular Biology/ Microbiology, ICMR-NITM*** *for providing me with the necessary resources for my research work and the whole team of* ***ICMR-NITM*** *for their valuable suggestion for*

my research work.

It's my privilege to thank my Ph. D committee: ***Prof. Dr. P. A. Patil****,* ***Prof. Dr. Sunil S. Jalalpure****, and* ***Prof. Dr. Alka Kale****, as well as Prof.* ***Dr. Roopa Bellad****, Director of Academic Affairs, KAHER, and* ***Dr. Daksha Dixit*** *(Former Director of Academic Affairs, KAHER) for their insightful comments and encouragement.*

This thesis becomes a reality with the kind support and help of many individuals. I would like to extend my sincere thanks to all my fellow researchers from the Department of Molecular Biology/Microbiology, ***Mrs. Aarthi. Bhathkande, Dr. Priyanka P. Patil, Mr. Vishal S. Patil, Dr. Vishwambhar. Bhandare and to my seniors Dr. Savita. C, Mrs. Nisha. Kode*** *for their constant support.*

Last, but not least, I extend my deepest appreciation to my mother Indira Devi and my son Shiva Agasthya for their immeasurable contributions and for being an unyielding source of support and love throughout my research journey.

Thank you

Mrs. Rajitha Charla

LISTOFABBREVIATIONS

ADP	**:**	Adenine diphosphate;
AME	:	*Aegle marmelos* hydroalcoholic extract;
ANOVA	:	Analysis of variance;
$AlCl_3$	:	Aluminium chloride;
AMR	:	Antimicrobial resistance;
BE	:	Binding energy;
BI%	:	Binding inhibition percentage;
CAE	:	*Careya arborea* hydroalcoholic extract;
CHO	:	Chinese hamster ovary;
CFR	:	Case fatality rate;
CID	:	Compound identification number;
CHL	:	Chlorogenic acid;
CT	:	Cholera toxin;
CFCF	:	Cell culture free filtrate;
CPCSEA	:	Committtee for the purpose of control and supervision of experiments on animals;
cfu	:	Colony forming unit;
cAMP	:	Cyclic adenylate monophosphate;
CTB	:	B subunit of Cholera toxin;
CTA1	:	A1 chain of Cholera toxin;
DMEM	:	Dulbecco's Eagle Modified Media;
DMSO	:	Dimethyl sulfoxide;
DLS	:	Drug-likeness score;
DNA	:	Deoxyribonucleic acid;

EDTA	:	Ethylenediaminetetraacetic acid;
EA	:	Ellagic acid;
FBS	:	Fetal Bovine Serum;
GM1 ELISA	:	Monosialotetrahexosylganglioside enzyme linked immuno-sorbent assay;
$G_{s\alpha}$	:	Heterotrimeric G protein subunit alpha;
GA	:	Gallic acid;
HPTLC	:	High Performance Thin Layer Chromatography;
H_2SO_4,	:	Sulphuric acid;
HAE	:	*Holarrhena antidysenterica* hydroalcoholic extract;
ICMR-NITM	:	Indian Council of Medical Research-National Institute of Traditional Medicine;
IC_{50}	:	The concentration of drug required for 50% inhibition;
MF	:	Molecular formula;
Mg	:	Milligram;
mL	:	Milliliter;
MHA	:	Mueller Hinton agar;
MHB	:	Mueller Hinton broth;
MTT	:	3-(4,5-dimethylthiazol-2-yl)-2,5-diphenyltetrazolium bromide;
MDR	:	Multidrug resistance:
mOsm/l	:	Milliosmomoles per litre;
MD	:	Molecular dynamics simulation;
MMPBSA	:	Molecular Mechanics Poisson-Boltzmann Surface Area;
Na_2CO_3	:	Sodium carbonate;
NaOH	:	Sodium hydroxide;

$NaNO_2$	:	Sodium nitrite;
NAD	:	Nicotinamide adenine dinucleotide;
NMDCY	:	Non-membrane damaging cytotoxin;
OCV	:	Oral cholera vaccine; **ORS**: Oral rehydration solution;
PDB	:	Protein data bank;
pH	:	Potential of hydrogen;
PBS	:	Phosphate buffered saline;
PHD	:	Phloridzin;
PCR	:	Polymerase chain reaction;
PLE	:	*Piper longum* hydroalcoholic extract;
PGAE	:	*Psidium guajava* hydroalcoholic extract;
PGRPE	:	*Punica granatum* hydroalcoholic extract;
QRTN	:	Quercetrin;
RMSD	:	Root mean square deviation;
RMSF	:	Root-mean-square fluctuation;
SD	:	Standard deviation;
SMILES	:	Simplified molecular-input line-entry system;
RTN	:	Rutin;
RNA	:	Ribonucleic acid;
TCBS	:	Thiosulfate–citrate–bile salts–sucrose agar;
TSA	:	Tryptic soy agar;
TPC	:	Total phenolic content;
TFC	:	Total flavonoid content;
UCSF	:	University of California, San Francisco.

ABSTRACT

Background: *Careya arborea, Punica granatum, Psidium guajava, Holarrhena antidysenterica, Aegle marmelos* and *Piper longum* are traditional medicines used to treat diarrheal diseases in India and supported by scientific literature. But their specific activity against Cholera toxin (CT) has not been explored yet.

Aim and objectives: The current study aimed to investigate the inhibitory activity of these plants against CT-induced cytotoxicity and enterotoxicity. Polyphenols were selected from plants that showed efficient neutralization activity against CT. The inhibitory activity of selected polyphenols against CTB binding to GM1 receptor was further investigated using computational and experimental approaches.

Methodology: CT in cell free culture filtrate of *V. cholerea* was quantified using GM1 ELISA and *in vitro* efficacy of hydro-alcoholic extracts of six plants against CT was investigated using cAMP assay and GM1 ELISA. Further *in vivo* studies were performed with *C. arborea, P. granatum, P. guajava* using adult mice model. Molecular modelling approach was used to investigate the intermolecular interactions of selected 20 polyphenolic compounds from these three plants with CT using DOCK6. Based on intermolecular interactions, two phenolic acids, Ellagic acid and Chlorogenic acid; two flavonoids, Rutin and Phloridzin were selected along with their respective standards, Gallic acid and Quercetrin. The stability of docked complexes was corroborated using molecular dynamics simulation. Furthermore, *in vitro* inhibitory activity of six compounds against CT was assessed using GM1 ELISA and cAMP assay. EA and CHL that showed prominent activity against CT in *in vitro* assays were investigated for their neutralizing activity against CT *in vivo*.

Results: Significant reduction in elevation of cAMP levels in CFCF treated CHO cell line was observed for all the selected extracts except *P. longum* whereas *C. arborea, P. granatum, H. antidysenterica* and *A. marmelos* showed >50% binding inhibition of CT to GM1 receptor. *C. arborea, P. granatum* and *P. guajava* that showed efficient anti-CT activity *in vitro* further reduced fluid accumulation caused by CT in ligated-ileal loops of adult mouse. The molecular modelling study revealed significant structural stability of the CT-EA, CT-CHL, and CT-PHD complexes compared to their respective controls. All the selected six compounds from these three plants significantly reduced CT-induced cAMP levels, whereas EA, CHL, and PHD exhibited > 50% binding inhibition of CT to GM1. The EA and CHL that showed prominent neutralization activity against CT from *in vitro* studies, also significantly decreased CT-induced fluid accumulation and histopathological changes in ligated-ileal loops of adult mouse.

Conclusion: Out of six selected traditional medicinal plants, *C. arborea, P. granatum* and *P. guajava* showed effective activity against CT as evident from *in vitro* and *in vivo* studies. Among the four selected polyphenols from these plants, Phenolic acids EA and CHL effectively inhibited CT binding to GM1 receptor preventing its internalization and further toxicity as evident from *in vitro* and *in vivo* studies. Our study not only validated their traditional use but also identified the bioactive compounds neutralizing CT toxicity.

Key words: Cholera toxin; Cell free culture filtrate; GM1 ELISA; Cytotoxicity; Docking; Molecular dynamics simulation.

TABLE OF CONTENTS

	14.4. Protective activity of six compounds against CT-induced cell elongation 15. ***In vivo* studies**	
5.	**RESULTS** **1. Estimation of total polyphenolic content** **2. Genomic DNA extraction and quantification** **3. PCR for identification of ctxAB gene** **4. Selection of single isolate of *V. cholerea* using cell based assays** **5. *In vitro* studies with seven plant extracts** *5.1. Cytotoxicity assay* *5.2. Estimation of Cholera toxin concentration in CFCF* 5.3. *Inhibitory activity of seven extracts against CFCF-induced cAMP levels* *5.4. Protective activity of seven extracts against CFCF-induced cell elongation* **6. Mining of bio-active compounds and Molecular docking** **7. Drug-likeness and side effects** **8. MD simulations of docked complexes** 8.1. *Structural stability of the docked complexes using MD* 8.2. *Intermolecular interactions in docked complexes* 8.3. *Secondary structural changes during simulation* 8.4. *Contribution of the binding pocket residues in the intermolecular interactions* **9. Quantification of selected polyphenols using HPTLC** **10. *In vitro* studies with six compounds** 10.1. *MTT cytotoxicity assay of six herbal compounds* 10.2. *Binding inhibition percentage of CT to ganglioside GM1 in presence of six compounds* 10.3. *Inhibitory activity of six compounds against CFCF-induced elevated cAMP levels* *10.4. Protective activity of six compounds against CFCF-induced cell elongation* **11. *In vivo* studies** *11.1. CFCF-induced fluid accumulation in ligated-ileal loops* *11.2. CFCF-induced cellular cAMP levels in ligated-ileal loops* 11.3. *Histopathology*	**50-90**

LIST OF FIGURES

LIST OF TABLES

INTRODUCTION

Diarrhea is a worldwide problem and the second leading cause of death in children under five years of age. Cholera, an ancient and devastating acute diarrheal disease caused by pathogenic strains of *V. cholerae* is a serious global problem as outbreaks of this disease are occurring in different regions around the globe. Each year 1.3 to 4.0 million cases and 21000 to 143000 deaths are estimated worldwide due to cholera [1]. *V. cholerae*, the causative agent of cholera is a facultative anaerobic Gram-negative, motile, non-spore-forming curved rod- shaped bacteria including both toxigenic and non-toxigenic strains that differ in their virulence gene contents and polysaccharide surface antigens [2].

Cholera toxin (CT), an 84Kd heterohexameric protein efficiently secreted into the culture supernatant by the type 2 secretion system of *V. cholerae* in soluble form is the key virulence factor responsible for diarrhea observed in cholera. CT binds to ganglioside GM1 located on the outer leaflet of apical membranes of intestinal epithelial cells [3] followed by endocytosis and then traffics retrograde from the plasma membrane to the trans-Golgi network, eventually reaching the endoplasmic reticulum (ER) [4]. Inside the ER, the A-subunit dissociates from the B pentamer, followed by cleavage between A1 and A2 polypeptide chains. From NAD, the A1 chain catalyzes ADP-ribose transfer to G protein $G_{s\alpha}$ in the cytoplasm leading to permanent ADP-ribosylation of $G_{s\alpha}$ and activation of adenylate cyclase. This results in a persistent elevation in cAMP levels which activates the cystic fibrosis transmembrane conductance regulator (CFTR), causing a dramatic efflux of ions and water from infected enterocytes, leading to diarrhea [5].

Despite CT being responsible for the pathogenesis observed in cholera, treatment majorly involves oral rehydration therapy and the use of antibiotics such as azithromycin and tetracycline targeting the bacteria. This is eventually leading to yet other outbreaks caused by the multidrug-resistant strains of *V. cholerae* [6]. Therefore, a number of phytocompounds have been investigated for anti-cholera activity. The potency of phytocompounds against CT has been demonstrated either by disruption of the binding of CTB to GM1 or by inhibition of CTA1 catalyzed ADP-ribosylation of $G_{s\alpha}$ [124]. A comprehensive analysis of available scientific literature revealed that most of the phytocompounds reported against CT were polyphenols [138,166,167].

Careya arborea, Punica granatum, Psidium guajava, Holarrhena antidysenterica, Aegle marmelos and *Piper longum* are commonly used traditional medicines against diarrheal diseases in India. These plants were also scientifically reported to act against diarrheal pathogens *viz. Shigella flexneri*, *V. cholerae*, enteropathogenic and enteroinvasive *Escherichia coli* (EPEC, EIEC), rotavirus and giardia. The decoction from unripe fruits of *A. marmelos* and leaves of *P. guajava* showed cidal activity against giardia, rotavirus, and inhibited the binding of CT and *E. coli* labile toxin to GM1 receptor [7,8]. The seeds and bark of *H. antidysenterica* have been shown to be effective against amoebic dysentery and *E. coli*- induced diarrhea in rats [9]. It has been reported that both the peel and juice extract of pomegranate seeds have gastroprotective activity and can prevent castor oil-induced enteropooling in rats [10]. Bark of *C. arborea* reduced castor oil-induced diarrhea in mice significantly [11]. Piperine, a major alkaloid found in the fruits of *P. longum* has been shown to have anti-diarrheal and antispasmodic properties [12].

All the six plants selected for the study are reported to show anti-diarrheal activity but their specific activity against *V. cholerae*-induced diarrhea was not fully demonstrated. Hence the present study aims to investigate the inhibitory activity of hydro-alcoholic extracts of these six plants against CT-induced cytotoxicity and enterotoxicity using *in vitro* and *in vivo* methods respectively. As polyphenols were reported to act against CT, phenolic acids and flavonoids were selected from plants that showed effective neutralization activity against CT from *in vitro* and *in vivo* studies. As the initial and critical step in CT pathogenesis involves its binding to the GM1 receptor on intestinal epithelial cells for internalization, we proposed to investigate and derive the role of selected polyphenols in neutralizing the CT-induced toxicities by using both molecular modeling and experimental studies**.**

AIM AND OBJECTIVES

Aim: To evaluate the inhibitory efficacy of traditionally used and scientifically reported six anti-diarrheal plants and their reported bio-active compounds against Cholera toxin using *in silico*, *in vitro,* and *in vivo* approaches.

Objectives of the study

1. To assess the inhibitory efficacy of hydro-alcoholic extracts of *C. arborea* (bark), *P. granatum* (fruit peel), *P. guajava* (leaves), *H. antidysenterica* (bark), *A. marmelos* (fruit), and *P. longum* (fruit) against CT using GM1 ELISA and cyclic AMP assay.
2. To screen and select the polyphenolic compounds from plants that are efficiently neutralizing CT *in vitro* using system biology tools.
3. To investigate the potency of selected polyphenolic compounds along with their respective standards against CT using *in vitro* assays
4. To evaluate the *in vivo* inhibitory efficacy of hydro-alcoholic extracts of plants and polyphenolic compounds that are showing notable activity against CT *in vitro* using a ligated-ileal loop model of adult mice.

REVIEW OF LITERATURE

1. Diarrheal diseases

Diarrhea which is annually killing more than 0.5 million children worldwide is the second leading cause of death in infants and children under five years of age [13,14]. It is caused by bacterial, viral or parasitic infections in the intestinal tract resulting from contaminated water sources, unhygienic food and improper sanitization strategies. Underlying malnutrition in children augments the symptoms and severity of disease [15]. Diarrhea is usually defined as the passing of more than three liquid stools per day which are categorized clinically into watery, inflammatory, and persistent diarrhea [16].

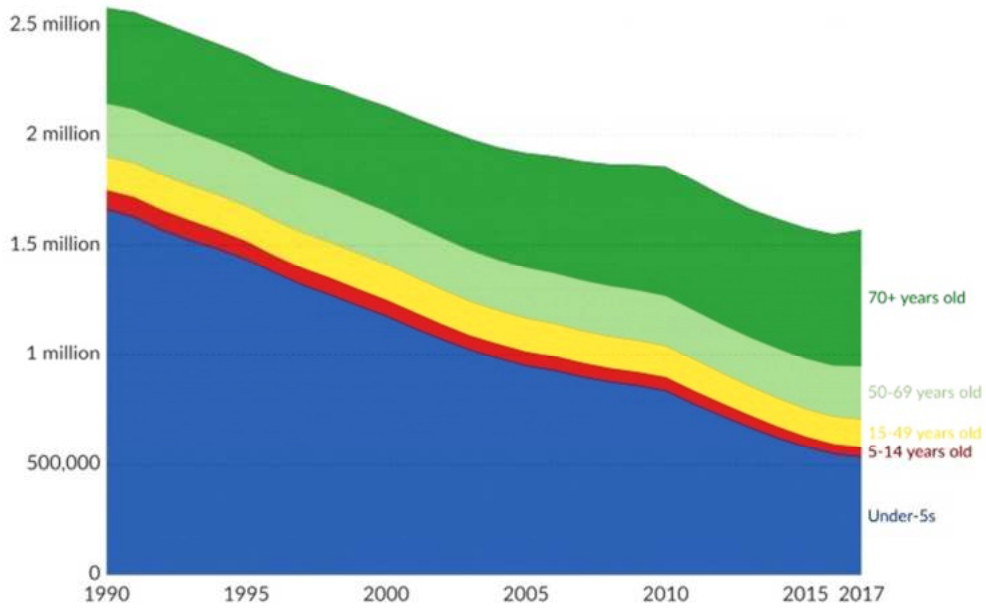

Figure 1 Death due to diarrhea by age from the year 1990-2017 (Source: IHME, Global burden of disease)

Watery diarrhea caused by *V.cholerae*, *E. coli,* and rotavirus leads to extensive loss of fluids and salts from the body which further progress to failure of critical organs and dysfunctional circulatory system. Acute watery diarrhea observed in cholera is caused by extensive loss of fluids and ions from enterocytes [17]. Treatment involves the replacement of lost fluids and electrolytes with ORS which can be life-saving by preventing further dehydration and progression of the disease.

Inflammatory diarrhea also called dysentery is caused by both invasive (EAEC, EHEC, *C. difficile*) and noninvasive (*Shigella flexneri, Camphylobacter jejani*) bacterial pathogens which invade the mucosal layer of the intestine and release the inflammatory mediators by stimulating the cytokine production [18]. This leads to the destruction of the mucosal layer and bloody diarrheal episodes observed in inflammatory diarrhea. Effective and early antibiotic treatment heals the degenerated mucosal tissue and decreases acute complications [19].

Diarrhea lasting more than 7-13 days is termed as persistent and it results in malnutrition due to loss of nutrients and poor absorption. Repeated exposure to few pathogens like *S. flexneri, S. dysenteriae,* and *G. intestinalis* were identified with the occurrence of persistent diarrhea [20].

2. Cholera

Cholera, an acute water-borne diarrheal disease is a serious global problem majorly in countries with improper sanitation strategies. This disease causes an estimated 21000 to 143000 deaths worldwide [21]. In 2017, 34 countries reported a total of 1227391 cases and 5654 deaths (CFR 0.5%) whereas the most recent 2020 cholera outbreak in Yemen reported 1384423 cases and 1574 deaths (CFR 0.11%) [22]. The

global burden of cholera is not known as most of the cases are not reported due to the lack of appropriate laboratories and proper epidemiological supervision. Annually, 1.3 billion people are at risk and 2.86 million cholera cases occur in endemic countries. Among these cases, there are an estimated 95,000 deaths and cholera has been reported to be the second leading diarrheal disease causing mortality and morbidity in children with less than five years of age [23].

2.1. *Etiology*

Cholera is caused by pathogenic strains of *V. cholerae,* a facultatively anaerobic, motile, non-sporing forming curved rod-shaped bacteria including both toxigenic and non-toxigenic strains [24]. In the year 1854, Filippo Pacini was the first to observe this bacteria in comma-shaped forms in stool samples of cholera patients. *V. cholerae* was first isolated in pure culture by Robert Koch in the year 1884. It is an aquatic Gram-negative rod-shaped bacteria characterized by the presence of single polar flagellum including both pathogenic and non-pathogenic strains differing in their virulence gene contents and polysaccharide surface antigens.

They are salt-loving aerobic bacteria with a generation time of 30 min, sensitive to low pH and grow actively under alkaline conditions. Based on the O-antigen present on the lipopolysaccharide of *V. cholerae*, more than 200 serogroups have been determined [25]. Among them, O1 and O139 serogroups are responsible for causing cholera which can be epidemic, endemic, and pandemic in nature [26,27]. The O1 serogroup has (a) two biotypes – Classical responsible for the first six cholera pandemics from 1817 to 1923 and EI Tor responsible for the seventh pandemic from 1961 to 1971 [28,29], (b) three serotypes – Ogawa, Inaba and Hikojima which differ in the expression of genes coding for A, B, and C somatic antigens [30,31]. The O139

serogroup of *V. cholerae* was initially identified in South Asia and it originated from the O1 El Tor biotype by lateral genomic transfer replacing the O1 antigen with O139 [32]. Reports of non-O1 and non-O139 serogroups have recently emerged and these are reported to cause severe cholera like gastroenteritis [33,34].

2.2. *Pathogenesis*

Primary transmission of *V.cholerae* occurs by the consumption of contaminated water from aquatic reservoirs in the environment whereas secondary transmission occurs from the infected individuals. Consumption of raw or undercooked sea food which is imported from cholera endemic regions also results in transmission of disease [35]. Clinical manifestations of cholera following an incubation period 6 to 48 hours ranges from mild without symptoms to severe and life threatening condition and if untreated, severe dehydration can rapidly lead to shock and death in hours [36].

The major virulence factors in *V.cholerae* are cholera toxin (CT) and toxin co-regulated pilus (TCP). The genome of *V.cholerae* is distributed in two circular chromosomes with a large 2.96Mb chromosome I and a small 1.07Mb chromosome II [37]. A non-lytic bacteriophage CTXΦ which carries the operon encoding CT integrates with the bacterial chromosome consists of a core region encoding for CT and proteins that are required for viral morphogenesis, as well as a RS2 region that codes for replication, regulation, and integration functions of the CTXΦ genome [38]. TCP is required for attachment and transmission of CTXΦ serving as its receptor [39]. The TCP operon is present in Vibrio pathogenicity island (VPI) that is located separately from CTXΦ in the large *V.cholerae* chromosome. The transcription of ctxAB and TCP operons are directly activated in a co-ordinated manner by a

regulatory protein ToxT encoded by VPI [40,41]. TCP P/TCP H and ToxR/ToxS tightly regulates the expression of ToxT[42]. After its assembly in the periplasm, CT is secreted from *V.cholerae* in a very efficient manner by Type II secretion system [43].

2.3. *Epidemiology*

Cholera outbreaks continue to happen in many parts of developing countries which lack proper sanitation strategies. It is grouped under emerging and reemerging infections with the highest rate of infection in children under five years. The first six pandemics of cholera caused by classical biotype occurred in India and spread to many countries [44].

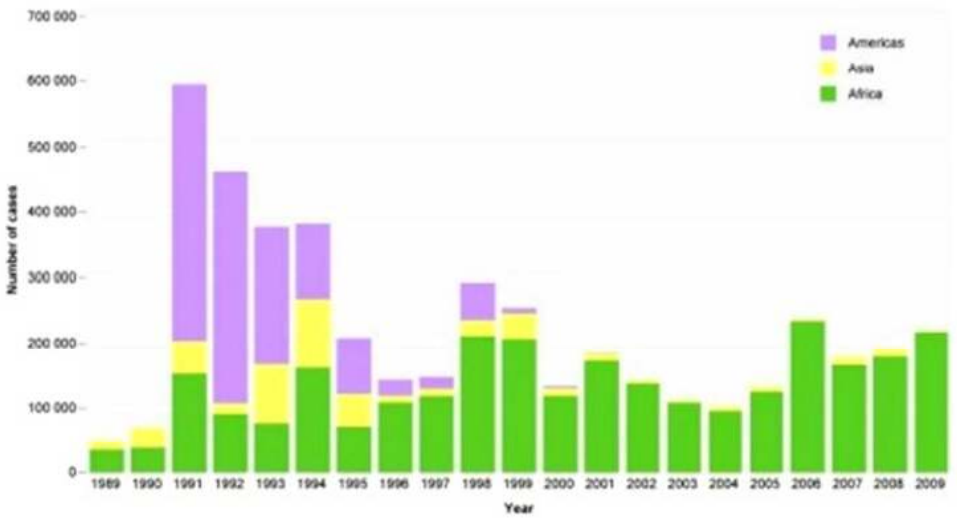

Figure 2 Cholera cases reported to WHO by continent and by year from 1989-2009 (Source:WHO Weekly Epidemiological Record no 31, 2010, 85, 293-308)

From the year 1830 to 1850, the second pandemic reached Canada and the British Isles through the infected immigrants on ships from Ireland [45]. The third and fourth pandemics were most prevalent in the US whereas the fifth pandemic

extensively affected South America. In the year 1899-1923, the Balkan Peninsula and middle east populations were affected by the sixth cholera pandemic [46]. The seventh pandemic caused by El Tor biotype on Sulawesi island, Indonesia was considered as an extensive pandemic as it was spread on large geographical sections for a long duration [47].

Table 1 Cholera pandemics since 1817

Year	Origin	Pandemic organism
1817-1823	India	Unknown
1829-1851	India	Unknown
1852-1859	India	Unknown
1864-1879	India	Unknown
1881-1896	India	*V. Cholerae* O1, Classical biotype
1899-1923	India	*V. Cholerae* O1, Classical biotype
1961-present	Sulawesi, Indonesia	*V. Cholerae* O1, El Tor biotype

Epidemiology of cholera is influenced by several factors which include - [i] proper hygiene, sanitation, and immunity of individuals, [ii] antibiotic resistance profile of epidemic strains which changes each year, [iii] seasonal changes, location, and high incidence of infection in children. The emergence of antibiotic resistant strains of *V. cholerae* is responsible for recent outbreaks in Bangladesh [48,49].

3. Entero-toxins produced by *V. cholerae*

Accessory Cholera toxin (ACE) stimulation of ANO6 (Anoctamin) function in intestinal epithelium causes chloride ion(Cl^-) secretion and induces diarrhea [50]. Zonula occludens toxin (ZOT) binds to the human α-1 chimaerin receptor increasing mucosal permeability and promoting the movement of macromolecules through the tight junction pathway [51]. Heat-stable enterotoxin (ST) causes elevation of intracellular cGMP by activating cystic fibrosis transmembrane conductance regulator (CFTR) chloride channel which induces anion secretion and diarrhea [52]. Cholix toxin (chx) has ADP-ribose transferase activity against ribosomal eukaryotic elongation factor-2 and it is involved in extraintestinal infections [53]. Multifunction autoprocessing repeats-in-toxin (MARTX) is a pore-forming accessory toxin that causes permanent dismantling cytoskeleton by the formation of covalent cross-links between monomeric G-actin forming oligomeric chains [54]. By utilizing the type-II secretion pathway, *V.cholerae* secretes Hemagglutinin protease (HAP), which targets multiple molecules to exacerbate infection severity. HAP modifies certain toxins, affects proteins associated with tight junctions, and degrades the protective mucus barrier [55]. Non-toxigenic strains of *V.cholerae* produce *V. cholerea* cytolysin (VCC), which is capable of damaging cell membranes and causing cell death. VCC forms a channel that selectively allows anions to pass through in planar lipid bilayers, resulting in vacuolation and eventual cell death [56]. Haemolysin produced by non-O1 and O1 El Tor biotypes of *V.cholerae* causes hemolysis of vertebrate erythrocytes [57], cytotoxicity in adrenal Y-1 cell line and Chinese hamster ovary cells [58] and also causes fluid accumulation in ligated intestinal loops of adult rabbits [59]. Non-membrane-damaging-cytotoxin (NMDCY) reported in non-O1 El Tor biotype causes

cell rounding in cultured HeLa cells and also induces accumulation of non-hemorrhagic fluid in rabbit ligated ileal loops [60].

4. Cholera toxin

Cholera toxin belongs to the larger family of AB toxins characterized by having an enzymatically active A-domain responsible for inducing toxicity and a cell-binding B-domain responsible for cell entry. A-subunit is comprised of an enzymatically active A1- chain which is non-covalently linked to the pentameric ring of B-subunits via the A2-chain. CT begins its intracellular journey by binding to the ganglioside GM1 located on the outer leaflet of apical membranes of intestinal epithelial cells [61]**.** The toxin enters the cell by various endocytic mechanisms including clathrin and caveolin dependent as well as caveolin and dynamin-independent mechanisms and traffics retrograde from the plasma membrane to the trans-Golgi network and ultimately reaches the endoplasmic reticulum (ER). The A2-chain has a KDEL sequence at its C-terminus which is responsible for retrograde transport of the toxin to ER [62]. Inside the ER, A-subunit dissociates from the B-pentamer followed by cleavage between A1 and A2 polypeptide chains. A1-chain is recognized by the reduced form of protein disulfide isomerase (PDI) which binds to and unfolds A1-chain [63]. The PDI-A1 chain complex is then targeted to a protein on the luminal membrane of the ER after which ER oxidase Ero1 oxidizes PDI to induce the release of the A1-chain. *Invitro* evidence suggests that HSP 70 chaperone BiP plays a major role in maintaining A1-chain in a soluble export competent state [63]**.**

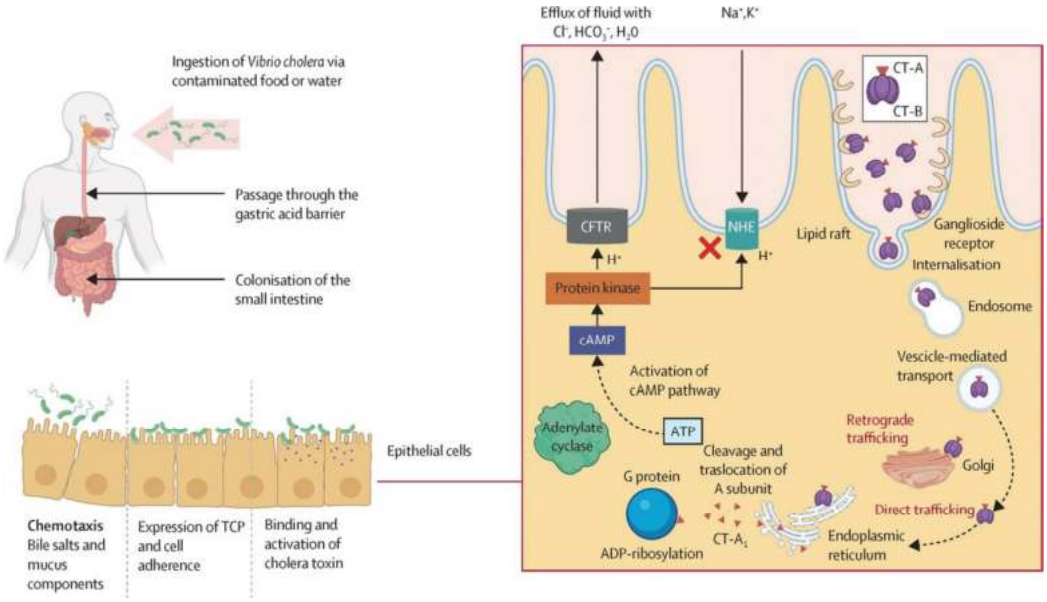

Figure 3 Mechanism of action of Cholera toxin (Source: The Lancet (2022), 399;10333, 1429-1440)

In the unfolded state, A1-chain is retro translocated through the Sec61p channel from ER lumen exploiting the ER-associated protein degradation pathway (ERAD) **[64].** A1-chain disguises itself as a misfolded protein to enter the ERAD pathway, escapes Ubiquitin-mediated protein degradation due to its low lysine content, and finally enters the cytosol. In the cytosol, the A1 chain catalyzes the transfer of ADP-ribose from NAD to G protein $G_{s\alpha}$ resulting in permanent ADP-ribosylation of $G_{s\alpha}$ and activation of adenylate cyclase which continuously stimulates the production of cyclic AMP **[65].** An increase in cyclic AMP levels leads to dramatic efflux of ions and water from intestinal cells causing severe "rice-water" diarrhea.

5. Treatment regimen for cholera

5.1. *Vaccines*

Currently, two types of oral cholera vaccines (OCVs) have been pre-qualified by the WHO. Dukoral®, which contains killed whole cells and a component of the cholera toxin, Shanthol™ and Evichol-Plus® which includes only killed whole cells [66]. Over two years of age, Dukoral® can be administered with a buffer solution to all individuals in two doses with not more than six weeks of delay between the two doses. This vaccine is mainly administered during travels and it gives protection against cholera for two years. A buffer solution is not required for the administration of Evichol-Plus® and it is given to all individuals above one year. The time gap between two doses should not exceed two weeks and this vaccine protects from cholera for three years. All three vaccines have a two-dose regimen with an interval of at least two weeks between the doses and they do not give lifelong immunity to the infection. Shanthol™ manufactured in India is used in private health care systems but not considered for use in national immunization programme [67].

5.2. *Oral rehydration therapy*

The main treatment for cholera is rapid rehydration, which can be achieved through oral rehydration therapy or by administering intravenous fluids in severe cases to replace fluids and electrolytes. Patients with mild or moderate dehydration are typically treated with oral rehydration salts. Salts of sodium and potassium with glucose as components in ORS are used in clinical management of diarrhea reducing the deaths caused due to diarrhea. WHO recommends ORS with reduced osmolarity of 245 mOsm/l when compared to the standard ORS with osmolarity of 311 mOsm/l

as an effective treatment for cholera [68]. Supplementation of new ORS with 20mg Zinc helps to minimize the diarrheal episodes in children with acute diarrhea whereas 10mg is recommended for infants less than six months old [69].

Table 2 WHO recommended composition of new ORS

New ORS	mmol/litre
Sodium	75
Chloride	65
Potassium	20
Citrate	10
Glucose anhydrous	75
Total osmolarity	245

5.3. *Antibiotic therapy*

In the treatment of cholera, along with fluid replacement, using of antibiotics is considered as a useful adjunct. Antibiotics belonging to the class of tetracyclines (tetracycline and doxycycline), quinolones (ciprofloxacin and norfloxacin), and macrolides (azithromycin and erythromycin) are commonly used against *V. cholerae.* Among these, azithromycin or tetracycline were observed to be effective compared to other tested antibiotics [70]. Antibiotics like tetracycline, doxycycline, furazolidone, erythromycin, ampicillin, and chloramphenicol are used thereby to reduce the length of hospital stays and break the cycle of transmission, especially during epidemics**.** For

treating cholera infection in children, WHO guidelines the use of tetracycline for three days. Due to changing antimicrobial resistance, currently, azithromycin and erythromycin are used as an effective treatment in paediatric cholera infection [71].

6. Antimicrobial resistance in *V. cholerae*

Antibiotics are chemical compounds synthesized and secreted naturally by fungal and bacterial species as a mode of defense against other micro-organisms in the surrounding environment or to maintain the balance in the microbial ecosystems [72]. Selective pressure placed on microorganisms by excessive use of antibiotics and mutations that arise has eventually led to the emergence of anti-microbial resistance (AMR). Multi-drug resistant (MDR) *V.cholerae* with epidemic outbreaks have been reported worldwide [73].

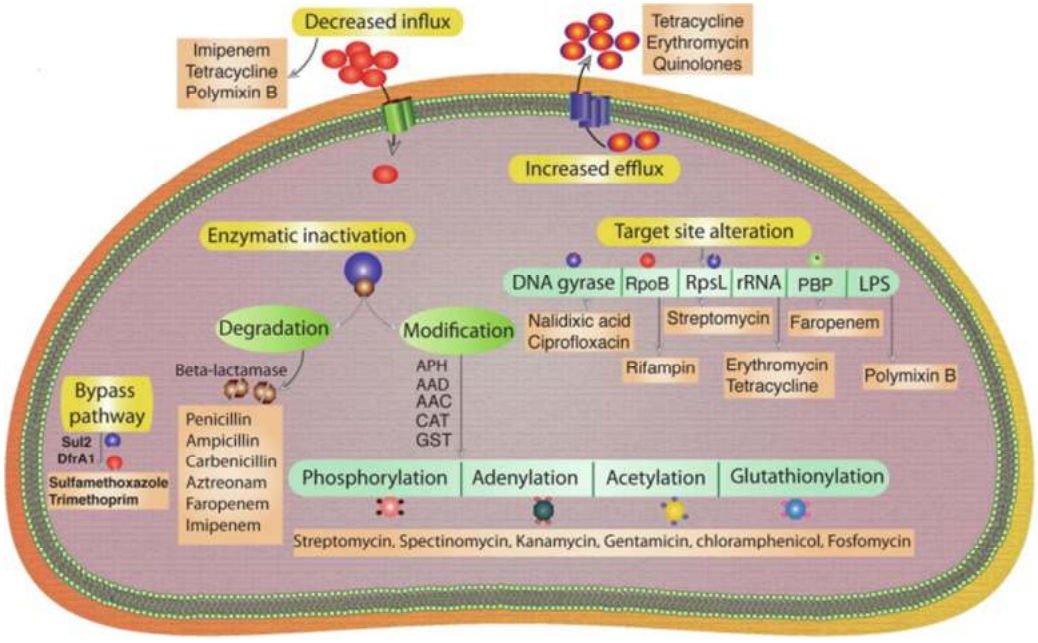

Figure 4 Mechanism of antimicrobial resistance in *V. cholerae* (Source: Vaccine, 2020 29;38:A83-92).

The genetic framework and competency are the vital factors responsible for acclimatization and resistance against the antimicrobials in *V. cholerae*. The emergence of AMR occurs naturally as an evolutionary process. Several factors such as environment, pattern of antibiotics used in public health, animal husbandry, and density of bacterial population in a specific habitat may contribute to the emergence of AMR. Horizontal gene transfer mediated by genetic recombination mechanisms such as conjugation, transformation, and transduction contributes to the chromosomal mutations and acquisition of extrachromosomal genetic elements in bacteria which is eventually leading to the emergence of AMR [74].

Antimicrobial resistance in *V. cholerae* is majorly contributed by the acquisition of extrachromosomal mobile genetic elements from related bacterial species. MDR in *V. cholerae o*ccurs by spontaneous mutations in antibiotic targets such as topoisomerases, RNA polymerase, and DNA gyrase. These mutations are facilitated by the horizontal transfer of transposons, insertion sequences, and ICEs from other related bacterial species [75]. MDR was first reported in the O1 serogroup of *V. cholerae* in 1970 against streptomycin and tetracycline. In the 1994 cholera outbreak in Eastern Zaire, this resistant strain was responsible for 12,000 deaths [76]. Recent studies have shown that most of the clinical isolates of *V. cholerae* have become resistant to commonly used antibiotics such as ciprofloxacin, tetracycline, chloramphenicol, streptomycin, and erythromycin. The quinolone resistance observed in *V. cholerae* was attributed to the point mutations in the gyrA gene encoding for topoisomerase enzyme [77]. The access of antibiotics to the target sites are inactivated by the bacterial enzymes and the mutations in these enzymes acquired through horizontal gene transfer are also contributing to AMR [78].

7. Traditional medicine in treating diarrheal infections

Traditional medicine in India is one of the ancient medical science in the world. The biodiversity in India offers a wide range of medicinal plants with are used in various systems of medicine such as Unani, Siddha, ayurveda, and homeopathy for diverse therapeutic applications. WHO supports the application of this traditional knowledge using medicines derived from plants for health care. It also encourages the interaction of indigenous systems of medicine with Western medicine to identify and develop safer drugs that can be effectively used against ailments [79]. These medicinal plants contain an array of phytocompounds belonging to the class of alkaloids, phenols, flavonoids, saponins, terpenoids, and steroids with distinct biological activities.

In Ayurvedic texts, more than 100 species of plants from 58 families were mentioned which were used to treat diarrhea [80]. Most of these plants are used in various diarrheal formulations which are available commercially. From an extensive review of available scientific literature, it is understood that most of the traditionally used plants against diarrhea were evaluated for their activity against diarrheal pathogens and chemically induced diarrhea. But there is very limited literature concerning the activity of these traditional medicines against enterotoxins. Therefore the present study selected six traditionally used plants against diarrhea i.e. *Careya arborea, Punica granatum, Psidium guajava, Holarrhena antidysenterica, Aegle marmelos,* and *Piper longum.* These plants are also reported to inhibit the growth of enteric pathogens such as *E. coli*, *V. cholerae*, rotavirus, *E. histolytica, S. flexneri,* and giardia but their specific activity against CT is not reported yet.

7.1. *Aegle marmelos*

7.1.1. Introduction

Aegle marmelos (L.) Correa which is commonly known as *Bael*/*Bilva* is a member of the Rutaceae family. It has been extensively utilized in traditional Indian medicine for its diverse medicinal properties. Unripe fruits of *A. marmelos* are used most prevalently in traditional medicine to treat chronic diarrhea and dysentery. A decoction from the unripe fruits is reported to significantly reduce the adherence of *S. flexneri*, enteropathogenic, and enteroinvasive *E. coli* to Hep-2 cells. It also showed cidal activity against giardia, rotavirus and prevented the binding of Cholera toxin and *E.coli* labile toxin to GM1 receptor [81]. The decoction of the root and root bark is useful in intermittent fever, hypochondriasis, melancholia, and palpitation of the heart [82,83]. The effectiveness of *A. marmelos* fruit in diarrhea and dysentery has resulted in its entry into the British Pharmacopoeia [84,85]. As fruits are highly rich in nutrients, various products such as bael toffee, bael candies, juice and beverages from fruits were prepared and marketed. The present study used hydro-alcoholic extract of matured but unripe fruits of *A. marmelos* to investigate its neutralizing activity against CT.

7.1.2. Reported bio-active compounds in fruit

Bael fruit is rich in fatty acids, sugars, fiber content, minerals, and vitamins A, B, and C. Both the fruit juice and fruit pulp are enriched with polyphenols such as carotenoids, flavonoids, coumarins, and glycosides which provide several health benefits [86]. Phenolic acids such as chlorogenic acid, ellagic acid, ferulic acid, gentistic acid, caffeic acid, and flavonoids quercetin, rutin, and catechin were reported in fruits

of *A. marmelos* [87]. Marmeline and marmelosin are the major alkaloids found in this plant and they are reported to protect against heavy metal toxicity [88].

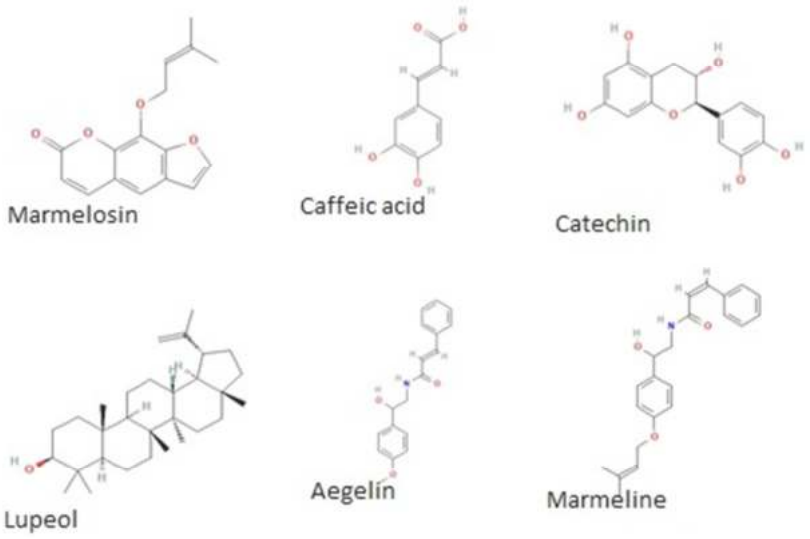

Figure 5 Reported bio-actives in fruit of *A. marmelos*

7.2. *Careya arborea*

7.2.1. Introduction

Careya arborea Roxb belonging to the family Lecythidaceae is a significant medicinal plant known as kumbhi in Ayurveda. The stem bark of *C. arborea* has long been used in traditional medicine for treating various ailments, including tumors, bronchitis, skin disease, epileptic fits, astringents, abscesses, and ulcers [89]. The fruits are prepared as a decoction to aid digestion, while the leaves and flowers are made into a paste and used to treat a range of skin disorders [90]. *C. arborea* bark methanolic extract is reported to significantly reduce castor oil-induced diarrhea in mice [91]. Hydro-alcoholic extract of bark is used in this study to determine its inhibitory activity against CT.

7.2.2. Reported bio-active compounds in bark

The phytochemicals in the stem and bark of *C. arborea* include flavonoids and triterpenoids such as betulin, and betulinic acid represented below. Phenolic acids such as ellagic acid and sterols were also found in bark. The methanolic bark extract significantly reduced carbon tetrachloride-induced liver toxicity and was also shown to possess anti-oxidant properties [92,93]. Antifungal activity against *C. albicans*, *A. flavus*, *A. niger* and antibacterial activity against enteric pathogens was studied using disc diffusion method [94]. The bark methanolic extract also showed anti-inflammatory and anti-ulcer activity [95].

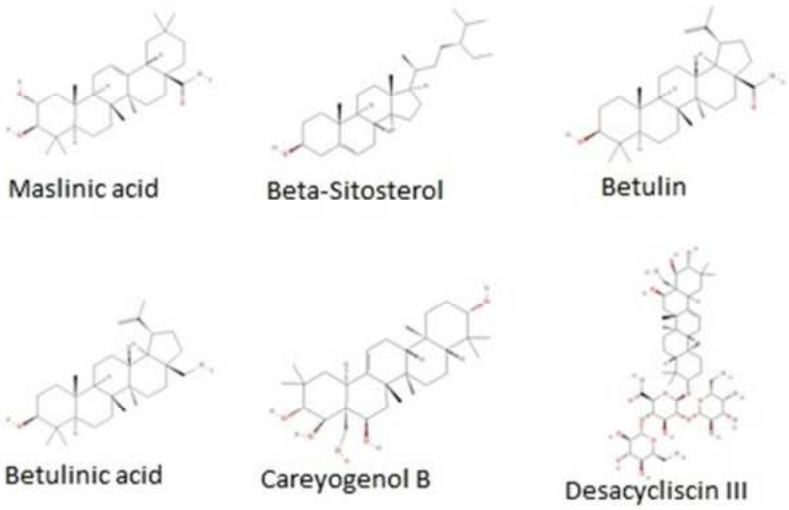

Figure 6 Reported bio-actives in bark of *C. arborea*

7.3. ***Holarrhena antidysenterica***

7.3.1. Introduction

Holarrhena antidysenterica (L.) Wall commonly known as kurchi belonging to the Apocynaceae family is a medicinal plant abundantly found in India, especially in the Himalayan ranges. Its uses are mentioned in the classical Ayurvedic literature

and by many folklore claims. In Ayurveda, this plant is used in classical formulations, namely, Kutajarishta, Kutajavleha and Kutajghan vati, Mahamanjishtadi Kashayam, Stanyashodhana Kashaya, and Patoladi Choornam [96]. It is classically known for curing Pravahika (amoebiasis), Atisara (diarrhea), Jwaratisara (secondary diarrhea), Asra (blood or blood-related disorders), Kustha (skin disorder), and Trsna (thirst) [97]. The plant is also of extreme economic importance as it is exported in the form of seed powder, bark powder, kutaja kwatha, Kutaja Prapati Vati, and as an herbal dietary supplement. The bark and seeds are reported to show activity against amoebic dysentery and *E. coli*-induced diarrhea in rats [98]**.** Anti-diarrheal formulation, Kutajarishta contains *H. antidysenterica* as a major ingredient. Aqueous and alcoholic bark extract showed antibacterial activity against enteric pathogens – EIEC, EPEC, *S. flexneri,* and *V. cholerae* [99]**.**

7.3.2. Reported bio-active compounds in bark

The methanolic bark extract inhibited biofilm formation by *V. cholerae* by down- regulating the expression of aph A and B genes which are responsible for the regulation of biofilm formation [100]. When petroleum ether bark extract was treated with EPEC, a reduction in plasma membrane damage and mitochondrial swelling was observed in INT 407 cell line [101]. The methanolic bark extract also exhibited antifungal activity against *C. albicans* [102]. Phytochemicals in bark include steroidal alkaloids such as conessine, conessimine, kurchinine, and holarrhine. Lupeol and ursolic acid are the triterpenes found in bark [103].

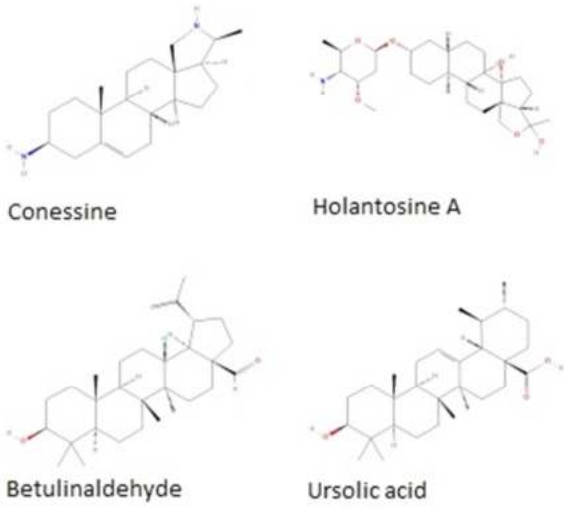

Figure 7 Reported bio-actives in bark of *H. antidysenterica*

7.4. *Punica granatum*

7.4.1. Introduction

Punica granatum L. belonging to the family Punicaceae has been used for thousands of years to cure a wide range of diseases across different cultures and civilizations. The fruit of this plant is used as food and as a diet in convalescence after diarrhea [104]. It is used in Siddha, Ayurvedha and Unani medicine, especially for the treatment of gastrointestinal (GI) diseases. The extract from the rind of *P. granatum* has been demonstrated to have gastroprotective activity through its antioxidant mechanism [105]. Many Ayurvedic antidiarrheal formulations contain *P. granatum* as one of the ingredients [106]. Fruit peel is traditionally used in treating gastrointestinal disorders. Both the peel and juice extract of *P. granatum* showed gastroprotective activity and also prevented castor oil- induced enteropooling in rats.

7.4.2. Reported bio-active compounds in fruit

Due to its rich nutritional content and health-enriching qualities, pomegranates are termed as a super fruit. It is marketed in various forms like fresh juices, capsules, and tablets with powdered extracts of fruit rind and seeds. Fruits are enriched with polyphenols comprising hydrolyzable tannins, and ellagitannins which are responsible for its antioxidant and anti-inflammatory properties [107]. Ellagic acid is converted to urolithins by the microflora of the intestine and it is reported that these urolithins possess anti-cancer and anti-aging activity [108].

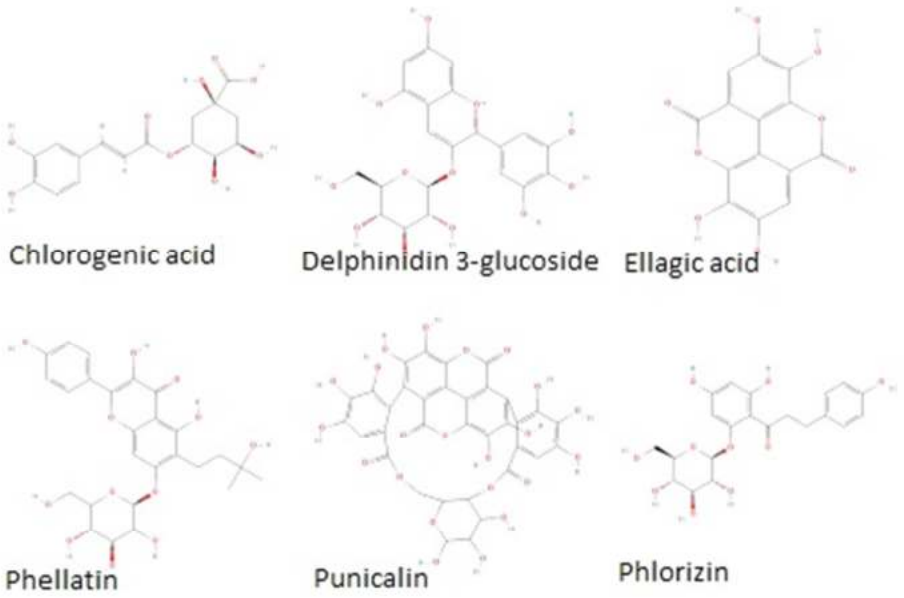

Figure 8 Reported bio-actives in fruit of *P. granatum*

7.5. *Piper longum*

7.5.1. Introduction

Piper longum L commonly called as pippali or long pepper belongs to the family Piperaceae. Ayurveda considers this herb highly valuable in traditional medicine, with its use being prescribed as a standalone remedy and also as part of

combination therapy for treating numerous ailments related to the respiratory and digestive system [109]. Long pepper is antioxidant, decongestant, carminative, expectorant, warming, analgesic, and detoxifier [110]. The use of this herb in Ayurvedic medicine is widespread, with applications in treating various health conditions. Long pepper is a key ingredient in Trikatu churna, which is a formulation used to enhance gastric function and alleviate dyspepsia [111]. Its traditional use also includes treating respiratory ailments such as asthma, bronchitis, cough, as well as digestive disorders. Studies with piperine, a major alkaloid in fruits of *P.longum* has shown anti-diarrrheal and antispasmodic activities. Similar to loperamide, piperine at the dose of 10 mg/kg provided complete protection from castor oil-induced diarrhea in mice [112].

7.5.2. Reported bio-active compounds in fruit

The fruits of *P. longum* are rich in alkaloids such as piperine, pipelongumine, pellitorine, refractomide, pipercide and piperidine. Unripe fruits are traditionally used in the treatment of infections related to the respiratory tract and also as an antitode for snake and scorpion bites [113]. In the ovalbumin-induced asthma model, piperine is reported to inhibit the production of Th-2-induced cytokines and infiltration of eosinophils resulting in hyper-response of airway [114]. Piperine also showed hepatoprotective activity as it reduced the hepatotoxicity induced by CCl_4 and d-galactosamine [115].

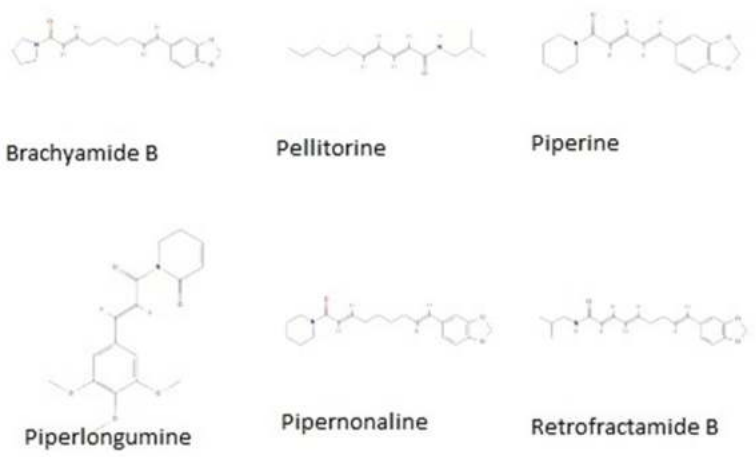

Figure 9 Reported bio-actives in fruit of *P. longum*

7.6. *Psidium guajava*

7.6.1. Introduction

Psidium guajava Linn. commonly called guava belongs to the family of Myrtaceae. Traditionally this plant has been used for decades across different cultures for treating diarrheal infections and disturbances in the respiratory tract. It is also used against wound healing, hypertension, inflammation, and diabetes [116]. In guinea pigs and rats, the leaf extract reduced the incidence of cough induced by aerosol of capsaicin and showed antibacterial activity against *S. aureus* and streptococcus bacteria [117]. Leaf and bark decoction is used for curing skin ailments. Young leaves are chewed for reducing toothaches and tincture from leaves is used for treating convulsions in children. A crude decoction from leaves showed antibacterial activity against *S. flexneri*, *V. cholerae* and also inhibited the adherence of enteropathogenic, enteroinvasive *E. coli* and *S. flexneri* to Hep-2 cells and binding of CT and LT to GM1 receptor [118].

7.6.2. Reported bio-active compounds in leaf

Among all the plant parts, leaves harbor a high amounts of bio-active compounds which are responsible for its antibacterial, anticancer, antidiabetic and antidiarrheal activities [119]. Guava leaves are a rich source of phenolic compounds and flavonoids. The essential oils from leaves contain caryophyllene which is reported to show antimicrobial and antioxidant properties [120]. Quercetin, a major bio-active compound found in guava leaves is reported to show anticancer and anti-inflammatory properties [121]. Flavonoids in guava leaves include procyanidin, quercetin, quercetrin, kaemferol, catechin, avicularin and epicatechin. Caffeic acid, chlorogenic acid, and gallic acid are the major phenolic compounds found in guava leaves [122].

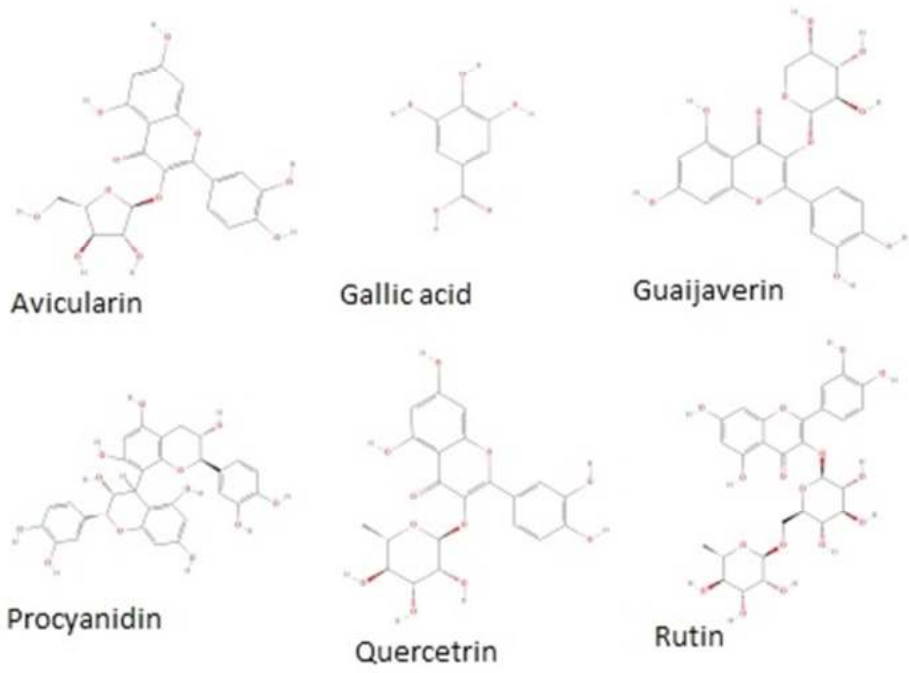

Figure 10 Reported bio-actives in leaf of *P. guajava*

8. Justification of the study and research hypothesis

From the extensive literature review, it is understood that despite CT being the major virulent factor responsible for cholera, treatment majorly involves the use of antibiotics targeting the bacteria but not the CT. This is resulting in yet another outbreaks caused by MDR strains of *V. cholerae*. Even though, access to clean water for drinking and a good sanitation system forms the pillars of cholera prevention and control, these are resource-intensive as well as time-consuming to implement.

Traditional medicine uses a variety of medicinal plants to treat diarrheal infections and most of these traditionally used plants were also scientifically reported to act against enteric pathogens. A comprehensive analysis of available scientific literature revealed that most of the phytocompounds that have been investigated to show anti-CT activity are polyphenols. The term "polyphenols" refers to a larger family of organic compounds synthesised by plants with structural phenolic features ranging from simpler phenolic acids to complex structures such as proanthocyanidins. The potency of these polyphenols against CT has been demonstrated either by disruption of the binding of CTB to GM1, subsequently preventing its internalization, or by inhibition of CTA1 catalysed ADP-ribosylation of $G_{s\alpha.}$ Among the different classes of polyphenols, flavonoids, and phenolic acids were experimentally investigated to show resistance against CT toxicity both through *in vitro* and *in vivo* studies.

Hence the hypothesis of the present study is that the polyphenols from selected six plants can inhibit CT toxicity by preventing its binding to the GM1 receptor on intestinal epithelial cells as shown in the image below.

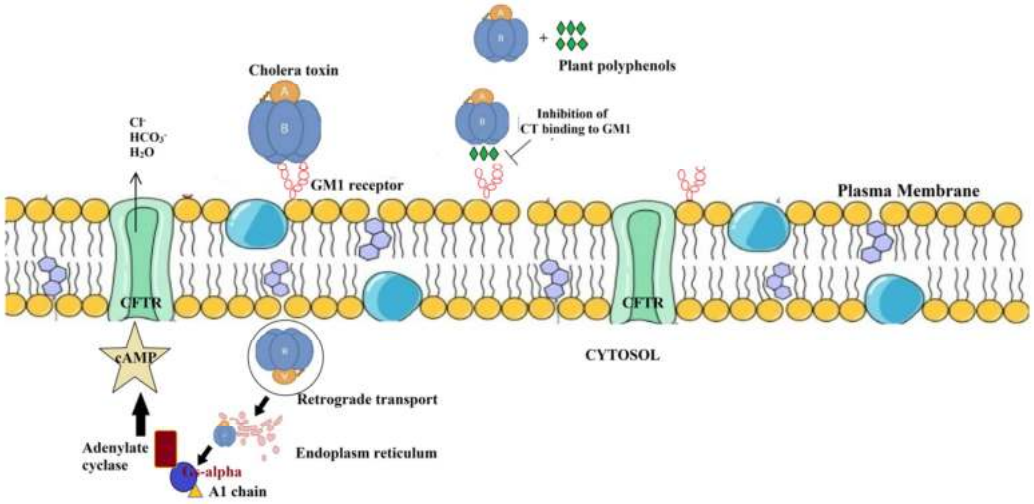

Figure 11 Research hypothesis representing binding inhibition of CT to GM1 by plant polyphenols

Workflow of the present study is represented as follows

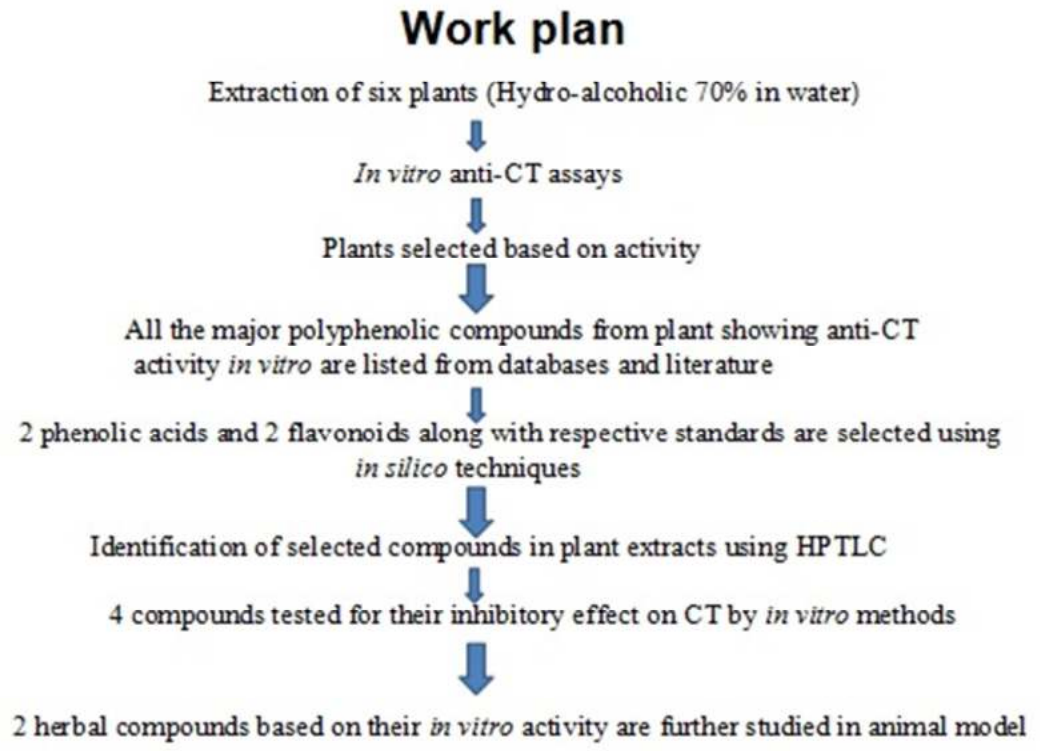

METHODOLOGY

1. Collection and authentication of plants

Unriped fully matured fruits of *Aegle marmelos* (Indian Bael); bark of *Careya arborea* (wild guava), *Holarrhena antidysenterica* (Kurchi); young leaves of *Psidium guajava* (common guava), fruits of *Punica granatum* (Pomegranate) and *Piper longum* (Indian long pepper) were collected from Belagavi district, Karnataka, India from March to May 2019. The collected plants were identified and certified by a plant taxonomist at ICMR-NITM. The voucher specimen has been deposited in ICMR-NITM with accession numbers 1588 (*Aegle marmelos*), 1590 (*Careya arborea*), 1591 (*Holarrhena antidysenterica*), 1589 (*Psidium guajava*), 1690 (*Punica granatum*), 1691 (*Piper longum*).

2. Plant extraction

All the plant parts were washed, shade dried, and powdered. The juice crushed from the seeds of pomegranate fruits after removal of the peel is filtered, lyophilized and stored at -20°C until further use. Before extraction, fruits of *Piper longum* are initially defatted using petroleum ether by Soxhlet apparatus. Deffated fruits of *P. longum* are then used for extraction. The extraction of six plants was carried out using cold maceration technique [123]. Powdered plant material (100 g) was mixed with fivefold 70% (v/v) ethanol and kept on a shaker at 120 rpm for 48 hrs at room temperature. The mixture was then filtered using Whatmann filter paper no-1 and the filtrate was distilled by rotary evaporator. The residual extract was freeze-dried by lyophilization. The extraction yield of seven extracts from six plants was calculated as weight of the dried extract/weight of powdered crude plant part * 100. All seven

extracts from six plants were stored at -20℃ for future use. Table 1 represents the extraction yield from six plants.

Table 3 Extraction yield from six plants and their respective coding

Name of the plant (part)	Extract code	Extraction yield
Careya arborea (bark)	CAE	7.67
Punica granatum (fruit peel)	PGRPE	5.83
Punica granatum (fruit juice)	PGRJ	6.87
Psidium guajava (leaf)	PGAE	9.58
Holarrhena antidysenterica (bark)	HAE	8.24
Aegle marmelos (fruit)	AME	4.86
Piper longum (fruit)	PLE	7.47

The selected six plants were evaluated for inhibitory activity against CT using *in vitro* anti-CT assays. Plants with efficient inhibitory activity against CT *in vitro* were selected and the bio-active compounds from these plants were screened against CT using computational tools. The phyto-compounds forming stable interaction with active sites residues at the GM1 binding site of CT were further evaluated using *in vitro* and *in vivo* studies.

3. Estimation of total polyphenolic content

As polyphenols were demonstrated to possess anti-Cholera toxin activity from the previously reported literature [124], total phenolic content (TPC) and total flavonoid content (TFC) in seven extracts were estimated using Folin-Ciocalteu [125] and $AlCl_3$ colorimetric methods respectively [126] with little modifications.

Folin-Ciocalteu reagent diluted at 1:20 in distilled water was added to seven extracts taken at three different concentrations (500 µg, 1 mg, and 2 mg/mL). To this, 4 mL of 7.5% Na_2CO_3 and distilled water were added to make the volume 15 mL. This mixture was allowed to stand for 2 hrs at room temperature and absorbance was taken at 750 nm. TPC was expressed as mg gallic acid equivalents per gram of dry extract.

Seven extracts at varying concentrations were added to the volumetric flask containing 4 mL distilled water and 0.3 ml $NaNO_2$ was added to this mixture. After 5 min, 0.3 mL of 10% $AlCl_3$ was added and 0.2 mL of 1 M NaOH was added at the 6^{th} min. Total volume was made to 10 mL with dis. H_2O and absorbance were taken at 510 nm. TFC was expressed as mg rutin equivalents per gram of dry extract.

4. Source of *V. cholerae* strains

The *V. cholerae* strains used in the present study were collected from clinical isolates during cholera outbreak from June 2012 to July 2013 [127,128]. All these strains were retrieved from the microbial strain repository of ICMR-NITM which were preserved as glycerol stocks at -80°C. Ten isolates were selected based on the presence of the virulence genes required for the pathogenesis, production of Cholera toxin and multi-drug resistant profile.

Table 4 Reference codes for selected ten clinical isolates of *V. cholerae* and their virulence genes profile

Code	Year	ctxA	ctxB	tcpA ET	tox S	tox R	tox T	VPI	ace	zot
DCHIP 79	2012	+	+	+	+	+	+	+	+	+
DCHIP 92	2012	+	+	+	+	+	+	+	+	+
DCHIP 93	2012	+	+	+	+	+	+	+	+	+
DCHIP 96	2012	+	+	+	+	+	+	+	+	+
DCHIP 99	2013	+	+	+	+	+	+	+	+	+
DCHIP 100	2013	+	+	+	+	+	+	+	+	+
DCHIP 103	2013	+	+	+	-	-	+	-	+	+
DCHIP 104	2013	+	+	+	+	+	+	+	+	+
DCHIP 105	2013	+	+	+	+	+	+	+	+	+
DCHIP 106	2013	+	+	+	+	+	+	+	+	+

5. Selective media and bacterial culture

The glycerol stocks were initially thawed and cultured in Mueller Hinton broth and incubated for 12 hrs at 37℃. Later the inoculum from broth cultures was streaked on selective TCBS media. *V. cholerea* grows on TCBS media forming yellow colonies [129]. A single colony from the TCBS plate was transferred to TSA media for pure culture and further analysis of the bacteria was performed using PCR.

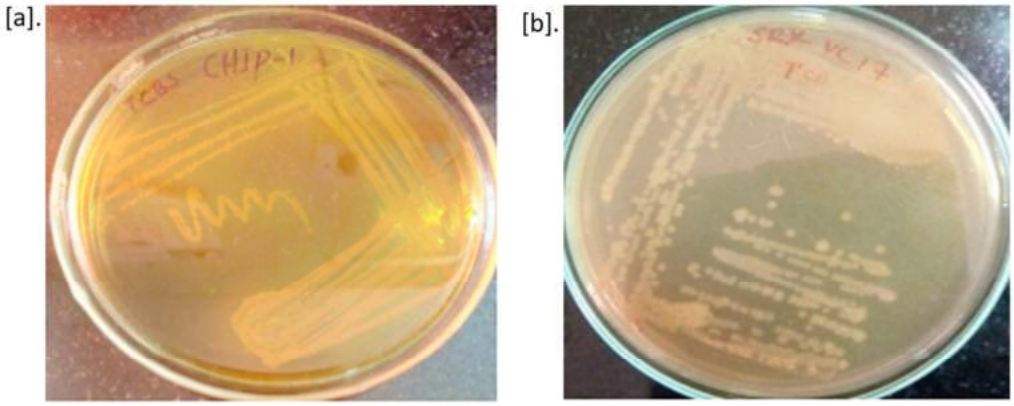

Figure 12 Yellow colonies of *V. cholerae* on TCBS media [a] and subculture of pure colonies on TSA media [b].

6. Genomic DNA extraction and quantification

DNA was extracted from 16 hrs pure cultures of selected ten strains in Mueller Hinton broth using enzymes and phenol/chloroform separation [130]. Overnight broth cultures in log phase were taken in 2 mL Eppendorf tubes and centrifuged at 8000 rpm for 20 min to pellet the bacterial cells. This bacterial pellet was resuspended in a buffer containing 10 µL of lysozyme and incubated for 1 hr at 37°C. After 60 min of incubation, 50 µL of SDS and 10µL of proteinase K were added and incubated at 60°C for 1 hr. PCI was added to this mixture and centrifuged at 12,0000 rpm for 20 min. The upper aqueous layer after centrifugation was carefully transferred to Eppendorf tube and an equal quantity of chilled absolute ethanol was added and further centrifuged for 20 min at 12,000 rpm. The supernatant was discarded and the pellet was carefully dried at 50°C and resuspended in TE buffer. Further quantification of DNA as nanogram/mL was performed using a nanodrop spectrophotometer at 260 nm and the quality of DNA was visually checked by running the genomic DNA on 1% agarose gel.

7. PCR for identification of ctxAB gene

PCR was performed with template DNA extracted from ten isolates of *V. cholerae* using the phenol/chloroform method. The forward and reverse primer sequences of the ctxAB gene were obtained from earlier studies [131].

ctxAB-F : 5′- CAGTCAGGTGGTCTTATGC – 3′

ctxAB -R : 5′- ATCGTGCCTAACAAATCCC– 3’

PCR amplification was carried out using 25 µL of the master mix comprising dNTP’s, Taq polymerase, Taq buffer, forward and reverse primers. The amplicon size of the ctxAB gene was 460 bp based on which the thermal cyclic conditions were maintained for 35 cycles with an initial denaturation at 95°C for 5 min, annealing at 56°C for 1 min, and final extension at 72°C for 7 min.

8. Preparation of cell free culture filtrate

AK1 media was used to induce the virulence genes expression and production of CT by *V. cholerae* as described [132,133]. Initially, the bacteria was streaked on MH agar medium and a single colony was picked and inoculated in MH broth and grown for 12 hrs. The inoculum size is adjusted to 10^5-10^7 cfu/mL and 1mL of inoculum was added to 10mL of AK1 medium taken in stationary tubes and incubated for 4 hrs at 37°C. The culture was then transferred to a flask and then kept on a shaker for 16 hrs. The culture fluid thus obtained was centrifuged at 14000 rpm for 20 min at 4°C to pellet the bacterial cells. The cell-free supernatant was filtered using a 0.22 µm syringe filter and stored as cell free culture filtrate (CFCF) at -20°C. Repeated freeze

thawing decreases the concentration of CT in CFCF and therefore multiple aliquots were prepared and stored at -20°C for future use.

9. Selection of single isolate of *V. cholerae* using cell based assays

CHO cell line was procured from NCCS, Pune and cultured in DMEM media with 10% FBS at 37°C and 5% CO_2. As CT produces cell elongation in the CHO cell line, cell elongation induced by CT in CFCF on the CHO cell line was analyzed as described [134] by direct observation with an inverted phase-contrast microscope. Briefly, CHO cells were seeded at $6x10^4$ in 12-well plate culture dishes in DMEM supplemented with 10% FBS and incubated for 24 hrs at 5% CO_2 and 37°C. Then the cells were washed and treated with different dilutions of CFCF of ten isolates in DMEM media with 2% FBS. After 18 hrs of incubation at 37°C and 5% CO_2, cells were observed under a phase contrast microscope at 40X magnification. CHO cells were also treated with similar dilutions of AK1 media to establish whether the media in itself is affecting the pH of tissue culture media. The CFCF of *V. cholerae* strain producing cell elongation in CHO cells even at the highest dilution was selected and was used further for *in vitro* and *in vivo* studies.

10. Estimation of Cholera toxin concentration in CFCF

CFCF-producing cell elongation in the CHO cell line at the highest dilution was selected for the estimation of CT concentration. Cholera toxin secreted into CFCF was estimated using GM1 ELISA as described by Dawson RM *et al* [135,136]. Cholera toxin (CTX), anti-Cholera toxin antibody, anti-rabbit IgG-peroxidase, monosialoganglioside G_{M1} used for the experiment were procured from Sigma Aldrich. Cholera toxin reconstituted as 5 mg/mL in deionized water was used for

plotting the calibration curve. Briefly Cholera toxin is taken at a known concentration from 1250 ng/mL serially diluted to 39 ng/mL and 100 µL of CFCF at different dilutions (1:5; 1:10; 1:20 and 1;30) in PBS (pH 7.4) were added to GM1(1.44 µM) pre-coated on 96-well micro titre plate. Distilled water used as solvent control for CTX and AK1 media for CFCF were taken as a negative control to provide baseline measurements. The total volume in each well was made to 100 µL with PBS and incubated for 1 hr at 37℃, wells were then washed thrice with 0.05% Tween20 in PBS buffer. ELISA was performed using polyclonal rabbit antiserum diluted 1:600 in PBS against CT and anti-rabbit IgG-peroxidase diluted 1:200 in PBS. To visualize the binding of CT to GM1, 50 µL of 0.04% (w/v) of OPD and 0.2% (v/v) of hydrogen peroxide in citrate buffer (pH-5.5) was added to each well and incubated for 5 min in dark. To stop the reaction, 50 µL of 2.5 N H_2SO_4 was added and absorbance was estimated at 492 nm using a Thermo Scientific ELISA plate reader. The concentration of CT secreted in CFCF was estimated from the Cholera toxin calibration curve. As the concentration of Cholera toxin produced by the bacterium is not constant, the concentration is determined for each batch of CFCF used.

11. *In vitro* studies with seven plant extracts

11.1. Cytotoxicity assay

Cytotoxicity of seven extracts was determined on the CHO cell line using MTT assay [137]. IC_{50} corresponds to the concentration of extract causing 50% cell death. The IC_{50} values of seven extracts were used to calculate their non-cytotoxic concentration. Two non-cytotoxic concentrations (NC1 and NC2) of each extract were determined that produces >90% cell viability using MTT assay. CHO cells were grown in Dulbecco's modified Eagle medium supplemented with 10% FBS, penicillin-

streptomycin and amphotericin b in the presence of 5% CO_2 at 37°C. The stock solutions of seven extracts was prepared as 10 mg/mL in 5% DMSO and filtered using a 0.22 µm syringe filter. CHO cells were seeded at $3x10^4$ per well in 96-well plate and incubated for 24 hrs at 37°C and 5% CO_2. After 24 hrs, the media was discarded and cells were washed with PBS. Then the cells were treated with increasing concentrations of seven extracts in triplicates. The total volume in each well was made to 200 uL with DMEM supplemented with 2% FBS and incubated for 24 hrs. Then the cells were washed with PBS and treated with 20 uL of 0.5% MTT solution in PBS and incubated for 4 hrs. The formazon crystals formed after 4 hrs was solubilized by adding 100 µL of DMSO. The absorbance was recorded at 570 nm and the cytotoxicity percentage was calculated as $(1- A_{test}/A_{control}) \times 100$.

11.2. Binding inhibition percentage of CT to ganglioside GM1 in presence of seven extracts

The inhibition of CT binding to GM1 by seven extracts was evaluated by GM1 ELISA as previously stated. The concentration of CT in CFCF was estimated from the standard curve and used for the experiment. The CFCF titre with a CT concentration 1600 ng/mL serially diluted to 100 ng/mL was initially used to estimate the CT concentration in CFCF that shows the highest absorbance using GM1 ELISA. Then this CFCF titre with CT concentration showing the highest absorbance is treated with two non-cytotoxic concentrations of each of the seven plant extracts and incubated for 4 hrs on shaker at 120 rpm at 37°C. Then this pre-incubated mixture of CFCF and seven plant extracts were added to pre-coated GM1 96-well micro titre plates in triplicates. Each concentration of seven plant extracts and CFCF were added

to the wells individually to provide the baseline measurements. The binding inhibition percentage was calculated as $(1-A_{test}/A_{control}) \times 100$.

11.3. Inhibitory activity of seven extracts against CFCF-induced cAMP levels

Cyclic AMP levels in CFCF-induced CHO cells was estimated using Abcam cyclic AMP *in vitro* competitive ELISA kit as per the instructions of the manufacturer. CHO cells were seeded at $4x10^4$ cells in Nunc 96-well flat bottom micro plate and incubated for 24 hrs at 5% CO_2 and 37°C. After 24 hrs, the used media was discarded; cells were washed and treated with a pre-incubated mixture of seven extracts at two non-cytotoxic concentrations and CFCF with a CT concentration of 100 ng/mL. The volume in each well was made to 200 µLwith DMEM supplemented with 2% FBS and incubated for 18 hrs. The cell lysate was prepared after 18 hrs by treating the cells with 0.1 M HCl and 1% tritonX-100. Uniform lysis of cells was observed under a microscope and lysate supernatant was obtained by centrifugation of cell lysate at 2000 rpm. Cell lysates of test samples were added to the kit wells in duplicates and assay was performed as per the instructions. Untreated cells, cells treated with CFCF and cells treated with each of seven extracts alone served as controls. Cyclic AMP levels were calculated as percent bound cAMP for cells treated with mixture of seven extracts with CFCF and control cells treated with each of seven extracts/ CFCF/DMEM.

11.4. Protective activity of seven extracts against CFCF-induced cell elongation

The protective activity of seven extracts against cell elongation induced by CT in CFCF on CHO cell line was analyzed as described [138] by direct observation with an inverted phase-contrast microscope. Two non-cytotoxic concentrations of seven

extracts were treated with CFCF containing 100 ng/mL of CT and incubated for 4 hrs under shaking conditions at 120 rpm. Briefly, CHO cells were seeded at $6x10^4$ in 12-well plate culture dishes in DMEM supplemented with 10% FBS and incubated for 24 hrs at 5% CO_2 and 37°C. After 24 hrs, cells were washed and the pre-incubated mixture of seven extracts with CFCF was added to the cells in DMEM media with 2% FBS. After 18 hrs of incubation at 37°C and 5% CO_2, cells were washed, replenished with fresh media and observed under a phase contrast microscope at 40X magnification. CHO cells were also treated with similar dilutions of AK1 media to establish whether the media in itself is affecting the pH of tissue culture media.

12. ***In silico*** **studies**

12.1. Mining of bio-active compounds and Molecular docking

C. arborea, P. grantum and P. guajava were observed to show efficient inhibitory activity against CT from our *in vitro* studies. Polyphenolic compounds from these three plants were mined from public database resources like PCIDB (Phytochemical interactions DB), Dr. Dukes DB and literature search. Structural and chemical information about these phytocompounds was obtained from PubChem small molecule database. This compiled dataset of bioactive compounds was filtered for duplicate entries and ubiquitous molecules. The virtual screening was performed using Dock6.9 software developed by UCSF [139]. We used a flexible docking approach for virtual screening as most of the herbal compounds had larger molecular weights. Also, flexible docking would help to accurately predict the binding mode and intermolecular interactions of selected 60 phytocompounds with the Cholera toxin (CT).

The three-dimensional structure of CT was retrieved from the RCSB structural database that has five β-subunits bound to the one α-subunit (PDB ID: 1XTC). We have prepared the structure of CT by adding missing residues and refining the generated models by energy minimization in gromacs. The grid was set at the region where CT binds to the GM1 receptor, the binding pocket residues were taken from the earlier reported structures [140]. The spheres were generated over the entire surface by producing one sphere per surface point. Further, we have chosen the spheres which are located at the GM1 binding interface of CT.

In the selected CT structure, β-subunits have five chains of which we have preferred chain F (shown in gold surface representation in Figure 13A) that formed a larger cavity at the GM1 binding interface, and hence considered as a potential binding site. The default parameters for flexible docking were selected in this study. Selected 20 polyphenolic compounds were prepared for docking by adding hydrogens and converting them into 'mol2' file format using Openbabel2.4. The ligand conformations were ranked by considering their grid score. Best-docked conformations were selected by analyzing their intermolecular interactions with the active site of CT causing the disruption of CT to the GM1 receptor.

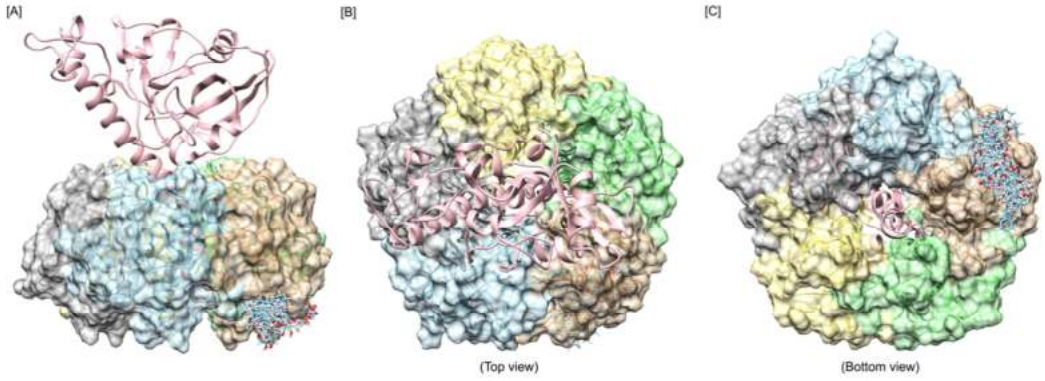

Figure 13 Binding of 20 phytocompounds to the largest binding pocket at chain F of 1XTC. [A] shows the front view, while the top (B) and bottom view (C) are also shown to highlight the orientation and architecture of whole CT having one alpha and five subunits of beta chains

12.2. Drug-likeness prediction

Drug likeness prediction and side effects of top 10 hits with 1XTC were performed by submitting the canonical SMILES of each molecule to an online prediction server ADMETlab 2.0 [141].

Based on the docking score and a total number of interactions with active site residues at the GM1 binding site of CT, we have chosen three phenolic acids (Ellagic acid, chlorogenic acid and gallic acid) and three flavonoids (rutin, phlorizin, and quercetrin) from the screened 20 compounds. Gallic acid and Quercetrin were used as a control for phenolic acid and flavonoids respectively as they were reported to show neutralizing activity against CT.

12.3. MD simulations of the docked complexes

Six complexes were selected based on their docking interactions with active site and grid score viz., CT-Ellagic acid (CT-EA), CT-Chlorogenic acid (CT-CHL), CT-Gallic acid (CT-GA), CT-Rutin (CT-RTN), CT-Phloridzin (CT-PHD) and CT-Quercetrin (CT-QRTN). The stability of these six complexes was studied by performing MD simulation using gromacs 2021 [142]. We used antechamber module of AmberTools21 to generate partial charges for the ligand molecules, x-leap was used to generate topology file for the entire complexes with Amber-99SBildn forcefield. Complexes were minimized using steepest descent followed by conjugate gradient method to obtain near global state of all the docked complexes. These minimized systems were equilibrated using canonical NVT and NPT ensembles, temperature and pressure was set to 300K and 1 bar respectively. Further, unrestrained all atom molecular dynamics simulations was performed for 100ns and trajectories at every 2fs were recorded. The parameters for the Protein-Ligand MD simulations were taken from the earlier similar studies [143,144,145]. The trajectories obtained were analysed using inbuilt gromacs tools, chimera was used to analyse individual snapshots and generate publication quality images. The tool *'g_mmpbsa'* was used to calculate the relative binding energy using MMPBSA approach [146]. The Grace 5.1.25 software package was used to represent all the plots generated by analysing the MD trajectories. Intermolecular interactions were investigated using Biovia-Discovery studio visualizer 2021 [147].

13. Quantification of selected polyphenols using HPTLC

Six herbal compounds, including three phenolic acids, Ellagic acid (EA), Chlorogenic acid (CHL), Gallic acid (GA), and three flavonoids; Rutin (RTN), Phloridzin (PHD), and Quercetrin (QTRN), selected using *in silico* studies were procured from Sigma Aldrich. Quantification of these six compounds in hydro-alcoholic extract was performed using High-Performance Thin-Layer Chromatography (HPTLC).

CAMAG-HPTLC system was used for the detection, separation, and densitometric analysis of hydro-alcoholic extracts of *C. arborea*, *P. guajava, P. granatum* for selected six compounds [148,149]. The stock solutions of extracts and standards were prepared as 1.0 mg/mL in methanol except EA which was dissolved in 99.7% DMSO. Analysis was performed on a pre-coated TLC silica gel G60 F_{254} plates (ALUGRAM) (10 × 10 cm) for phenolics (EA, CHL, and GA) and RP-18W/UV_{254} (ALUGRAM) (10 × 10 cm) for flavonoids (RTN, PHD, and QRTN). Standards and sample bands (6 mm) were applied using CAMAG Linomat-5 TLC Sampler using a 100 µL syringe. Band length 6 mm, application rate 50 µL/s distance from the bottom of the plate (Y) 10 mm, distance from the edge of the plate (X) 10 mm, the distance between bands were auto set. The plates were developed up to a distance of 80 mm with toluene: ethyl acetate: methanol: formic acid in the ratio of 3:3:0.8:0.6 v/v (for phenolics) and tetrahydrofuran: water: formic acid in the ratio of 4: 6: 0.5 v/v (for flavonoids) as mobile phase. The details of peaks were recorded at 280 nm (for phenolics) and 310 nm (for flavonoids) using CAMAG TLC scanner 3, WinCATS–Planar Chromatography Manager, (Version 1.4.4.6337), Switzerland.

14. *In vitro* studies with six polyphenolic compounds

14.1. MTT cytotoxicity assay

Six herbal compounds, including three phenolic acids, Ellagic acid (EA), Chlorogenic acid (CHL), Gallic acid (GA), and three flavonoids; Rutin (RTN), Phloridzin (PHD), and Quercetrin (QTRN), were procured from Sigma Aldrich, and CHO cell line was obtained from NCCS, Pune. Cytotoxicity of these six compounds on the CHO cell line was determined using the MTT assay as described [137]. CHO cells were seeded at a density of 20,000 cells/well and incubated for 24 hrs at 37°C and 5% CO_2. The stock solutions of CHL, GA, RTN, PHD, and QRTN were prepared as 2 mg/mL in 0.05% DMSO, whereas EA stock was prepared as 2 mg/mL in 99.7% DMSO and filtered using 0.22 μm syringe filters. After 24hrs, CHO cells were treated with increasing concentrations of six compounds, ranging from 18 to 700 μg/mL each, in triplicates in DMEM media supplemented with 2% FBS and incubated for 24 hrs at 37°C and 5% CO_2. Simultaneously, untreated cells and cells treated with DMSO were taken as cell control and vehicle control, respectively. Subsequently, cells were washed twice with PBS and treated with 20 μL of 0.5% MTT solution in PBS for 4 hrs, and formazan crystals formed after 4 hrs were solubilized using DMSO. The absorbance was taken at 570 nm and the IC_{50} of six compounds on the CHO cell line was estimated using the cytotoxicity percentage.

Using IC_{50} values, two non-cytotoxic concentrations (NC1 and NC2) for each of the six compounds were determined by employing 25% and 12.5% of their respective IC_{50} values, and the viability percentage was estimated by the MTT assay.

14.2. Binding inhibition percentage of CT to ganglioside GM1 in presence of six compounds

The binding inhibition of CT to GM1 by selected phenolic acids (EA and CHL) and flavonoids (RTN and PHD) along with their respective standards was determined by GM1 ELISA as described earlier [135,136]. Initially, the CT concentration in CFCF was estimated from the CT standard curve. CFCF titre with a CT concentration of 3200 ng/mL was diluted twofold up to 100 ng/mL to plot the CFCF absorbance curve and to select the CT concentration exhibiting maximum absorbance at the highest dilution. The selected CFCF titre was treated with NC1 and NC2 of each of the six compounds and incubated on a shaker at 120 rpm for four hours at 37°C. Later, this pre-incubated mixture was added along with CFCF control to a pre-coated GM1 96-well micro-titre plate, and GM1 ELISA was performed in triplicates. Simultaneously, each concentration of six compounds was also added in triplicates to get the background measurements, and the binding inhibition percentage was calculated.

14.3. Inhibitory activity of six compounds against CFCF-induced elevated cAMP levels

Elevated cAMP levels in CT-induced CHO cell lines were evaluated using the Abcam cAMP *in vitro* competitive ELISA kit as per the manufacturer's instructions. CHO cells seeded at a density of $4x10^4$ cells/well in a 96-well microtitre plate were treated with a pre-incubated mixture containing CFCF (CT=100ng/mL) and each of six compounds at NC1 and NC2 in duplicates. Untreated CHO cells and cells treated with CFCF alone were taken as cell control and positive control, respectively. Concurrently, cells were also treated with each of the six

compounds to establish that the selected compounds have no effect on the intracellular cAMP levels. The inhibitory activity of six compounds against CT-induced cAMP levels in the CHO cell line was evaluated as an increase in bound percent (B%) of cAMP *w.r.t.* CFCF control.

14.4. Protective activity of six compounds against CT induced cell elongation

The protective activity of six compounds against CT-induced cell elongation in the CHO cell line was analyzed as described by Saha (2013). CHO cells were seeded at a density of $6x10^4$/well in 12-well culture plates supplemented with 10% FBS + DMEM media and incubated for 24 hrs at 5% CO_2 and 37°C. CFCF titre with CT concentration 100 ng/mL was treated with NC1 and NC2 of each of six compounds and incubated at 37°C under shaking conditions at 120 rpm for 4 hrs. After 24 hrs, the pre-incubated mixture was added to CHO cells in duplicates supplemented with 2% FBS+DMEM media and further incubated for 18 hrs at 5% CO_2 and 37°C. CHO cells were also simultaneously treated with six compounds alone to check their effect on cell morphology. After 18hrs, cells were washed twice with PBS, replenished with fresh media, and observed for morphological changes under a phase contrast microscope.

15. *In vivo* studies

Based on the results from *in vitro* experiments with plant extracts and phyto-compounds, three plant extracts (CAE, PGRPE, and PGAE) and three phenolic acids (EA, CHL, and GA) were further studied against CFCF-induced fluid accumulation and histopathological changes *in vivo* using adult mice ligated-ileal loop model [150].

Animal experiments using adult mice were approved by the Institutional Animal Ethical Committee of ICMR-NITM, Belagavi (Registration number: 1388/GO/Re/S/10/CPCSEA, July 17th, 2018). Six-week-old Swiss albino mice weighing 25-30g were procured from CPCSEA-approved Central Research Laboratory, Belagavi, Karnataka, and acclimatized under controlled conditions of temperature, humidity, and light at the Animal Research Facility of ICMR-NITM, Belagavi.

A total of 84 Swiss albino mice were randomized into 14groups (n=6) and the grouping is detailed as (A) Normal (Untreated): received 100ul of PBS/loop; (B) CFCF control: received CFCF with CT concentration (1µg/loop); (C) CAE1: 100µg of CAE + CFCF (CT 1µg)/loop; (D) CAE2: 50µg of CAE + CFCF (CT 1µg)/loop; (E) PGRPE1: 100µg of PGRPE + CFCF (CT 1µg)/loop; (F) PGRPE2: 50µg of PGRPE + CFCF (CT 1µg)/loop; (G) PGAE1: 100µg of PGAE + CFCF (CT 1µg)/loop; (H) PGAE2: 50µg of PGAE + CFCF (CT 1µg)/loop.

(P) EA1: 50µg of EA + CFCF (CT 1µg)/loop; (Q) EA2: 25µg of EA + CFCF (CT 1µg)/loop; (R) CHL1: 50µg of PGRPE + CFCF (CT 1µg)/loop; (S) CHL2: 25µg of CHL + CFCF (CT 1µg)/loop; (T) GA1: 50µg of GA + CFCF (CT 1µg)/loop; (U) GA2: 25µg of GA + CFCF (CT 1µg)/loop.

Group C-H received a pre-incubated mixture of each of three plant extracts at two variable concentrations with CFCF into each ligated-ileal loop whereas group P-U received a pre-incubated mixture of each of three phenolic acids at two variable concentrations with CFCF.

The mice were fasted overnight prior to the experiment providing free access to the water and then they were anaesthetized by intraperitoneal injection of Ketamine-Xylazine (87.5 mg/kg; 12.5 mg/kg). A small abdominal incision was made through which a loop of distal ileum 2-3 cm in length was exteriorized and tied at both ends using surgical thread. These sealed ileal loops were then injected with PBS/CFCF/plant extracts + CFCF/phenolic acids + CFCF without causing injury to the tissue, gently restituted, and sutured. These mice were then allowed to recover from anesthesia, placed in proper cages and given free access to food and water. After 18 hrs, mice were sacrificed by overdosing with anaesthesia and ileal loops were excised from the carcass. The length and weight of the ileal loops were measured and the weight/length ratio was calculated to determine the protective activity of selected three extracts and phenolic acids against CFCF-induced fluid accumulation in mice, cellular cAMP levels and histopathological changes in ligated-ileal loops.

RESULTS

1. Estimation of total polyphenolic content

Total phenol (TPC) and flavonoid content (TFC) was estimated for 1 mg of seven extracts in terms of gallic acid and rutin gram equivalents based on the calibration curve of gallic acid ($y = 0.0001x + 0.236$; $R^2=0.995$) and rutin ($0.0002x + 0.126$; $R^2=0.992$) respectively.

TPC was observed to be highest for CAE, PGRPE, PGAE, and HAE whereas CAE, PGRPE, and PGAE showed a higher percentage of flavonoid content (Figure 14).

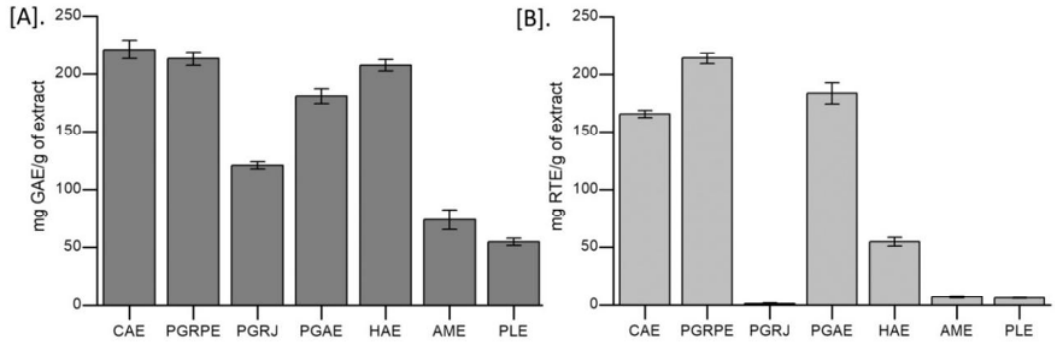

Figure 14 Total phenolic content (TPC) and total flavonoid content (TFC) in seven extracts [A] TPC in seven extracts expressed as mg gallic acid equivalents/g of extract; [B] TFC in seven extracts expressed as mg rut in equivalents/g of extract.

2. Genomic DNA extraction and quantification

Genomic DNA extraction from selected ten clinical isolates was performed using phenol/chloroform method and the obtained DNA was quantified using nanodrop spectrophotometer (Figure 15).

A.

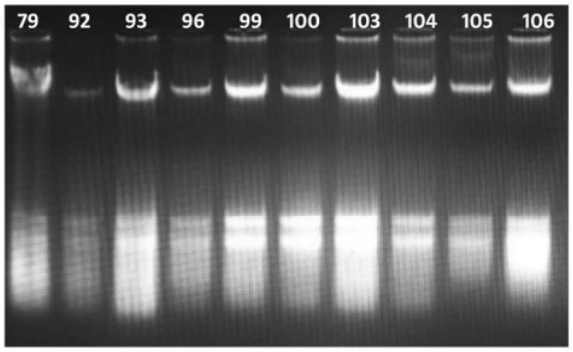

B.

Code	Conc in ng/ul	260/280 ratio
DCHIP79	275.1	2.13
DCHIP92	200.1	2.17
DCHIP93	432.2	2.22
DCHIP96	185.9	2.15
DCHIP99	280.3	2.10
DCHIP100	235.4	2.18
DCHIP103	353.6	2.17
DCHIP104	185.8	2.10
DCHIP105	386.1	2.13
DCHIP106	277.8	2.17

Figure 15 Visual quality of genomic DNA on agarose gel (A) and its quantification using nanodrop (B).

3.PCR for identification of ctxAB gene

Cholera toxin gene in selected Vibrio isolates was identified using ctxAB primers. All the ten isolates were positive to CTX gene (Figure 16).

Figure 16 PCR for identification of ctxAB gene in selected ten isolates

4. Selection of single isolate of *V. cholerae* using cell based assays

CT induces cell elongation in the CHO cell line. CFCF of the *V. cholerae* isolates efficiently secreting CT was identified by treating the CHO cell line with different dilutions of CFCF for 18 hrs and observed for cell elongation using a phase contrast microscope. It was observed that DCHIP100 showed cell elongation at the highest dilution among the selected ten isolates and therefore taken further for quantification of CT in CFCF using GM1 ELISA (Table 5).

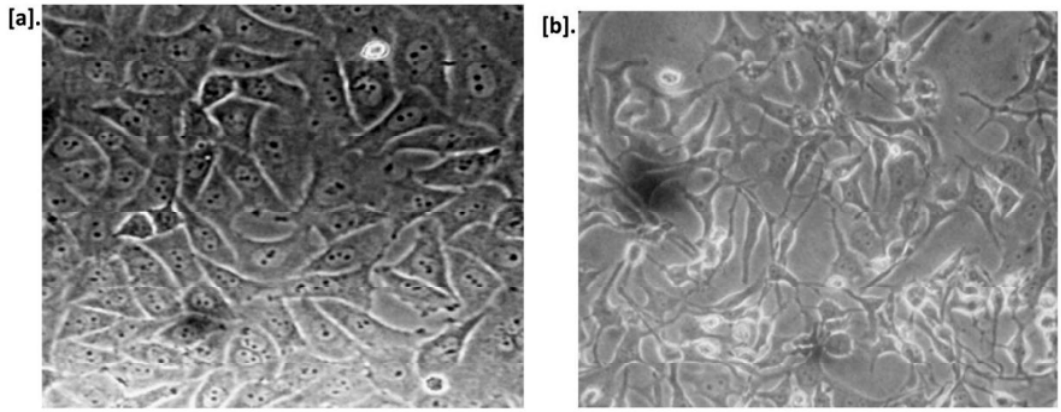

Figure 17 (a) Control CHO cell line and CFCF-induced CHO cell line (b) at 40X magnification observed under a phase-contrast microscope.

Table 5 CFCF-induced cell elongation at different dilutions for the selected ten clinical isolates of *V. cholerae*

Ref no.	CFCF-induced cell elongation (without dilution)	CFCF-induced cell elongation (1:5 dilution)	CFCF-induced cell elongation (1:10 dilution)
DCHIP79	No effect	No effect	No effect
DCHIP92	Observed	Observed	No effect
DCHIP93	No effect	No effect	No effect
DCHIP96	No effect	No effect	No effect
DCHIP99	Observed	No effect	No effect
DCHIP100	Observed	Observed	Observed
DCHIP103	No effect	No effect	No effect
DCHIP104	Observed	Observed	No effect
DCHIP105	Observed	No effect	No effect
DCHIP106	No effect	No effect	No effect

5. *In vitro* studies with seven plant extracts

5.1. Cytotoxicity assay

IC_{50} indicates the concentration of the extract where 50% of cell death has been observed on the CHO cell line by using MTT assay. Among the seven extracts, PLE showed higher toxicity with IC_{50} 128.9±14.2 µg/mL and AME showed least toxicity with IC_{50} 646.3±33.7 µg/mL whereas PGRJ was observed to be non-cytotoxic to CHO cells even at 1 mg/mL concentration of lyophilized juice (Figure 18). Two non-cytotoxic concentrations (NC1 and NC2) for each of the seven extracts were determined by taking 25% and 12.5% of IC_{50} values and the viability percentage at these concentrations was estimated as ≥ 90% on CHO cells (Table 6).

Table 6 IC_{50} and two non-cytotoxic concentrations (NC1 and NC2) of seven extracts:

Plant name	IC_{50} (µg/mL)	NC1 (µg/mL)	Viability %	NC2 (µg/mL)	Viability %
Careya arborea bark (CAE)	349.3 ± 19.3	85	90.1	42.5	95.1
Punica granatum peel (PGRPE)	446 ± 5.1	110	93.6	55	98.6
Punica granatum juice (PGRJ)	ND*	500	98.8	250	98.4
Psidium guajava leaf (PGAE)	486.4 ± 30.8	120	90.7	60	96.2
Holarrhena antidysenterica (HAE)	321.4 ± 22.1	80	89.9	40	91.2
Aegle marmelos fruit (AME)	646.3 ± 33.7	160	97.6	80	98.8
Piper longum fruit (PLE)	128.9± 14.2	35	91.3	17.5	96

ND* Not determined

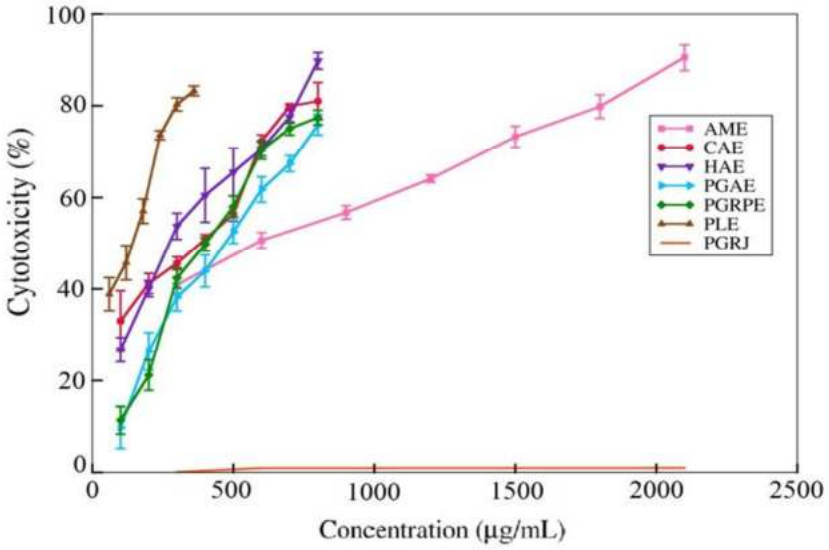

Figure 18 IC_{50} of seven extracts estimated using MTT assay

5.2. Estimation of Cholera toxin concentration in CFCF

A single clinical isolate of *V. cholerae* (DCHIP100) was selected that showed cell elongation in the CHO cell line at the highest concentration of CT in CFCF. Cholera toxin concentration in CFCF calculated using GM1 ELISA was 18.76 µg/mL±0.2. This concentration was not consistent for each batch of CFCF prepared and calculated each time along with the standard curve using GM1 ELISA.

Binding inhibition of CT to GM1 was determined using CFCF of *V. cholerae*. GM1 ELISA was initially performed with CFCF (1:5 dilution) and the concentration of CT was determined. CFCF titre with CT concentration at 1600 ng/mL serially diluted to 100 ng/mL was used to get the CT concentration with maximum absorbance by GM1 ELISA. Using this absorption curve, CFCF titre with 1600 ng/mL of CT was observed to show the highest absorbance. The CFCF titre with CT concentration of 1600 ng/mL was treated with each of the seven extracts at two non-

cytotoxic concentrations and the percentage of binding inhibition was calculated. CAE, PGRPE, PGRJ, and HAE displayed highest binding inhibition percentage which demonstrates their CT neutralization activity by disrupting its binding to the GM1 receptor on intestinal epithelial cells (Figure 19).

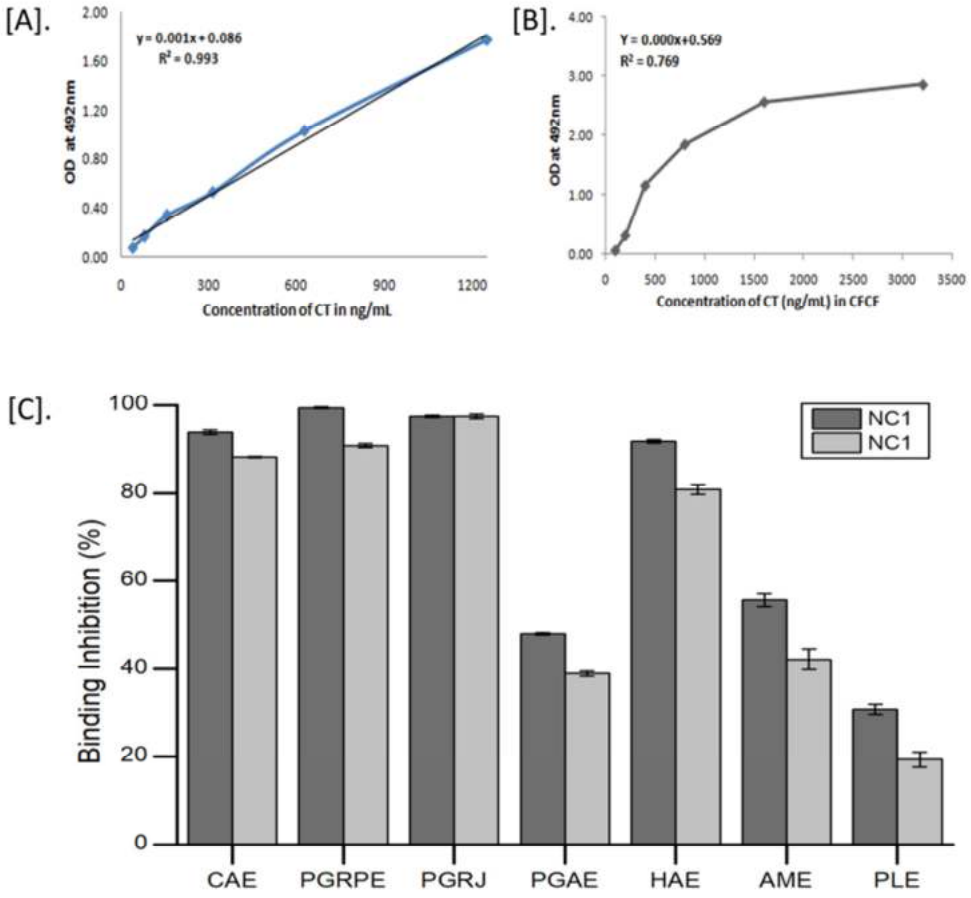

Figure 19 Determination of CT concentration in CFCF and its binding inhibition to GM1. (A) Calibration curve of CT plotted using GM_1 ELISA (B) Absorbance curve of CFCF titre (C) Binding inhibition percentage (BI%) of CT to GM1 in presence of seven extracts.

5.3. Inhibitory activity of seven extracts against CFCF-induced cAMP levels

Elevation in cellular cAMP levels induced by CFCF on the CHO cell line was investigated using competitive ELISA. A significant increase in cAMP levels was observed in CFCF control ($^{\Delta\Delta\Delta}p < 0.001$) compared with CHO cell control. Except PLE, CAE, PGRPE, PGRJ, PGAE, and HAE at both NC1 and NC2 significantly (***$p < 0.001$) reduced cellular cAMP levels compared with CFCF control (Figure 20).

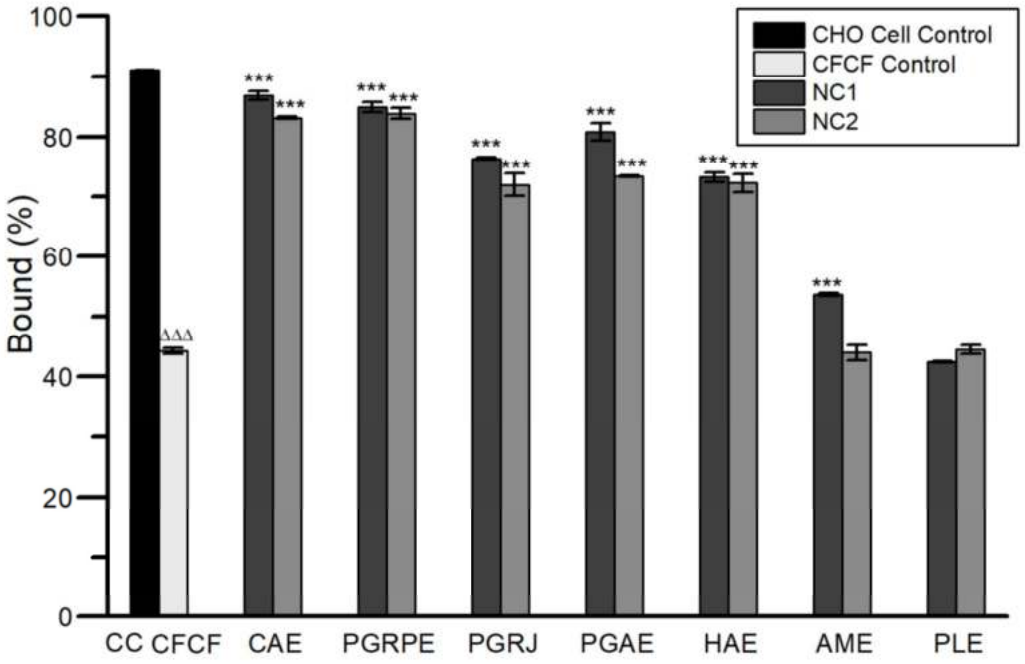

Figure 20 Effect of seven extracts on increased cAMP levels in CFCF induced CHO cell line. All values were expressed as mean ± SD, One Way Analysis of Variance (ANOVA) followed by Dunnett test. $^{\Delta\Delta\Delta}p<0.001$, compared with CHO cell control. ***$p<0.001$ compared with CFCF control.

5.4. Protective activity of seven extracts against CFCF-induced cell elongation

The protective activity of seven extracts against CFCF (CT=100 ng/mL) induced cell elongation in the CHO cell line was investigated by direct observation under phase contrast microscopy at 40X. Except for PLE, all the selected extracts showed protective activity against CFCF-induced cell elongation (Figure 21). CAE, PGRPE, and PGAE were observed to be more effective compared to the other selected extracts which were consistent with the results from the cAMP assay.

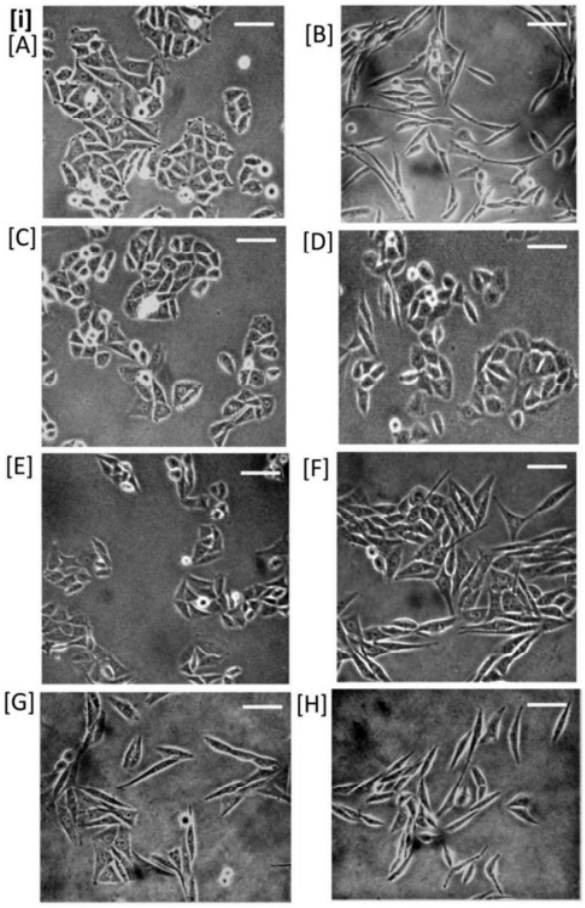

Figure 21 Protective activity of seven extracts (NC1) against CFCF-induced cell elongation. **(i)** CHO cell control (A), CHO cells treated with CFCF (CT=100ng/mL) (B), CAE+CFCE (C), PGAE+CFCE (D), PGRPE+CFCE (E), PGRJ+CFCE (F), HAE+CFCE (G), AME+CFCE (H).

6. Mining of bio-active compounds and Molecular docking

Previously reported 20 polyphenolic compounds were chosen from three plants, excluding the pervasive molecules (Table 7).

Table 7 List of 20 polyphenolic compounds selected from *C. arborea, P. granatum,* and *P. guajava* using databases and literature survey.

S. No.	Plant name	Name of the compound	PubChem ID	Classification
1.	*Punica granatum*	Catechin	9064	Flavonoid
2.	*Psidium guajava, Careya arborea, Punica granatum*	Quercetin	5280343	Flavonoid
3	*Psidium guajava, Careya arborea, Punica granatum*	Ellagic acid	5281855	Phenolic acid
4	*Punica granatum*	Chlorogenic acid	1794427	Phenolic acid
5	*Punica granatum*	Kaempferol	5280863	Flavonoid
6	*Punica granatum, Psidium guajava*	Rutin	5280805	Flavonoid
7	*Punica granatum*	Luteolin	5280445	Flavonoid
8	*Punica granatum*	Cyanidin	128861	Flavanoid
9	*Psidium guajava, Punica granatum*	Gallic acid	370	Phenolic acid
10	*Punica granatum*	Phlorizin	6072	Flavonoid
11	*Punica granatum*	Caffeic acid	689043	Phenolic acid
12	*Punica granatum*	Phellatin	44258781	Flavonoid
13	*Punica granatum*	Delphinidin 3-glucoside	443640	Flavonoid
14	*Punica granatum*	Ferulic acid	445858	Phenolic acid
15	*Psidium guajava*	Gentisic acid	3469	Phenolic acid
16	*Psidium guajava*	Procyanidin b1	11250133	Flavonoid
17	*Psidium guajava*	Procyanidin b2	122738	Flavonoid
18	*Psidium guajava*	Procyanidin b3	146798	Flavonoid
19	*Psidium guajava*	Quercitrin	5280459	Flavonoid
20	*Psidium guajava*	Eugenol	3314	Phenolic acid

The docking study reveals the stable binding of selected 20 compounds to the preferred binding site (expected to bind to the GM1 receptor) with varying binding affinity. The grid score cut off for flavonoids and phenolic acids was selected based on grid scores of standards QRTN (-37.249) and GA (-28.355) (Tables 8 and 9).

Table 8 The grid score resulted from flexible virtual screening and other energy components van der Waals (vdw), electrostatic energy (es) of 13 flavonoids docked with 1XTC (Chain F).

Pubchem CID	Compound name	Grid_Score (kcal/mol)	Grid_vdw_energy (kcal/mol)	Grid_es_energy (kcal/mol)
5280805	Rutin	-48.042801	-45.469723	-2.573079
6072	Phlorizin	-44.387592	-40.547153	-3.840439
44258781	Phellatin	-43.699451	-40.455997	-3.243455
122738	Procyanidin b2	-43.479301	-40.645905	-2.833396
11250133	Procyanidin b1	-42.414948	-39.893745	-2.521202
146798	Procyanidin b3	-40.048206	-39.379646	-0.668559
443650	Delphinidin	-38.179119	-32.950298	-5.22882
5280459	Quercetrin	-37.249252	-34.549435	-2.699819
5280343	Quercetin	-35.541042	-31.458048	-4.082994
5280863	Kaempferol	-34.439274	-30.487968	-3.951307
5280445	Luteolin	-33.997169	-29.748465	-4.248707
128861	Cyanidin	-32.527771	-27.560312	-4.967459
9064	Catechin	-31.774496	-28.145555	-3.628941

Table 9 The grid score resulted from flexible virtual screening and other energy components van der Waals (vdw), electrostatic energy (es) of 7 phenolic acids docked with 1XTC (Chain F).

Pubchem ID	Compound name	Grid_Score	Grid_vdw_energy	Grid_es_energy
1794427	Chlorogenic acid	-39.264503	-34.880714	-4.383787
5281855	Ellagic acid	-36.419472	-31.110126	-5.309345
689043	Caffiec acid	-28.51786	-23.899292	-4.618569
370	Gallic acid	-28.355522	-23.503485	-4.852037
445858	Ferulic acid	-27.67881	-22.11463	-4.24631
3469	Gentistic acid	-26.730343	-22.38484	-4.345502
3314	Eugenol	-25.38118	-22.887379	-2.4938

We have carefully analyzed the top 10 hits (including standard-gallic acid) to get more structural insights into their intermolecular interactions. All the selected 10 top hits from the flexible virtual screening show maximum binding affinity when compared to the standard GA. Table 10 represents the list of top 10 hits, their grid scores, and intermolecular interactions. The maximum number of combined H-bonding and other interactions are observed in the complex CT-Ellagic acid (10), followed by CT-Procyanidin B3 (9) and CT-Delphinidin (9).

Table 10 List of top 10 hits interacting with active site residues of 1XTC (chain F) binding to GM1 receptor using Dock6.9.

Compound name	Grid Score	Hydrogen bond interactions (No. of interactions)	Van der Waals, Pi-Alkyl, CH, Pi-Cation, Pi-Sigma, Pi-Pi stacked, Pi-Pi T-shaped interactions (No. of interactions)	Active site residues within interactions	Total no. Of interactions with active site residues
Rutin (Flavonoid)	-48.042	Asn14, Gln61, Glu51, Gln56(2)	His13	Asn14, GLN61, Glu51, Gln56, His13	6
Phlorizin (Flavonoid)	-44.3875	Asn90, Asn14, Glu51	His57, Trp88(2), Ile58	Asn90, Asn14, Glu51 Trp88, Ile58	6
Phellatin (Flavonoid)	-43.699	Glu51, Glu11, Glu56, Gln61	Trp88, His13(2)	Glu51, Glu11, Glu56, Gln61 Trp88, His13	7
Procyanidin B2 (Flavonoid)	-43.4793	His13, Gln61, Glu51, His57, Gln56	Trp88(3), Ile58	His13, Gln61, Glu51, Gln56, Trp88(3), Ile58	8
Procyanidin B1 (Flavonoid)	-42.4149	Trp88, Glu51(2), Ser55, Asn90	Trp(88)	Trp88, Glu51, Asn90	5
Procyanidin B3 (Flavonoid)	-40.0482	Gly33, Gln61, Glu51, Gln56, Glu11(2), His57	Trp88(2), Ile58	Gly33, Gln61, Glu51, Gln56, Glu11, Trp88, Ile58	9
Chlorogenic acid (Phenolic acid)	-39.2645	Gly33, Gln61, Trp88, Lys91, Gln56(3), Gln61	Nil	Gly33, Gln61, Trp88, Lys91, Gln56, Gln61	8
Delphinidin (Flavonoid)	-38.1791	His13(2), Asn90, Glu51, Gly33	Trp88(4)	His13, Asn90, Glu51, Gly33, Trp88	9
Quercetrin (Flavonoid)	-37.2493	Asn14, Gln61, Gln56	His57, Trp88	Gln61, Gln56, Trp88	3
Ellagic acid (Phenolic acid)	-36.4194	Gln61(2), Asn90(2), Glu51, Gly33, His57	Trp88(5)	Gln61, Asn90, Glu51, Gly33, Trp88	10
Gallic acid (Phenolic acid)	-28.355	Gln61(2), Asn90(2), Glu51, His57	Trp88(2)	Gln61, Asn90, Glu51, Trp88	7

7. Drug-likeness and side effects

The ADMET profile and drug-likeness of the top 10 hits are listed in Table 11**.** Phenolic acids showed a more favourable ADMET profile and drug-likeness compared to flavonoids.

Table 11 ADMET profile and drug-likeness of top 10 compounds

Compound name	LogS	LogD	LogP	[1]HIA	Caco-2	[2]PPB (%)	[3]NPL	Ames	Carcinogenicity	Lipinski rule	GSK rule
Rutin (Flavonoid)	-3.93	0.69	-0.76	0.92	-6.34	83.81	2.01	0.80	0.06	Rejected	Rejected
Phlorizin (Flavonoid)	-3.07	0.94	-0.26	0.95	-6.32	65.30	1.80	0.52	0.24	Accepted	Rejected
Phellatin (Flavonoid)	-3.67	0.95	0.58	0.82	-6.17	89.11	2.06	0.77	0.05	Rejected	Rejected
Procyanidin (Flavonoid)	-3.96	1.66	1.85	0.96	-6.77	88.71	1.93	0.27	0.03	Rejected	Rejected
Delphinidin3-glucoside (Flavonoid)	-3.09	0.59	-0.20	0.87	-6.42	85.93	2.08	0.68	0.04	Rejected	Rejected
Quercetrin (Flavonoid)	-4.03	1.59	0.82	0.53	-6.14	89.52	2.16	0.82	0.07	Rejected	Rejected
Chlorogenic acid (Phenolic acid)	-1.19	0.01	-0.16	0.87	-6.13	67.19	2.25	0.03	0.06	Accepted	Accepted
Ellagic acid (Phenolic acid)	-4.60	0.79	1.12	0.198	-5.31	78.23	0.59	0.38	0.31	Accepted	Accepted
Gallic acid (Phenolicacid)	-1.2	0.34	0.64	0.08	-5.73	53.49	0.98	0.05	0.02	Accepted	Accepted

From among the top 10 hits, we selected two phenolic acids and two flavonoids complexes with their respective standards based on their grid score and drug-likeness for further molecular dynamics simulation studies (CT-Ellagic acid, CT-Chlorogenic acid, CT-Gallic acid, CT-Rutin, CT-Phloridzin, and CT-Quercetrin).

These complexes are abbreviated as CT-EA, CT-CHL, CT-GA, CT-RTN, CT-PHD, CT-QRTN, and these abbreviations are used in the entire manuscript hereafter. The binding modes (in 3D) and their atomic level intermolecular interactions (2D) for these six selected complexes are represented in Figures 22 and 23.

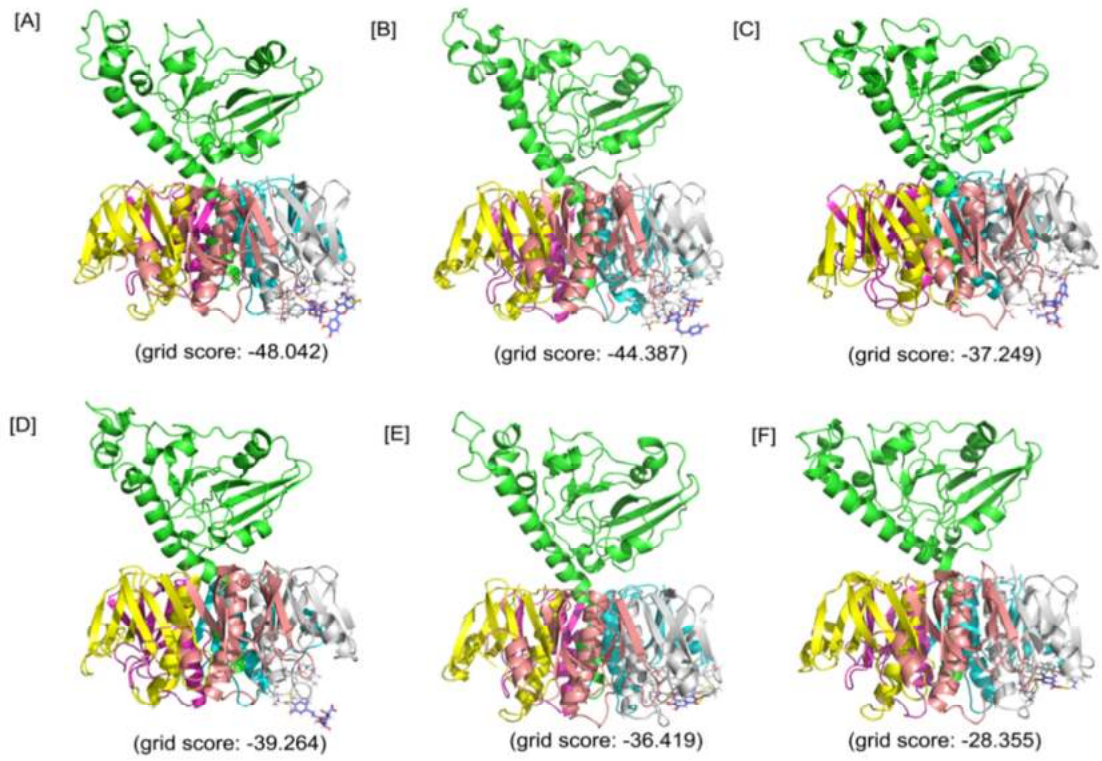

Figure 22 The 3D representation of binding mode and the interactions of the six selected compounds with 1XTC with their respective grid score. (A) CT-RTN, (B) CT-PHD, (C) CT-QRTN, (D) CT-CHL, (E) CT-EA, (F) CT-GA.

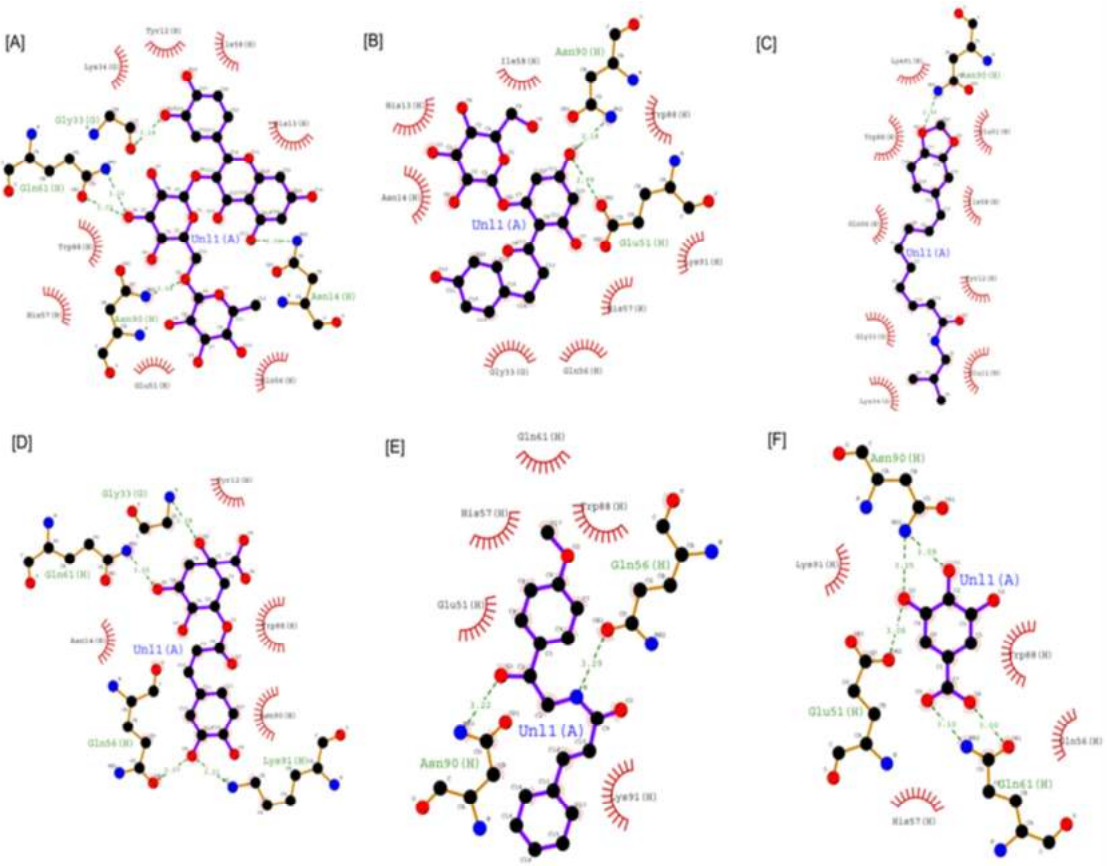

Figure 23 The 2D representation of the binding mode and atomic level intermolecular interactions of six selected compounds with 1XTC. (A) CT-RTN, (B) CT-PHD, (C) CT-QRTN), (D) CT-CHL, (E) CT-EA, (F) CT-GA.

8. MD simulations of the docked complexes

Out of the 20 studied complexes, phenolic acids and flavonoids were selected based on a number of interactions with active site residues of the GM1 binding site of CT. We have selected two phenolic acids (CT-EA, CT-CHL) and two flavonoids (CT-RTN, CT-PHD) complexes with their respective standards CT-GA acid and CT-QRTN for further molecular dynamics simulation studies.

8.1 Structural stability of the docked complexes using MD

These six complexes are used for investigating their structural stability and intermolecular interactions using molecular dynamics simulations. The quality check performed over the 100 ns trajectory generated using gromacs by analyzing the potential energy of the simulated systems and equilibration of the simulated complexes was confirmed by plotting the temperature and pressure over the MD simulation trajectory. It is observed that the temperature, pressure and potential energy of the simulated complexes are stable with no considerable fluctuations. The temperature and pressure were maintained constant at 300 K and 1 bar during the simulation in all the studied complexes (Figure 24).

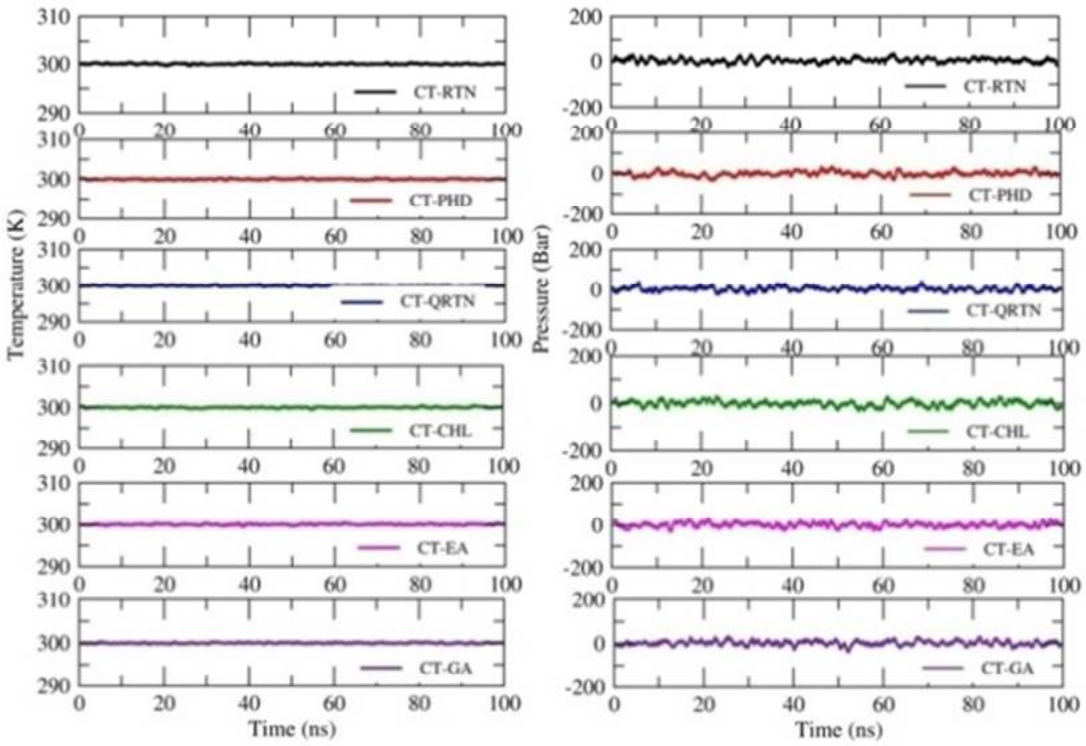

Figure 24 Temperature and pressure equilibration plot of six complexes

The average backbone RMSD value of these six complexes ranges between 1.5 and 3.5 Å. It was observed that these complexes are well equilibrated during the 0 to 60 ns of the simulation and thereafter show stable dynamics throughout the simulation period (Figure 25A). The RMSD of chain F is stabilized at a value below 2.25 Å except for the CT-GA complex, which showed a maximum RMSD value after 60 ns of simulation time (Figure 25B). The complex CT-EA and CT-PHD show the lowest RMSF values except for the flexible loop at the binding pocket region in the CT. The residues participating in the non-bonded interactions showed fewer fluctuations as their flexibility was arrested by stable intermolecular interactions (Figure 25C).

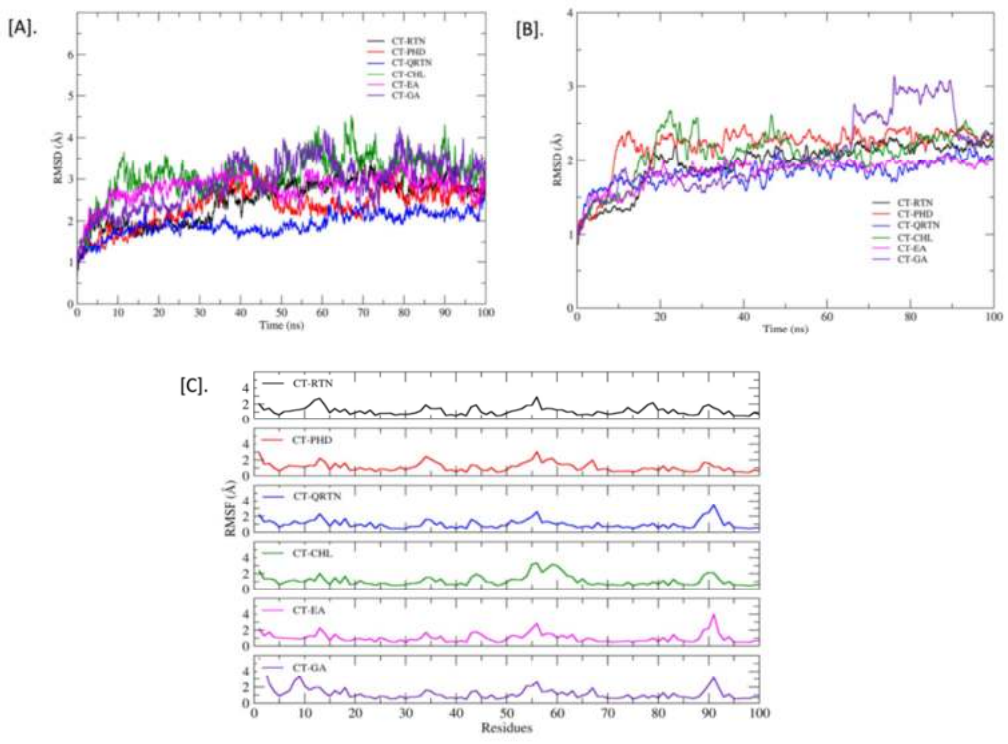

Figure 25 (A) The structural stability of the simulated complexes analysed by plotting backbone RMSD of CT-complexes (B) RMSD of chain F i.e. GM1 binding pocket (C) Residual fluctuations of GM1 binding pocket

The R*g* value, analyzed for the entire CT complex and separately for Chain F, also revealed the stable dynamics during the 100 ns simulation in all the complexes (**Fig. 5A, 5B**). A similar observation was made for solvent-accessible surface area analysis of the overall CT complex. However, variations in the SASA value of chain F (GM1 binding pocket) were observed during the simulation. The graphical representation of SASA with for CT and chain F is shown in Figure 26C and Figure 26D, respectively.

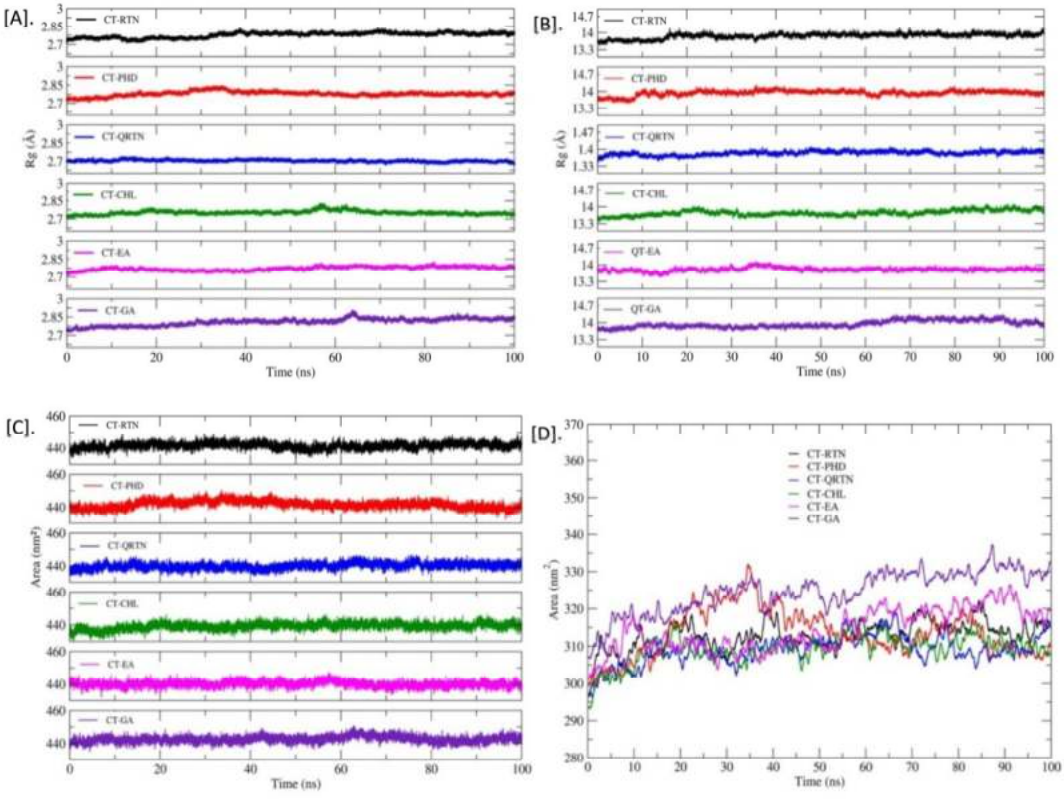

Figure 26 The compactness of the CT-complexes and chain F GM1 binding pocketis shown as (A) and (B) respectively. The hydrophobicity of CT-complexes is also quantified by analysing solvent accessible surface area for the entire CT-complex (C) as well as chain F (D).

8.2. Intermolecular interactions in docked complexes

From structural stability analysis, it is observed that docked complexes are well stabilized during the simulation. Therefore, we characterized intermolecular interactions in the initial and final MD simulation conformations. Furthermore, we also noted the intermolecular interactions precisely with the active site residues. The maximum number of H-bonds formed between CT and ligands during the MD simulations in all six complexes is shown in Figure 27**.**

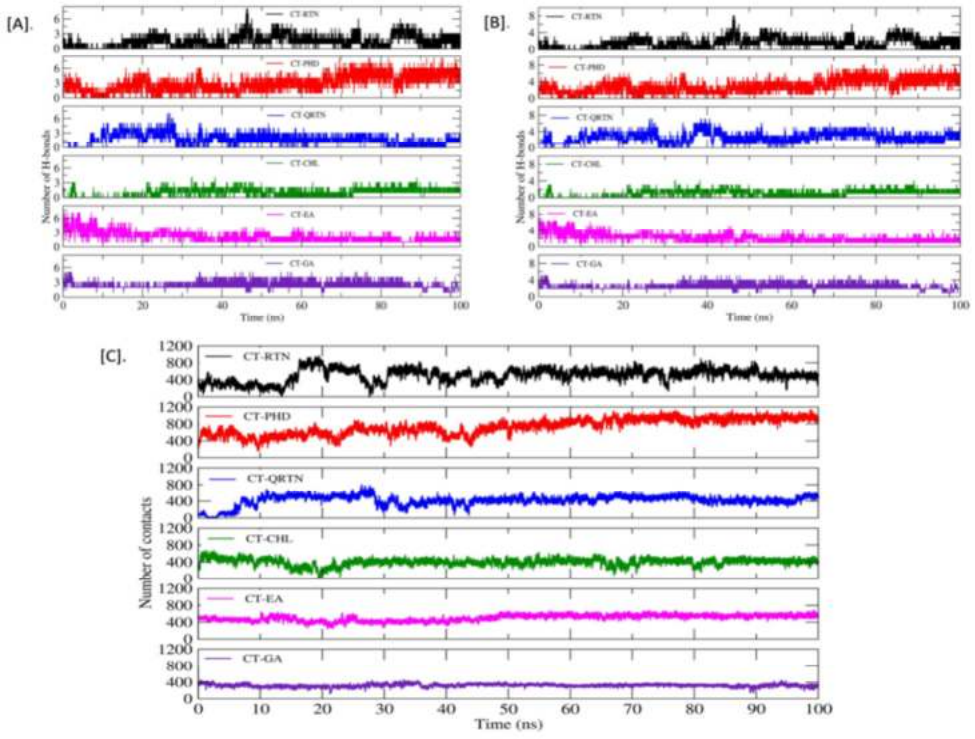

Figure 27 The maximum number of H-bonds promoting stable complex formation for all the CT-complexes are shown in A and number of H-bonding interactions between CT chain F are shown in B. The number of non-bonded contacts including hydrophobic and electrostatic interactions observed between the pentameric CT subunits and ligands are shown in C for all the complexes.

The list of all the nonbonded interactions (H-bonds, hydrophobic interactions, etc.) that trigger stable complex formation before and after simulations is given in **Table 5**. Total non-bonded interactions are increased in the complexes CT-PHD (6 to 9) and CT-QTRN (3 to 12), whereas other complexes showed a decrease in the total non-bonded interactions in initial and final MD conformations. This revealed the consistent interactions with the binding pocket residues are increased in the complexes CT-PHD and CT-QRTN, whereas in other complexes these interactions are not consistent. The initial (0 ns) and final (100 ns) snapshots of the MD simulation trajectory are shown in Figure 28.

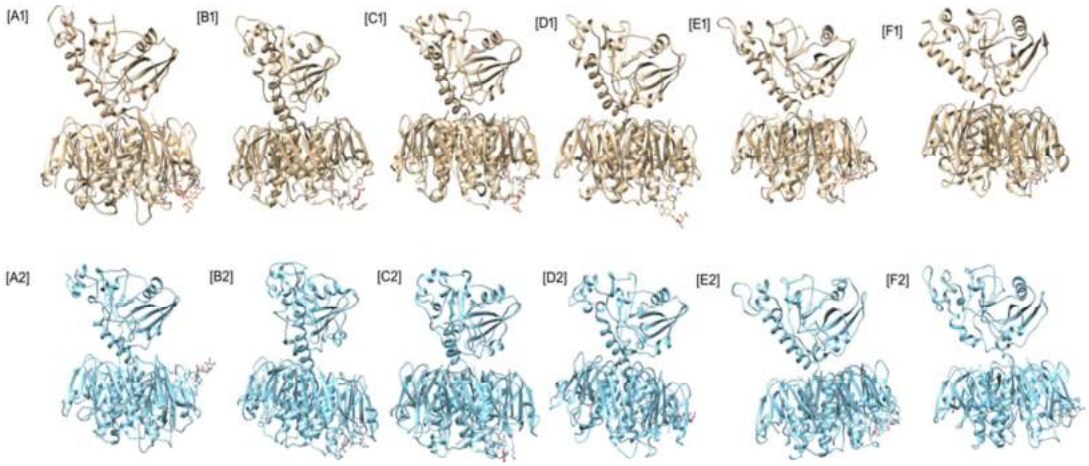

Figure 28 The MD simulation snapshots revealing the stable complex formation during the 100ns of simulation. The starting MD conformations are shown in gold (A1-F1) while MD simulation end structure (100ns) are shown in cyan (A2-F2), where A, B, C, D and E represents complexes CT-RTN, CT-PHD, CT-QRTN, CT-CHL, CT-EA and CT-GA respectively.

To gain more structural insights into these intermolecular interactions, we plotted the minimum distance between the six compounds and CT chain F (**Figure 29**). It showed the distance of CT-EA and CT-PHD is constant <2.5 Å, whereas in other complexes it showed significant fluctuations (up to 7 Å).

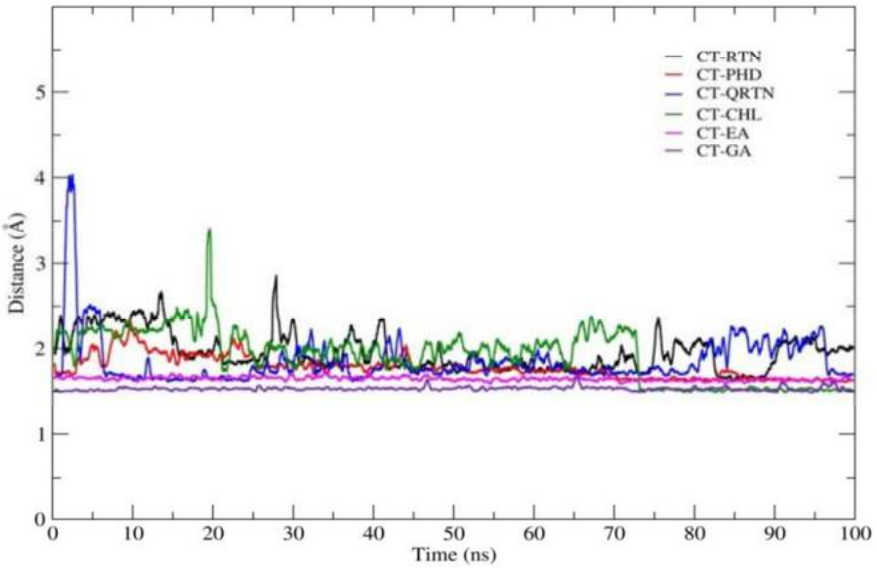

Figure 29 The variations in the minimum distance observed between the GM1 binding pocket (chain F) with the six phytochemicals during the simulation

The relative binding energy of six complexes was calculated using the MM/PBSA approach and is represented in Table 2. The order of binding free energy was observed as CT-EA > CT-CHL > CT-GA for phenolic acids and CT-PHD > CT-QRTN > CT-RTN for flavonoids. The selected polyphenolic compounds showed much higher binding affinity than their respective controls (Table 12). This highlights the potency of these compounds in the successful inhibition of CT.

Table 12 Calculation of binding free energy (in kcal/mol) of six complexes using *'gmx_MMPBSA'* tool

Complexes	ΔE_{VDW}	ΔE_{ELE}	ΔE_{GB}	ΔE_{SURF}	ΔG_{GAS}	ΔG_{SOLV}	ΔTOTAL
CT-EA	-31.86 ± 0.02	-34.04 ± 2.61	42.68 ± 0.58	-3.78 ± 0.01	-65.9 ± 2.61	38.9 ± 0.58	-27 ± 2.67
CT-CHL	-7.86 ± 0.28	-78.25 ± 4.2	62.39 ± 1.69	-2.11 ± 0.02	-86.11 ± 4.21	60.27 ± 1.69	-25.83 ± 4.54
CT-GA	-7.27 ± 0.01	-81.88 ± 1.57	67.01 ± 0.55	-2.1 ± 0	-89.15 ± 1.57	64.91 ± 0.55	-24.25 ± 1.66
CT-PHD	-33.33 ± 0.65	-76.09 ± 2.98	80.48 ± 3.16	-5.21 ± 0.06	-109.42 ± 3.05	75.27 ± 3.16	-34.16 ± 4.39
CT-QRTN	-28.5 ± 1.26	-38.14 ± 3.51	42.6 ± 1.33	-4.03 ± 0.03	-66.64 ± 3.73	38.57 ± 1.33	-28.07 ± 3.96
CT-RTN	-24.62 ± 1.18	-19.52 ± 8.84	29.71 ± 3.92	-3.31 ± 0.21	-44.14 ± 8.92	26.4 ± 3.92	-17.74 ± 9.75

E_{VDW} = van der Waals contribution; E_{ELE} = electrostatic energy; E_{GB} =electrostatic contribution to the solvation free enrgy; G_{SURF} = solvent-accessible surface area; G_{SOLV} = polar solvation free energy; TOTAL= Binding free energy.

8.3. *Secondary structural changes during simulation*

We analyzed conformational changes at the binding site over the simulation period using the DSSP tool. Figure 30 represents the distortions in the secondary structure calculated in all the complexes (A-F). The binding pocket architecture was well stabilized in complexes CT-EA and CT-PHD compared to other complexes, mainly due to the increased helical content in the chain-F.

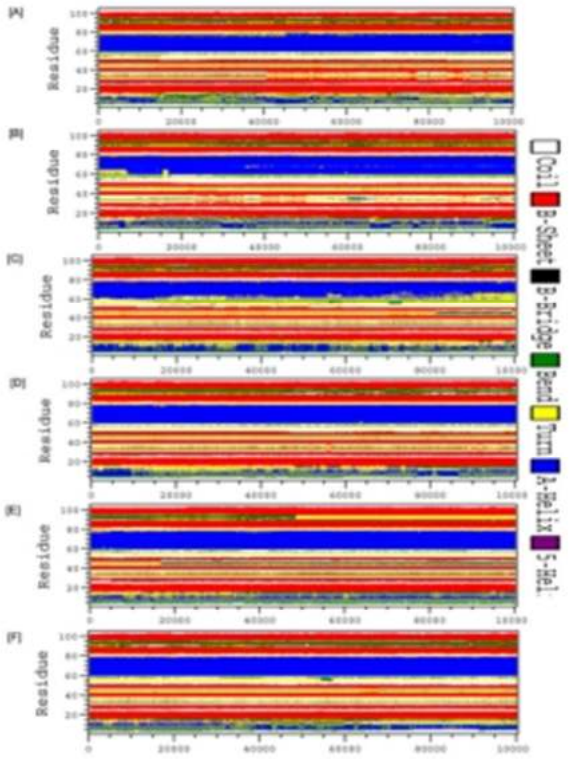

Figure 30 The distortion in the secondary structures during the 100ns MD simulation for complexes CT-RTN[A], CT-PHD[B], CT-QRTN[C], CT-CHL[D], CT-EA[E], CT-GA[F].

8.4. Contribution of the binding pocket residues in the intermolecular interactions

The residue decomposition energy calculated over the stable trajectory revealed the contribution of the individual resides in the binding energy (Figure 31). The positive contribution energy refers to the specific residue that does not favour the interactions, while the negative contribution energy refers to favourable interactions, binding pocket residues show the least binding energy. Most of the residues in complexes CT-EA, CT-PHD, and CT-CHL showed negative contribution energy. But in other studied complexes, the contribution energies varied a lot, which makes it hard for them to form stable complexes.

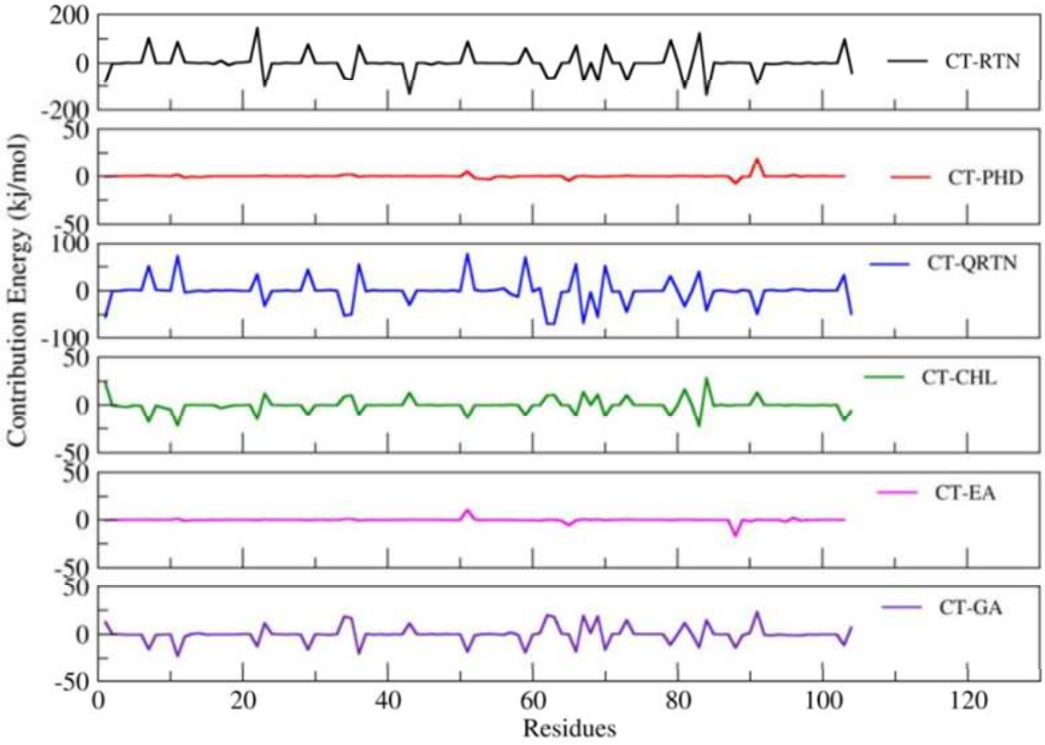

Figure 31 Per residue decomposition energy reveals the contribution of key binding site residues in the binding energy.

9. Quantification of selected polyphenols using HPTLC

Quantitative analysis of phenolics (EA, CHL, and GA) and flavonoids (RTN, PHD, and QRTN) in hydro-alcoholic extracts of *C. arborea, P. guajava,* and *P. granatum* performed using HPTLC is represented in Table 13. The HPTLC-PDA chromatogram is represented separately for phenolic acids and flavonoids in Figure 32**.**

Table 13 HPTLC analysis of six compounds in *C. arborea, P. guajava* and *P. granatum*

Compound name	*C. arborea*	*P. guajava*	*P. granatum*	Linearty
Ellagic acid	0.3 ± 0.01	0.7 ± 0.02	10.30 ± 0.76	y = 47780x - 1459.5
Chlorogenic acid	0.4 ± 0.05	0.45 ± 0.03	0.6 ± 0.02	y = 14317x - 37.442
Gallic acid	458.25 ± 26	732.4 ± 19.7	ND	y = 6610.2x + 1578.99
Rutin	ND	2.31 ± 0.15	19.70 ± 0.06	y = 7053.3x + 163.01
Phloridzin	ND	4.83 ± 1.06	ND	y = 6964.6x + 259.35
Quercetrin	ND	5.60 ± 1.5	20.60 ± 2.8	y = 8577.3x + 224.48

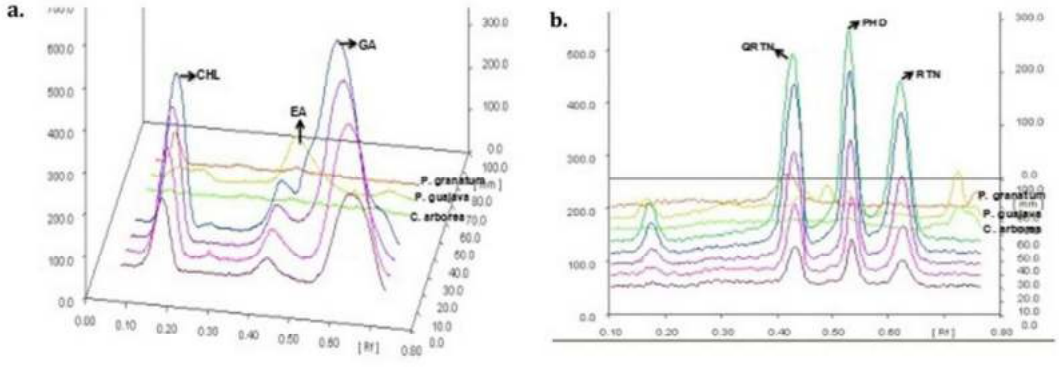

Figure 32 HPTLC-PDA chromatogram of phenolics (a) at 280nm and flavonoids (b) at 310nm in *C. arborea, P. guajava* and *P. granatum*

10. *In vitro* studies with six compounds

10.1. MTT cytotoxicity assay of six herbal compounds

Among the six selected compounds, GA was observed to be more cytotoxic to CHO cells with an IC_{50} of 102.7±1.14 µg/mL whereas CHL, with its IC_{50} value of 398.2±5.4 µg/mL, showed the least cytotoxicity (Figure 33). The MTT assay revealed that two non-cytotoxic concentrations (NC1 and NC2) of each of the six compounds showed > 90% viability on the CHO cell line. Table 14 lists the IC_{50} of six compounds along with their respective NC1 and NC2.

Table 14 The IC_{50} of six herbal compounds and their non-cytotoxic concentrations (NC1 and NC2).

Plant name	IC_{50} (µg/mL)	NC1(µg/mL)	Viability (%)	NC2 (µg/mL)	Viability (%)
Rutin (RTN)	287.4±6.9	70	92.4	35	97.6
Phloridzin (PHD)	297.9±3.9	75	94.8	37.5	97.6
Quercetrin (QRTN)	233.5±3.7	60	91	30	96.3
Chlorogenicacid (CHL)	398.2±5.4	100	90.5	50	97.2
Ellagic acid (EA)	115.5±9.6	30	93.2	15	97.5
Gallic acid (GA)	102.7±1.1	25	93.5	12.5	97.9

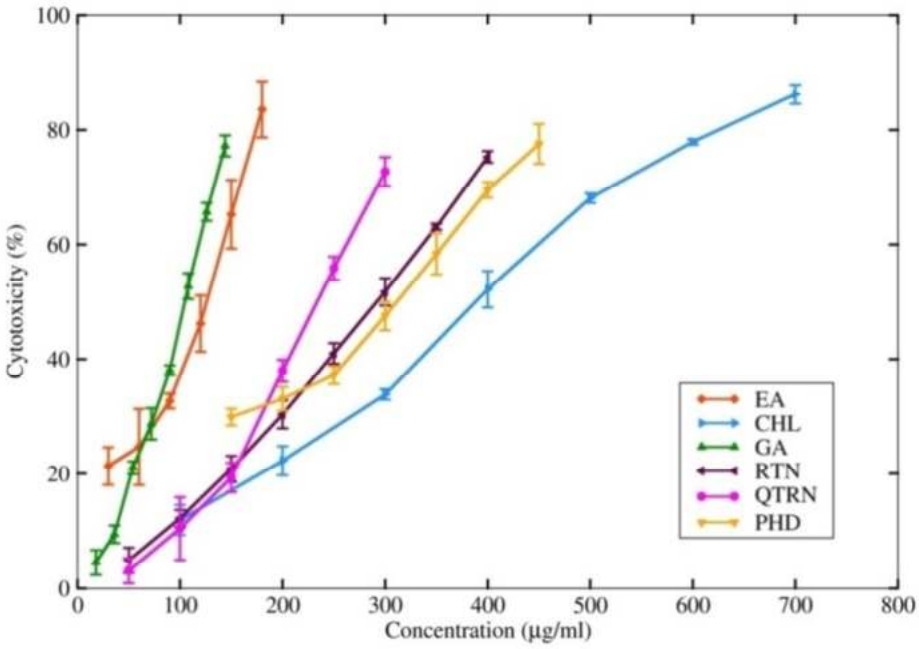

Figure 33 IC_{50} of six herbal compounds determined by MTT assay on CHO cell line

10.2. Binding inhibition percentage of CT to ganglioside GM1 in presence of six compounds

Using the CT standard curve, the average concentration of CT in CFCF was calculated as 19.78±0.52 µg/mL. The maximum absorbance shown by the highest dilution of CFCF with a CT concentration of 1600 ng/mL indicated the saturation of GM1 with CT. The selected six compounds (NC1 and NC2) were pre-incubated with CFCF titre with a CT concentration of 1600 ng/mL and binding inhibition percentage (BI%) was evaluated using GM1 ELISA. Phenolic acids, EA, and CHL showed distinct activity against CT binding to GM1 compared to the standard GA, whereas, among flavonoids, PHD showed higher BI% (Figure 34).

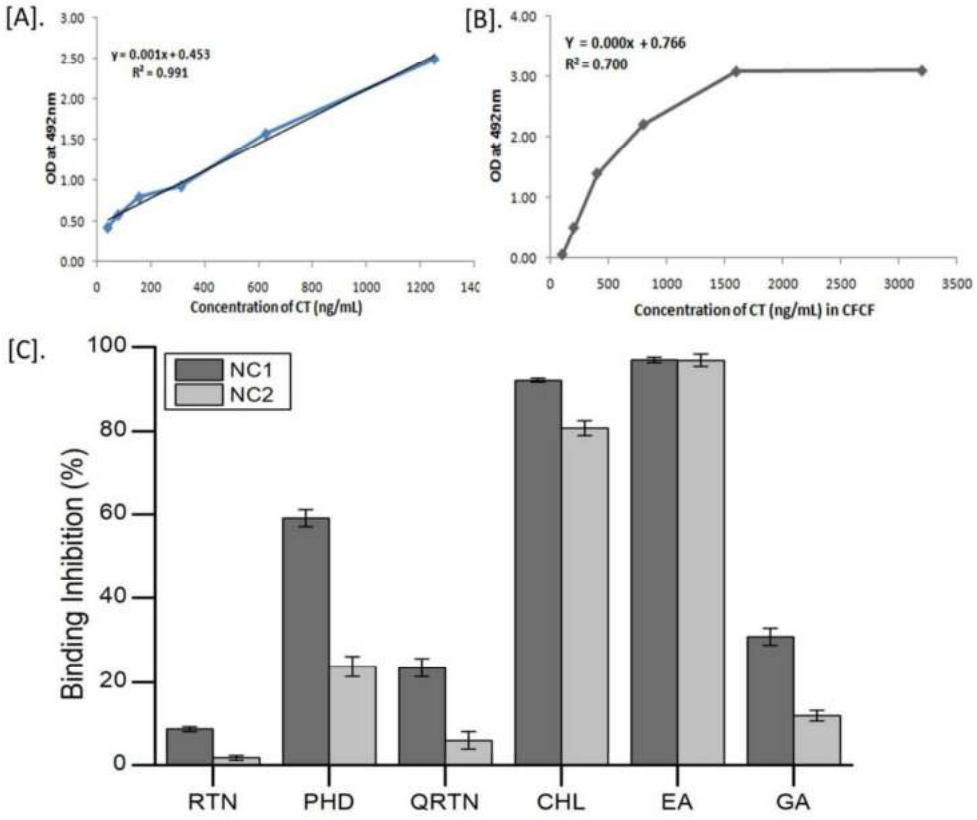

Figure 34 Binding inhibition percentage (BI%) of six herbal compounds to GM1.

(A) CT calibration curve; (B) CFCF absorbance curve; (C) BI% of three phenolic acids (CHL, EA, GA) and three flavonoids (RTN, PHD, QRTN) to GM1 at their respective non-cytotoxic concentrations (NC1 and NC2) using GM1 ELISA.

10.3. Inhibitory activity of six compounds against CFCF-induced elevated cAMP levels

The elevation of cAMP levels in the CHO cell lines was determined as the bound percent (B%) of cAMP using competitive ELISA (cellular cAMP levels are inversely proportional to B%) following kit instructions. Significant reduction in cAMP levels (***p<0.001) was observed for all three phenolic acids compared with CFCF control at both NC1 and NC2, whereas flavonoids showed a significant reduction in cellular cAMP levels (***p<0.001) at NC1 only (Figure 35)

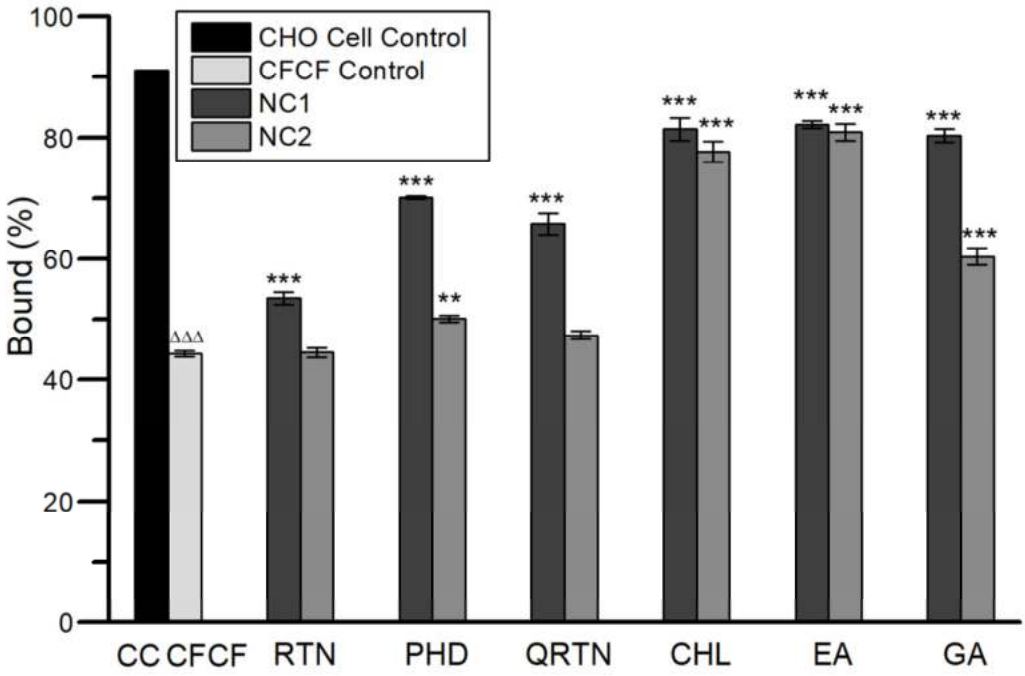

Figure 35 Efficacy of six herbal compounds against elevated cAMP levels in CHO cell line. $^{\Delta\Delta\Delta}p<0.001$ compared with CHO cell control. ***$p<0.001$ compared with CFCF control.

10.4. Protective activity of six compounds against CFCF-induced cell elongation

The protective activity of phenolic acids and flavonoids against CFCF (CT=100 ng/ml) induced cell elongation was investigated by phase contrast microscopy. All the selected compounds, excluding RTN, showed protection against CT-induced cell elongation at both NC1 and NC2. Further, EA and CHL showed greater protective activities among the selected six compounds (Figure 36).

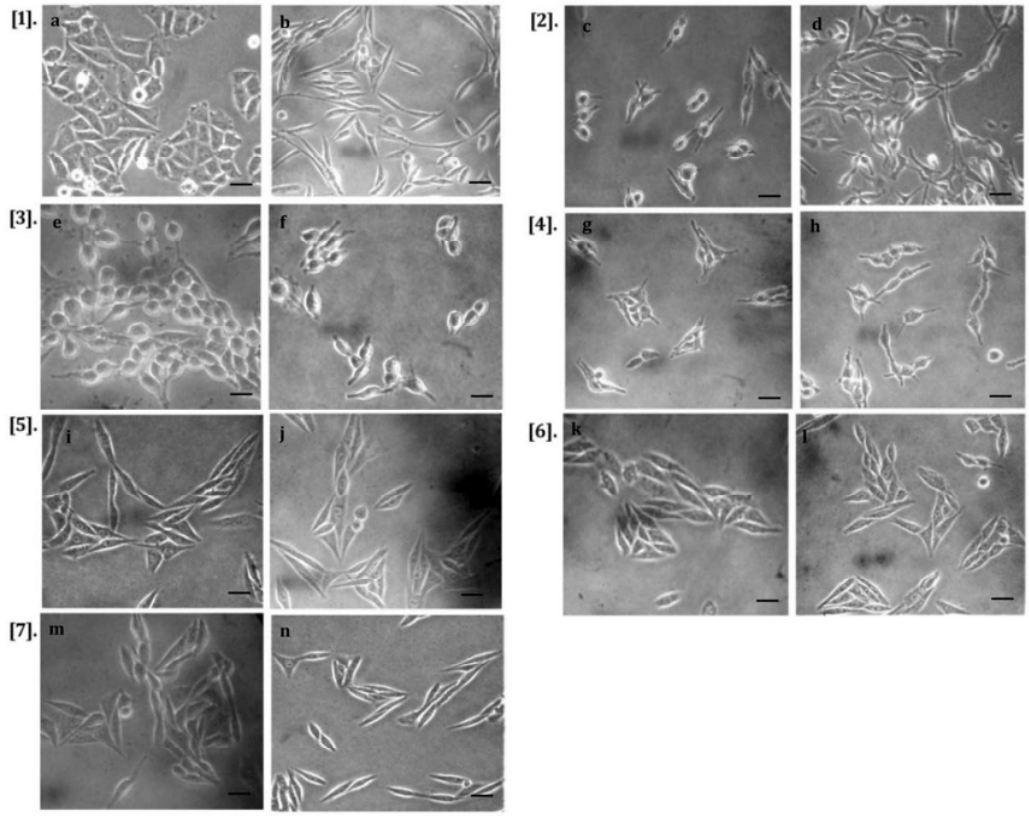

Figure 36 Protective activity against CT-induced cell elongation in CHO cell line. [1] a. CHO cell control, b. CFCF control (CT=100ng/mL); [2] c. RTN (NC1)+CFCF, d. RTN (NC2)+CFCF; [3] e. PHD (NC1)+CFCF, f. PHD (NC2)+CFCF; [4] g. QRTN (NC1)+CFCF, h. QRTN (NC2)+CFCF; [5] i. EA (NC1)+CFCF, j. EA (NC2)+CFCF; [6] k. CHL (NC1)+CFCF, l. CHL (NC2)+CFCF; [7] m. GA (NC1)+CFCF, n. GA (NC2)+CFCF at 40X magnification (scale bar 5µm).

11. *In vivo* studies

Based on results from *in vitro* studies, three plant extracts CAE, PGRPE, PGAE and two phenolic acids, EA and CHL showed efficient inhibitory activity against CT. All these three extracts along with the standard GA were further analyzed *in vivo* using adult mice ileal-ligated loop model.

11.1. *CFCF-induced fluid accumulation in ligated-ileal loops*

Initially, we determined the amount of fluid accumulated in ligated ileal loops of 2-3 cm in length of adult Swiss albino mice by instilling CFCF containing 1µg of Cholera toxin following the incubation period of 18 hrs. The mean weight/length ratio of CFCF-treated ileal loops was determined as 0.249 g/cm ± 0.02 whereas that of untreated ileal loops instilled with PBS was 0.078 g/cm ± 0.01. It was observed that the mice ileal loops treated with CFCF containing 1µg of CT caused prominent intestinal fluid accumulation after 18 hrs of incubation period showing the diarrhegenic potential of CFCF.

The test groups categorized into 12 groups (n=12) were treated with a pre-incubated mixture containing two concentrations (100µg and 50µg) of each of three extracts – CAE, PGRPE, PGAE and CFCF (CT=1µg) and each of the three phenolic acids EA, CHL and GA at two variable concentrations (50 µg and 25 µg) into each ligated loop. Among the three selected extracts, a significant reduction in intestinal fluid accumulation in test groups expressed as $*P < 0.001$ was observed for CAE (0.091 g/cm, 0.184 g/cm) and PGRPE (0.080 g/cm, 0.190 g/cm) at 100 µg and 50 µg respectively. PGAE (0.150 g/cm) showed a significant reduction ($*P < 0.001$) in fluid accumulation at 100 µg concentration only (Figure 37(i), (ii)). Both EA (0.091g/cm and 0.094 g/cm) and CHL (0.132 g/cm, 0.176 g/cm) showed a significant decrease *(***p<0.001)* in mean W/L ratio at 50 ug and 25 µg respectively, whereas standard GA (0.188 g/cm) showed a significant reduction (***p<0.01)* at 50 ug in fluid accumulation compared to CFCF control (Figure 37(iii), (iv)).

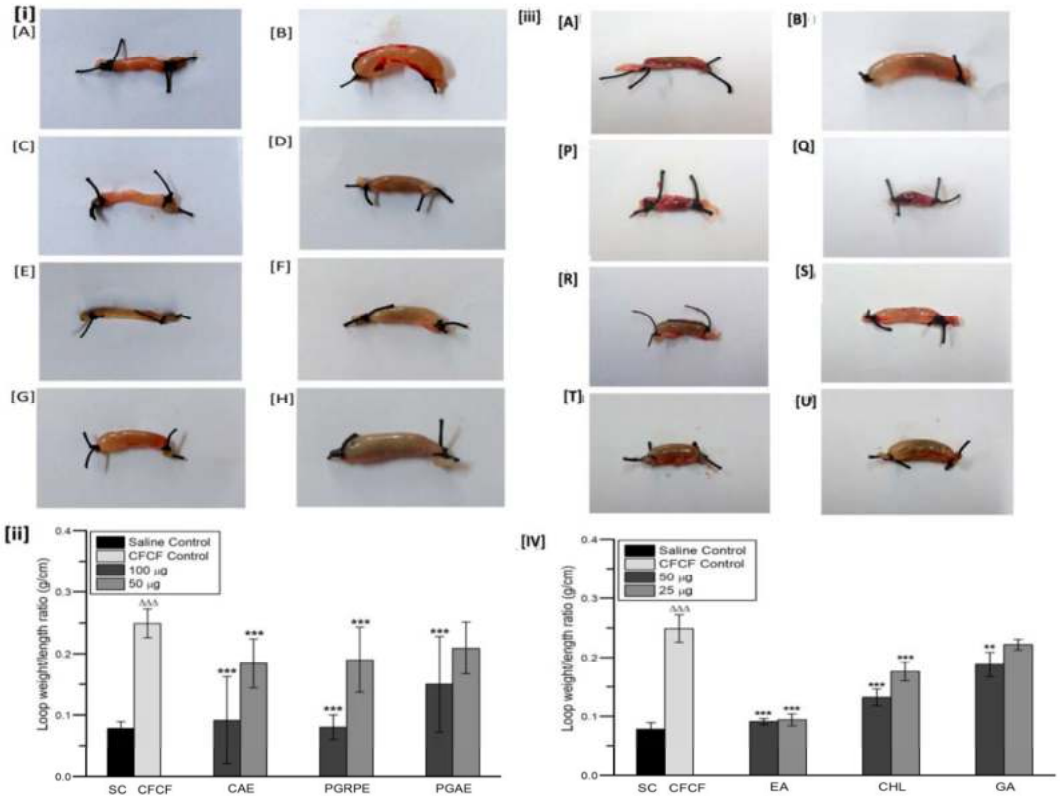

Figure 37 Inhibitory activity of plant extracts and phenolic acids against CFCF induced fluid accumulation.

[i]. [A] Saline control (100µl PBS), [B] CFCF control(CT=1µg/loop), [C] CAE(100µg)+CFCF, [D] CAE(50µg)+CFCF, [E] PGRPE(100µg)+CFCF, [F] PGRPE(50µg)+CFCF, [G] PGAE(100µg)+CFCF, [H] PGAE(50µg)+CFCF. [iii]. [A] Saline control (100µl PBS), [B] CFCF control (CT=1µg/loop), [P] EA (50µg)+CFCF, [Q] EA (25µg)+CFCF, [R] CHL(50µg)+CFCF, [S] CHL (25µg)+CFCF, [T] GA (50µg)+CFCF, [U] GA (25µg)+CFCF.

[ii], [iv] Weight/length ratio of mice ligated-ileal loops; All values were expressed as mean ± SEM (n=6) One Way Analysis of Variance (ANOVA) followed by Dunnett

test. $^{\Delta\Delta\Delta}p<0.001$, compared with saline control. ***p<0.001 compared with CFCF control.

11.2. CFCF-induced cellular cAMP levels in ligated-ileal loops

Cellular cAMP levels in ligated-ileal tissues were estimated as an increase in bound percent (B%) using competitive ELISA. When compared to the Saline control group, there was a significant increase in cAMP levels in the CFCF control ($^{\Delta\Delta\Delta}p$<0.001). CAE, PGRPE, and PGAE inhibited CFCF-induced cAMP levels in ileal tissues significantly (***p<0.001) at 100 µg and 50 µg, as evidenced by their reduction in cellular cAMP levels (Figure 38[A]). All three selected phenolic acids also showed significant reduction *(***p<0.001) in* CFCF-induced elevation of cAMP levels in ileal tissues at both concentrations (50 µg and 25 µg) (Figure 38 [B]).

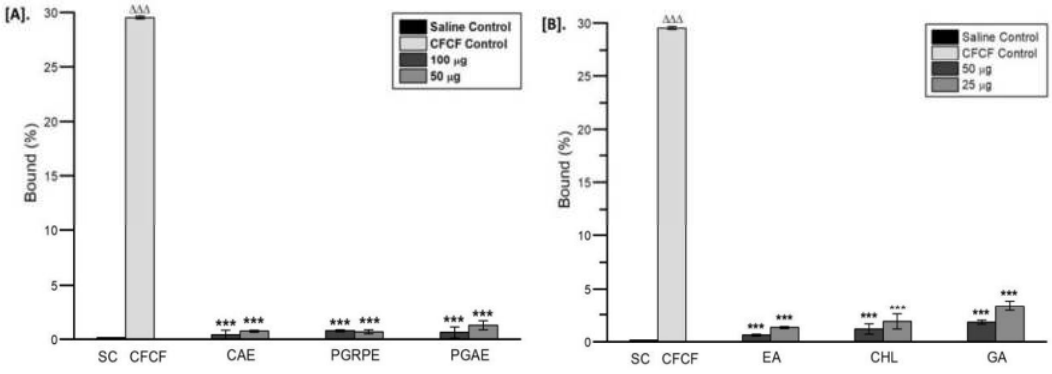

Figure 38 Cellular cAMP levels in ligated-ileal tissues

All values were expressed as mean ± SD, One Way Analysis of Variance (ANOVA) followed by Dunnett test. $^{\Delta\Delta\Delta}p<0.001$, compared with Saline control. ***$p<0.001$ compared with CFCF control.

11.3. *Histopathology*

Histological examination of CFCF-treated ileal loops revealed significant changes in intestinal tissues when compared to the Saline control group. After 18 hrs of CFCF administration into ligated-ileal loops, there was prominent inflammatory cellular infiltration in the submucosa (green arrows, Figure 8.2c), as well as further mucosal layer degeneration and diffused edema in the intestinal villi (red arrows, Figure 8.2d). The morphology of the mucosal and submucosal layers was normal in the Saline control group. Among the three plant extracts, 100 µg of CAE and PGRPE greatly reduced the histopathological changes induced by CFCF in mice ileal loops as indicated by the decreased infiltration of inflammatory cells and edema. Among the three selected phenolic compounds, 50 ug of EA and CHL showed substantial protective activity against CFCF-induced histopathological changes as evidenced by decreased inflammation and edema in the intestinal tissues (Figure 39). However, indistinct amelioration in histopathological changes was observed for the standard GA compared to CFCF control.

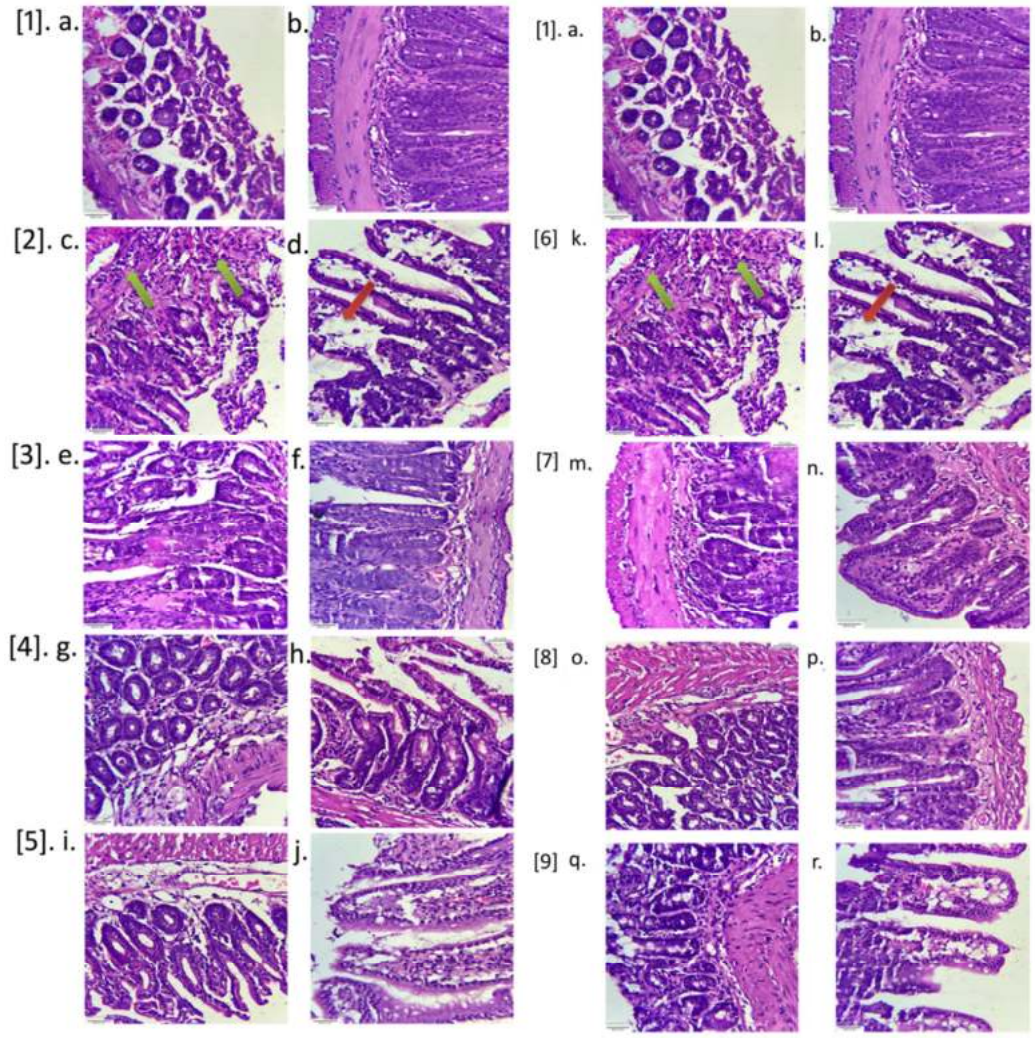

Figure 39 Histopathological analysis of mice ileal loops

Intestinal tissues of mice ileal sections stained with hematoxylin, eosin and observed at 40X magnication (scale bar=30µm). Green arrows represent inflammation in submucosa; red arrows represent mucosal layer degeneration and diffused edema.

[1a,b] Saline control; [2c,d; 6k,l] CFCF control (CT=1µg); [3e,f] CAE (100µg)+CFCF (CT=1µg); [4g,h] PGRPE(100µg)+CFCF(CT=1µg); [5i,j] PGAE(100µg)+CFCF (CT=1µg) [1a,b] Saline control; [2c,d] CFCF control; [7m,n] EA+CFCF; [8o,p] CHL+CFCF; [9q,r] GA+CFCF.

Other outcomes of the study

CFCF of a selected clinical isolate of *V. cholerae* contains non-membrane damaging cytotoxin (NMDCY) along with Cholera toxin. When CFCF was treated with CHO cell line, we observed different morphology in CHO cells unlike cell elongation induced by CT on CHO cells. CHO cells when treated with increasing concentration of CFCF showed cell rounding and further cell death without accompanying membrane damage. From the literature review, there were earlier reports about NMDCY which causes dramatic cytotoxic effects characterized by cell rounding observed in CHO and HeLa cell lines and eventually cell death without accompanying membrane damage [151]. It is also shown to possess enterotoxigenic potential as it causes non-haemolytic fluid accumulation in rabbit ileal loops. It is also the main cause of diarrhea in non-toxigenic clinical strains of non-O1 and non-O139 *V. cholerae* [152] as well as in residual diarrhea elicited in OCV (oral cholera vaccines) individuals [153].

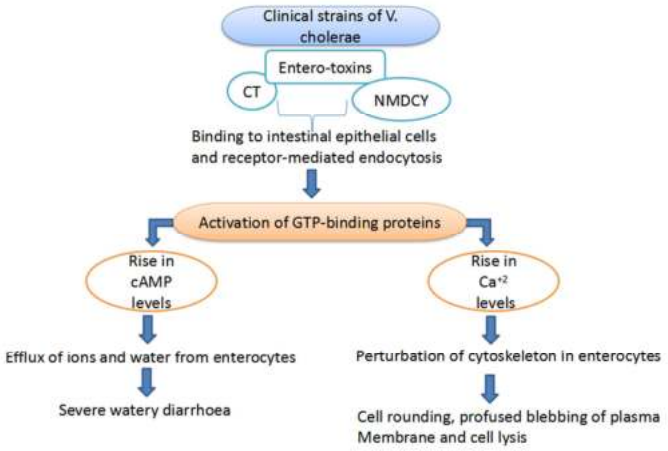

Figure 40 Flow chart depicting the mechanism of action of CT and NMDCY

There are reports which stipulated the secretion of NMDCY by both O1, O139, and non-O1, O139 serogroups of *V. cholerae.* The percentage positivity of NMDCY was determined to be 81.3% in the case of clinical O1 strains [151] underlining the relevance of this secretogenic protein in cholera pathogenesis which augmented our interest to study the inhibitory activity of selected plants against this cytotoxin also.

1. Inhibitory activity of plant extracts against NMDCY-induced cytotoxicity in CHO cell line

The cytotoxicity in NMDCY-induced CHO cell line was analysed was estimated using MTT assay. Briefly CHO cells were seeded at $6x10^4$ in 12-well plate culture dishes in DMEM supplemented with 10% FBS and incubated for 24 hrs at 5% CO_2 and 37°C. Then the cells were washed and treated with equal volumes of twofold serial dilutions of non-concentrated CFCF in the same media. Untreated cells and cells treated with AK1 media were taken as cell control and solvent control respectively. The total volume in each well was made to 200 µL with DMEM supplemented with 2% FBS and incubated for 24 hrs. After 24 hrs, cells were washed with PBS and treated with 20 µL of 0.5% MTT solution in PBS and incubated for 4 hrs. The formazan crystals formed after 4 hrs was solubilised by adding 100 µL of DMSO. The absorbance was recorded at 570 nm and cytotoxicity percentage was calculated.

In the succeeding experiment, the two non-cytotoxic concentrations (NC1 and NC2) of all seven plant extracts were pre-incubated with IC_{50} titre of CFCF for 4 hrs at 120 rpm at 37°C and treated with CHO cells for 24 hrs. Untreated cells served as

cell control and CHO cells treated with CFCF was used as CFCF control. MTT assay was performed as previously described and the inhibitory activity of seven extracts against CFCF induced cytotoxicity was expressed as viability percentage.

$$\text{Viability percentage} = \frac{A\ test}{A\ cell\ control} \times 100$$

CFCF at its 16-fold dilution produced 50% viability in the CHO cell line using MTT assay and is considered as IC_{50} titre of CFCF (Figure). In the subsequent experiment, when CHO cells were treated with a pre-incubated mixture comprising of NC1 and NC2 of each of seven extracts and IC_{50} titre of CFCF, a significant increase in cell viability% (***p<0.001) was observed for CAE, PGRPE, and PGAE compared with CFCF control.

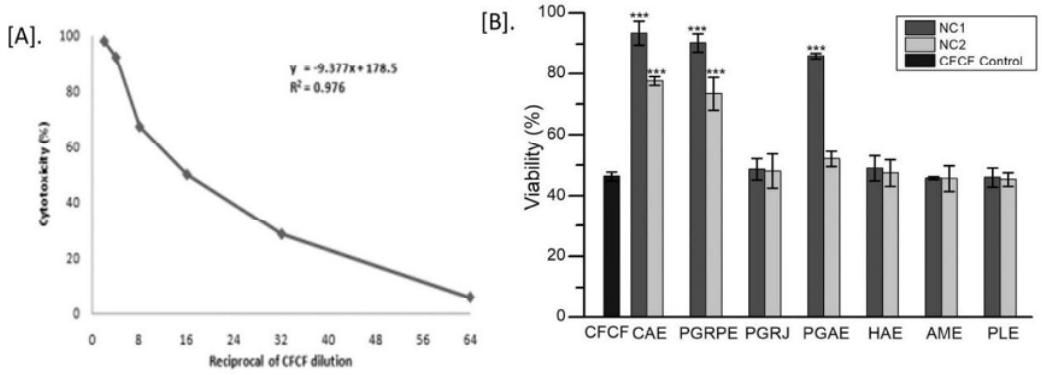

Figure 41 IC_{50} of CFCF on CHO cell line using MTT assay [A]. Viability percentage in CFCF treated CHO cell line [B]. All values are expressed as a mean ± SD (n=3), One Way Analysis of Variance (ANOVA) followed by Dunnett test, ***p<0.001 compared with CFCF control.

2. Inhibitory activity of plant extracts against NMDCY-induced morphological alterations in CHO cell line

The morphological changes in the NMDCY-induced CHO cell line were analyzed as described with slight modifications [154] by direct observation with an inverted phase-contrast microscope. Briefly, CHO cells were seeded at $6x10^4$ in 12-well plate culture dishes in DMEM supplemented with 10% FBS and incubated for 24 hrs at 5% CO_2 and 37°C. The cells were washed and treated with equal volumes of twofold serial dilutions of CFCF in DMEM media with 2% FBS. After 24 hrs of incubation at 37°C and 5% CO_2, cells were observed under a phase contrast microscope at 40X magnification. CHO cells were also treated with similar dilutions of AK1 media as a negative control. The reciprocal of the highest dilution of CFCF at which 100% of CHO cells showed two levels of morphological changes i. e. cell-rounding and cell death induced by NMDCY was quantified and taken as 100% tissue culture infective dose ($TCID_{100}$). The NC1 and NC2 of each of the seven extracts is treated with $TCID_{100}$ of CFCF producing two different morphological alterations and incubated on a shaker at 120 rpm for 4 hrs at 37°C. This CFCF pre-incubated with the extracts was then treated with CHO cells seeded at $6x10^4$ in a 12-well plate in duplicates; cells treated with only CFCF served as positive control and untreated cells as cell control.

The cells were then incubated at 5% CO_2 and 37°C for 24 hrs after which the media was discarded and cells were washed. The cells were replenished with fresh media, observed for morphological changes under the microscope and photographed at 40X magnification. Among the selected seven extracts, three plant extracts *viz.*

CAE, PGRPE, and PGAE showed effective protective activity against NMDCY-induced cell rounding [Figure 5.ii(I) to ii(L)] and cell death [Figure 5 iii(M) to iii(P)] compared with CFCF control.

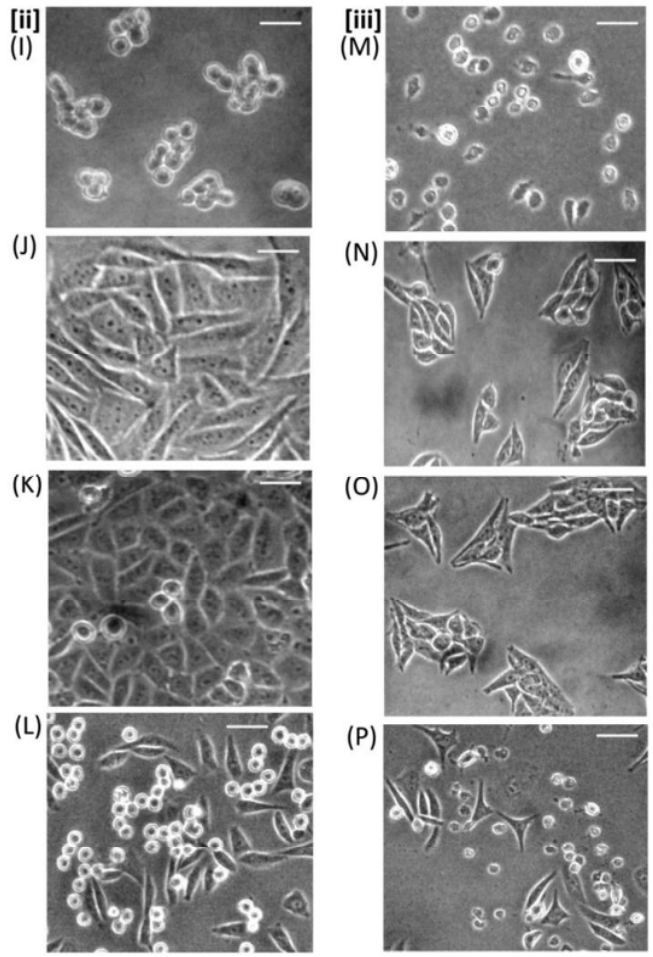

Figure 42 Protective activity of seven extracts (NC1) against NMDCY-morphological alterations. **(ii)** CHO cell control treated with CFCF $TCID_{100}$ for cell rounding (CFCR) (I), CAE+CFCR (J), PGRPE+CFCR (K), PGAE+CFCR (L). **(iii)** CHO cells control treated with CFCF $TCID_{100}$ for cell death (CFCD) (M), CAE+CFCD (N), PGRPE+CFCD (O), PGAE+CFCD (P) using phase contrast microscopy at 40X magnification (scale bar-5µm).

DISCUSSION

Our current research validates the traditional use of six plants and their bio-active compounds in counteracting CT which is the major virulent factor in cholera pathogenesis using *in silico*, *in vitro,* and *in vivo* approaches. Initially *in vitro* studies were performed with CFCF which includes binding of CT in CFCF to GM1 receptor using GM1 ELISA and estimation of CT concentration in CFCF followed by cytotoxic effects and elevation of cyclic AMP levels in CFCF treated CHO cells. The protective activity of seven extracts against CFCF-induced morphological alterations was analyzed by treating CHO cells with $TCID_{100}$ of CFCF. The results from *in vitro* studies showed the promising inhibitory activity of three plant extracts i.e. CAE, PGRPE, and PGAE against CFCF. Among the 20 screened polyphenolic compounds from these three plants, two phenolic acids (EA, CHL) and two flavonoids (RTN, PHD) along with their respective standards (GA and QRTN) were selected using computational tools based on their interaction with active site residues of GM1 binding site of CT. The presence of these compounds in selected plants was investigated using HPTLC. All the selected herbal compounds along with respective standards were analyzed for inhibitory activity against CT using GM1 ELISA and cAMP assay. Phenolic acids, EA and CHL exhibited effective neutralizing activity against CT compared to standards GA and QRTN. These two compounds along with CAE, PGRPE and PGAE that showed prominent activity against CT from *in vitro* studies were further studied using adult mice ligated-ileal loop model.

1. Production of CT and NMDCY into CFCF of *V. cholerae*

This study utilized the cell-free culture filtrate of O1 El Tor Ogawa *V. cholerae* isolated from clinical samples during cholera outbreaks in Karnataka, India [127,128] for both *in vitro* as well as *in vivo* studies. It has been well reported that O1 El Tor Ogawa strain of *V. cholerae* produces Cholera toxin [155], Non-membrane damaging cytotoxin [154] into culture supernatant along with other toxins such as Accessory Cholera toxin [50], Zonula occludens toxin [51], Multifunction autoprocessing repeats-in-toxin [54], Haemolysin [57] which are responsible for the pathogenesis of *V. cholerae*. It was reported in earlier studies that both CT and NMDCY are efficiently secreted by the bacterium in AK1 media [132,133]. The clinical strain of *V. cholerae* used in the current study when grown in AK1 media produced both CT and NMDCY into the culture filtrate.

2. Estimation of CT in CFCF

The concentration of CT in CFCF was estimated as 18.76 µg/mL ± 0.2 using GM1 ELISA whereas NMDCY showed IC_{50} on CHO cell line at 16-fold dilution of CFCF by MTT assay. Both CT and NMDCY produce cytotoxic effects on the CHO cell line; CT induces elevation of cAMP levels and alters the cell morphology in the CHO cell line. Cell elongation observed in CFCF-treated CHO cells is the distinctive effect of CT secreted into CFCF by the bacterium. This elongation morphology observed in CHO cells treated with CT is due to elevated levels of cAMP caused by permanent ADP-ribosylation of $G_{s\alpha}$ and activation of adenylate cyclase which continuously stimulates the production of cAMP [5]. It was observed that 100 ng/mL of CT in CFCF caused cell elongation and a significant increase in cellular cAMP levels in the CHO cell line; an earlier study by Saha et al., (2013)[138] also reported similar results.

3. Estimation of NMDCY in CFCF using cell based assays

NMDCY secreted into CFCF produced cell rounding and cell death in the CHO cell line as reported in a similar study by Saha et al., (1996) [154]. The morphological changes observed in CFCF-treated CHO cells in our study showed a close resemblance with that of NMDCY-induced cellular intoxication observed in CHO and HeLa cells. Evidently, with a further increase in concentration of CFCF, CHO cells switched from cell rounding to cell death without accompanying the membrane damage as observed under the phase contrast microscope. Cell death is caused by a cascade of events that includes major alterations in cellular synthetic, secretory, cell cycle-dependent functions during the earlier phase of NMDCY intoxication and disorganization of cytoskeleton at the later phase [151]. The assay for cytotoxic activity of NMDCY on CHO cell line producing cell rounding and cell death was performed using 100% tissue culture infective dose ($TCID_{100}$) and direct observation under phase contrast microscope as reported in previous study [152]. $TCID_{100}$ was estimated as the reciprocal of the highest dilution of CFCF producing a 100% cytotoxic effect on CHO cell line. The present study showed 100% cell rounding and cell death in the CHO cell line at 8-fold and 2-fold dilutions of CFCF respectively, while the earlier study by Saha [152] showed 100% cell rounding at 16-fold dilutions of CFCF.

4. *In vitro* studies with seven plant extracts

Seven extracts from six plants (*A. marmelos, P. guajava, H. antidysenterica, C. arborea, P. granatum, and P. longum*) were selected based on their traditional use and reported anti-diarrheal activity. Their efficacy against CFCF-induced cellular toxicities was investigated using their non-cytotoxic concentration (NC1 and NC2)

that showed >90% cell viability on the CHO cell line. The initial and crucial step in CT intoxication involves binding of its B subunit to the GM1 receptor on intestinal epithelial cells through which CT is transported retrograde into cytosol [156]. A subunit of CT that accesses the cytosol of enterocyte has ADP-ribosyl transferase activity and catalyzes the permanent ADP-ribosylation of $G_{s\alpha}$. This results in continuous stimulation of adenylate cyclase and a rise in cellular cAMP levels. Elevated cAMP levels in host cell activate cystic fibrosis transmembrane conductance regulator (CFTR) causing a dramatic efflux of ions and water from infected enterocytes leading to diarrhea [157].

4.1. Binding inhibition percentage of seven plant extracts

As CT binds with ganglioside GM1 with high affinity and specificity, we investigated the inhibition of CT binding to GM1 (BI%) by seven extracts using GM1 ELISA. Among these six plants, *A. marmelos* fruits and *P. guajava* leaves showed 55% and 40% binding percentage of CT to GM1 with 10% of their respective decoctions in an earlier study [7,8]. In our study, hydroalcoholic extracts of *A. marmelos* and *P. guajava* showed 55% and 48% binding inhibition of CT to GM1 at NC1 respectively. However, no previous reports were found for other plants. The BI% of the other four plants was estimated as CAE (94%, 88%), PGRPE (99%, 91%), PGRJ (97%, 97%), HAE (92%, 81%), PLE (31%, 19%) at NC1 and NC2 respectively. The results from GM1 ELISA explain that excluding PLE all other extracts exhibited anti-CT activity by inhibiting the binding of CT to the GM1 receptor.

4.2. Protective activity of seven extracts against CFCF-induced elevated cAMP levels

Elevation of cyclic AMP levels is the chief attribute of CT toxicity. Using competitive cAMP ELISA, the efficacy of seven extracts against CT-induced elevation of cAMP in CHO cell line was evaluated as an increase in bound percent (B%) of cAMP. From selected seven, five extracts showed a significant increase ($p<0.001$) in B% i.e. CAE (87%, 83%), PGRPE (85%, 84%), PGRJ (76%, 72%), PGAE (81%, 73%), and HAE (73%, 72%) at NC1 and NC2 respectively compared with CFCF control (44%). The results from the cyclic AMP assay were correlated with the protective activity of seven extracts against CT-induced cell elongation in CHO cell line. The protection against CT-induced cell elongation in CHO cells was observed to be prominent in the presence of CAE, PGRPE, PGRJ, PGAE, HAE, and AME which were consistent with the results from the cAMP assay. The cumulative results of *in vitro* studies corresponding to anti-CT activity of seven extracts conclude that except PLE all other extracts showed varying degree of neutralizing activity against CT which validates the traditional use of these plants in treating CT-induced diarrheal infections.

4.3. Counteracting activity of seven extracts against NMDCY-induced celluar toxicities

The counteracting activity of seven extracts against NMDCY-induced cytotoxicity was determined as viability% using MTT assay. CFCF control (16-fold dilution) showed 50% cell viability in the CHO cell line and two plant extracts CAE (93%, 78%), PGRPE (90%, 73%) showed a significant defensive activity ($p<0.001$) against NMDCY induced cytotoxicity at NC1 and NC2 whereas PGAE (86%, 52%) showed significant protective activity at NC1. The results from the MTT assay were

observed to be correlated with protective activity of the seven extracts against the NMDCY-induced morphological alterations in CHO cell line. CAE, PGRPE and PGAE also showed efficient protective activity against NMDCY-induced cell rounding and cell death in CHO cell line whereas PGRJ, HAE, AME, PLE showed no activity against NMDCY.

From our *in vitro* studies performed with CFCF of *V. cholerae*, it is apparent that there is differential activity of seven extracts against CT and NMDCY-induced cellular toxicities. Except for PLE, all other plants exhibited anti-CT activity whereas only CAE, PGRPE and PGAE showed neutralizing activity against NMDCY in CFCF. Interestingly a correlation was observed between the total phenolic and total flavonoid content in extracts to binding inhibition of CT to GM1, decrease in CT-induced elevated cAMP levels and NMDCY- induced cell rounding in CHO cells. Specifically, the plants with higher phenolic content i.e. CAE, PGRPE, PGRJ, and HA exhibited >90% BI% of CT to GM1, whereas plants with higher flavonoid content i.e. CAE, PGRPE and PGAE showed more protection against CT induced cAMP and NMDCY induced cytotoxicity. The current study substantiates the effectiveness of hydroalcoholic extracts of *C. arborea, P. granatum,* and *P. guajava* extracts against cytotoxicity induced by CT as well as NMDCY secreted by *V. cholerae*.

5. *In silico* studies with polyphenolic compounds

Using molecular modeling studies, two phenolic acids (EA and CHL) and two flavonoids (PHD and RTN) were selected from *C. arborea, P. granatum, P. guajava* based on their binding affinity and interactions with active site amino acid residues involved in stable binding of CTB to the GM1 receptor on intestinal epithelial cells.

Further, GA was selected as a standard for phenolic acids as it is reported to inhibit CT binding to GM1 receptor [8] and QRTN as a flavonoid standard as it was reported to decrease CT-induced cAMP levels [124].

5.1. Molecular docking of 20 polyphenolic compounds against β-subunit (chain F) of CT

The 3D structure of CT (1XTC) was retrieved from the RCSB structural database and missing residues in the structure were added. Among five β-subunits of CT (chain B, C, D, E, F), we have considered chain F as it formed a larger cavity at the GM1 binding interface, and the grid box was set around binding pocket residues that interacted with GM1 *viz.* Glu11, His13, Gly33, Glu51, Gln56, Gln61, Trp88, Asn90, and Lys91 [140]. Substitution of Gly33 residue with Asp was reported to abolish the binding affinity of CTB to GM1 [2]. From the selected 20 compounds, EA, CHL, Delphinidin, and Procyanidin B3 showed H-bond interactions with Gly33. The maximum number of interactions with active site residues was observed for Ellagic acid (10), followed by Procyanidin and Delphinidin. Based on the drug-likeness score, grid score, and a total number of interactions, CT-EA (-36.42, 10), CT-CHL (-39.26, 9), CT-RTN (-48.02, 6), and CT-PHD (-44.39, 6) complexes were further analyzed for their stability by 100ns MD simulations along with their standards, CT-GA (-28.35, 7) and CT-QRTN (-37.25, 3).

5.2. Molecular dynamics simulation studies of docked six complexes with CT using gromacs

Simulation studies using gromacs were performed for ligand-CT complexes (CT-EA, CT-CHL, CT-GA, CT-RTN, CT-PHD, CT-QRTN), and their structural

stability was studied by analyzing the root mean square deviation (RMSD), root mean square fluctuation (RMSF), radius of gyration (Rg), and solvent accessible surface area (SASA).

5.2.1. Structural stability of the docked complexes using MD

The complexes CT-RTN, CT-EA, and CT-PHD showed relatively stable dynamics and reached an equilibrium state earlier within 35ns, of which the flavonoid standard QRTN showed the least RMSD value amongst all the studied complexes. RMSF analysis over the C-α atoms of the chain having binding pocket showed a similar trend in the residual fluctuations in all the complexes. Also, it is interesting to observe that phenolic acid complexes (CT-EA and CT-CHL) showed the least RMSF values compared to the GA standard. However, flavonoid (CT-PHD) showed relatively less fluctuation than the standard (CT-QRTN). The R*g* values for complex CT-EA and CT-PHD showed much more stable R*g* values after the equilibration period of 40 ns. The CT-QRTN complex also showed a stable R*g*value comparable to the CT-PHD. The complexes CT-EA, CT-PHD, and CT-GA showed stable dynamics through the conserved binding pocket interactions as observed in the MD simulation movies. During the MD simulation, EA and PHD fit well in the binding pocket, while RTN moves away from the binding pocket after 30 ns. The complex CT-GA chain-F showed an increased SASA value, highlighting the exposure of chain F to the solvent. Complex CT-PHD and CT-EA showed large variations in the SASA value in chain F and it further decreased, hence making these complexes very stable during the course of simulation of 100 ns.

5.2.2. Intermolecular interactions in docked complexes

CT-PHD shows the maximum number of H-bonding interactions (8) formed during MD simulation; these interactions are consistent throughout the simulation period, whereas the number of H-bonds decreased from 5 to 2 for CT-RTN. CT-QRTN also shows a decrease in the H-bonding interactions during simulation. In general, flavonoids complexed with CT show a relatively higher number of H-bonds than phenolic acids. CT-EA complex initially showed ~7 H-bonding interactions, but steadily these interactions decreased to 3, which were consistent throughout the simulation. We also analyzed other non-bonded contacts of six compounds with CT. This shows that in complexes CT-PHD and CT-EA, the number of contacts steadily increases, making these complexes very stable. However, in other complexes, the number of contacts is either decreasing or steady but less in number. It is interesting to note that the flavonoids and phenolic acids selected have maximum contact when compared to their respective standards.

5.2.3. Secondary structural changes during simulation

We have analyzed conformational changes at the binding site over the simulation period using the DSSP tool. The binding pocket architecture is well stabilized in complexes CT-EA and CT-PHD compared to other complexes mainly due to the increased helical content in the chain-F.

5.2.4. Contribution of the binding pocket residues in the intermolecular interactions

Calculations of residue decomposition energy showed negative contribution energy by most of the residues in CT-EA, CT-CHL, and CT-PHD, favouring their stable complex formation. From the cumulative analysis of results from MD

simulations, it is evident that CT-EA and CT-PHD showed stable dynamics compared with standards CT-GA and CT-QRTN. The order of stability of six complexes as observed through 100ns MD simulations and binding free energy were ranked as CT-EA > CT-CHL > CT-GA for phenolic acids and CT-PHD > CT-QRTN > CT-RTN for flavonoids. Subsequently, the efficacy of six complexes against CT binding to ganglioside GM1 was further validated experimentally by *in vitro* assays.

6. *In vitro* studies with selected six polyphenolic compounds

6.1. HPTLC analysis of C. arborea, P. granatum and P. guajava extracts

Both the qualitative and quantitative analysis of phenolic acids and flavonoids selected using *in silico* studies was performed HPTLC. The phytochemical analysis showed the presence of phenolic acids, EA and CHL in all three plants; GA in *C. arborea* and *P. guajava* whereas flavonoids PHD, RTN, and QRTN in *P. guajava* and *P. granatum* in varying concentrations. EA, an organic hetero-tetracyclic compound formed by the dimerization of gallic acid, is the most active and abundant phytocompound found in *P. granatum* [158]. It is an investigational drug and reported to show several therapeutic properties as an anti-oxidant and anti-proliferative agent [159,160]. CHL, an ester formed by the condensation of caffeic acid and quinic acid, is found majorly in coffee and black tea [161]. It is reported to activate the immune system and also acts as a potent anti-oxidant and carcinogenic inhibitor [162,163]. RTN prevents displacing of reduced CTA1 from CT holotoxin in the endoplasmic reticulum of the host cell by inducing conformational changes in protein disulfide isomerise (PDI), thus restricting the translocation of CTA1 into the cytosol as reported [164].

6.2. MTT cytotoxicity and binding inhibition percentage of six compounds

MTT cytotoxicity assay was performed with six compounds on the CHO cell line to determine their non-cytotoxic doses that showed > 90% cell viability, and further *in vitro* assays were carried out using their respective NC1, NC2. The neutralizing activity of selected phenolic acids and flavonoids against CT (1600 ng/mL) binding to the GM1 receptor was evaluated as BI% using the GM1 ELISA. Phenolic acids EA (97%, 97%) and CHL (92%, 81%) demonstrated remarkable BI% at NC1 and NC2 when compared to their standard GA (31%, 12%). Among flavonoids, PHD (59%, 24%) showed prominent BI% compared with RTN (9%, 2%) and standard QRTN (23%, 6%) at NC1 and NC2 respectively. Earlier similar studies with GA (50mM) showed 40% binding inhibition of CT to GM1 [8] and in another study, binding of FITC-CTB to Vero cells in the presence of 10 µg/ml GA and QRTN was inhibited by 23% and 20%, respectively [124]. These results explain that the interaction of phenolic acids EA and CHL with β-pentamer efficiently inhibits CT binding to GM1 receptor and eventually neutralizes CT toxicity by preventing its internalization into enterocytes. Further confirmatory studies were performed to investigate the protective activity of six compounds against CT-induced cell elongation and elevation of cAMP levels in the CHO cell line.

6.3. Inhibition of CFCF-induced cell elongation and cAMP levels by six compounds

The hallmark of CT toxicity is an increase in cellular cAMP levels that results in the dramatic efflux of ions and water from infected enterocytes, leading to diarrhea [165]. The protective activity of six compounds against CT-induced elevation of cAMP in the CHO cell line was evaluated using competitive cAMP ELISA as an increase in bound percent (B%) of cAMP. Phenolic acids showed a significant increase

(*p<0.001*) in B%, i.e. EA (82%, 81%), CHL (81%, 78%), and GA (80%, 60%) at NC1 and NC2 respectively compared with CFCF control (44%). Flavonoids showed the least protective activity compared to phenolic acids, i.e. PHD (71%, 50%), RTN (53%, 44%), and QRTN (66%, 47%) at NC1 and NC2 respectively. Surprisingly, EA, CHL, and PHD showed efficient defensive activity against CT-induced cAMP levels compared to standard GA and QRTN. Similar results were observed in an earlier study that showed 76% and 59% of the decrease in cAMP with 10 µg/mL of GA and QRTN compared to CT control [124]. However, no previous reports were found for the remaining four compounds. The results from the cAMP assay were correlated with the protective activity of six compounds against CT-induced cell elongation in the CHO cell line. The protection against CT-induced cell elongation in CHO cells was observed to be prominent in the presence of EA and CHL, which were consistent with the results from the cAMP assay.

From the cumulative results of *in silico* and *in vitro* studies, it is apparent that there is a differential activity of phenolic acids and flavonoids against CT. From docking and simulation analysis, it is evident that EA, CHL, and PHD formed more stable complexes with CT. However, phenolic acids EA and CHL were found to be effective in inhibiting CT binding to the GM1 receptor and also significantly reduced CT-induced cAMP levels and cell elongation in CHO cell lines *in vitro*. When MD simulation analysis of six complexes was compared with *in vitro* results, EA, CHL, and PHD were observed to form stable complexes with CT during simulations as well as inhibit CT binding to GM1 and further CT toxicities.

7. *In vivo* studies

Among the selected seven extracts, CAE, PGRPE, and PGAE showed prominent inhibitory activity against CT from the studied six polyphenolic compounds, EA and CHL showed distinguished activity against CT *in vitro* which were further validated *in vivo* against CT-induced fluid accumulation using adult mice ligated-ileal loop model along with standard GA.

7.1. Inhibition of CFCF-induced fluid accumulation in ligated-ileal loops by CAE, PGRPE, and PGAE

CT has potent enterotoxigenic activity and causes fluid accumulation in ligated-ileal loops of adult mice (Saito et al., 2002). CFCF containing 1 µg of CT when instilled into distal ligated ileal loops of 2-3 cm in length, elicited fluid accumulation after 18 hrs and loop mean (n=6) weight/length ratio was estimated at 0.25 g/cm±0.023 whereas a similar study by Sawasvirojwong (2013) [150] showed 0.192±0.042 g/cm. This fluid accumulation induced by CFCF was observed to be significant ($p<0.001$) compared with the saline control group (0.09±0.1 g/cm). A pre-incubated mixture of CFCF containing 1µg of CT and three extracts at two different concentrations (100 µg,50 µg) showed significant reduction ($p<0.001$) CFCF induced fluid accumulation.

7.2. Decrease in CFCF-induced elevated cAMP levels and histopathological changes by CAE, PGRPE, and PGAE

The pooled ileal tissues from each group were estimated for their cellular cAMP levels as an increase in bound percent (B%) using competitive ELISA. Significant increase in cAMP levels ($p<0.001$) were observed in the CFCF control

group (29.5%) compared to the Saline control (0.1%). CAE (0.41%, 0.73%), PGRPE (0.76%, 0.66%) and PGAE (0.6%, 1.2%) showed a significant reduction in cAMP levels *($p<0.001$)* at 100 µg and 50 µg respectively. Histopathological analysis of CFCF-treated ileal loops showed inflammation in sub mucosa and diffused edema in the mucosal layer of the intestine and similar results were also reported previously [150]. CFCF-treated ileal loops in the presence of CAE and PGRPE showed a prominent reduction in inflammation and edema. However, amelioration of histopathological changes in PGAE was found to a lesser extent compared with CFCF control. Previous studies with tea polyphenols [166] and apple polyphenols [167] reported decreased CT induced fluid accumulation in ligated-ileal loop of rabbits and adult mice reflected the anti-diarrheal effect of polyphenols in these plant extracts. The higher polyphenolic content in CAE and PGRPE could be responsible for their efficient enterotoxic activity against CT- induced fluid accumulation.

7.3 *Inhibitory activity of EA, CHL and GA against CFCF-induced fluid accumulation, cellular cAMP levels, and histopathological changes in ligated-ileal loops of adult mice*

A pre-incubated mixture of CFCF containing 1µg of CT and EA/CHL at two different concentrations (50 µg, 25 µg) showed a significant reduction ($p<0.001$) in CT-induced fluid accumulation. GA showed a significant decrease ($p<0.01$) against CT-induced fluid accumulation at a higher concentration but was found to be less effective at a lower concentration (25 µg). Cellular cAMP levels in ligated-ileal tissues were estimated as an increase in bound percent (B%) of cAMP using competitive ELISA. Significant increase in cAMP levels *($p<0.001$)* were observed in the CFCF control group (29.5%) compared to the Saline control (0.1%). EA (0.62%,

1.31%), CHL (1.18%, 1.89%), and GA (1.79%, 3.39%) showed a significant reduction in cAMP levels ($p<0.001$) at 50 µg and 25 µg respectively. Histopathological analysis of CFCF-treated ileal loops showed inflammation in sub mucosa and diffused edema in the mucosal layer of the intestine and similar results were also reported previously [150]. CFCF treated ileal loops in the presence of EA and CHL showed a prominent reduction in inflammation and edema. However, with GA, amelioration of histopathological changes was found to a lesser extent compared with CFCF control.

Polyphenols were reported to show anti-CT activity either by inhibiting CTB binding to GM1 receptor thus blocking CT entry into host cells or by interfering with CTA1- induced catalysis of ADP-ribosylation of Gsα that results in continuous stimulation of adenylate cyclase and increased cellular cAMP levels. Tea catechins and 6-gingerol have been shown to provide resistance to *V. cholerae*-induced fluid accumulation in rabbit ligated intestinal loops by blocking CT binding to GM1 and preventing its internalization into enterocytes [166,138]. Apple and grape polyphenols were also reported to inhibit CT toxicity by various mechanisms, which included their interference with CTA1 catalytic activity and CTB binding to GM1 receptor [167,124]**.** These leads from the literature encouraged us to further investigate the role of polyphenols in preventing CT-induced diarrhea.

CONCLUSION

The current study investigates the efficacy of traditionally used six anti-diarrheal plant extracts and their reported bioactives against CT-induced cyto- and enterotoxicities. Among the selected six plants, the hydroalcoholic extracts of *C. arborea, P. granatum,* and *P. guajava* showed notable activity against CT from our *in vitro* studies. In addition to CT, these three plants also significantly reduced NMDCY-induced cell rounding and cell death in the CHO cell line. Further *in vivo* studies with these plants decreased CT-induced fluid accumulation and histopathological changes in adult mice ligated-ileal loop model. Our study demonstrates the use of these three plant extracts as a supplement with regular oral rehydration therapy in treating cholera and is also expected to minimize the excessive use of antibiotics against these enteropathogens in treating the infection in cost-effective way with health and environmental benefits. Polyphenolic compounds were screened and selected using system biology tools from these three plants based on their intermolecular interactions with active site residues of GM1 binding site on B-pentamer of CT.

Based on computational screening, two flavonoids and two phenolic acids were selected along with reported known inhibitors (GA and QRTN) for further experimental validation. Among the selected six compounds, EA and CHL showed efficient inhibitory activity against CT-induced toxicities *in vitro*. Further, *in vivo* studies with EA and CHL were correlated with *in vitro* results as evidenced by decreased CT-induced fluid accumulation and histopathological changes in the adult mouse ligated-ileal loop model. Thus, our observations from computational molecular modeling studies are in good agreement with experimental results. Our study elucidated the inhibitory activity of EA and CHL against CT by interacting with B-

pentamer and subsequently inhibiting CT binding to the GM1 receptor on enterocytes. Clinical studies would further help to validate the application of hydro-alcoholic extracts of three plants (CAE, PGRPE, and PGAE) and their reported bioactive compounds, EA and CHL as a supplement to standard therapies during cholera outbreaks.

SUMMARY

Anti-Cholera toxin activity of hydro-alcoholic extracts of *C. arborea* (bark), *P. granatum* (fruit peel), *P. guajava* (leaves), *H. antidysenterica* (bark), *A. marmelos* (fruit), and *P. longum* (fruit) was initially investigated using *in vitro* assays. From the selected six, *C. arborea, P. granatum, P. guajava* exhibited prominent neutralization activity against CT by inhibiting its binding to GM1 receptor and eventual reduction in CT-induced elevated cellular cAMP levels. Further animal studies with these three plants also significantly reduced CT-induced fluid accumulation, cAMP levels, and histopathological changes in ligated-ileal loops of adult mice correlating with the results from *in vitro* studies. The results from *in vitro* and *in vivo* studies encouraged us to further explore the bio-active compounds from these plants that has the potential to neutralize CT toxicity. As polyphenols were reported to show anti-CT activity, four polyphenolic compounds from these plants interacting with CT were screened and selected using system biology tools.

Based on molecular docking and dynamics simulation studies, two phenolic acids (Ellagic acid, Chlorogenic acid) and two flavonoids (Rutin, Phloridzin) were selected along with their respective standards (Gallic acid and Quercetrin) for evaluating their potency against CT using *in vitro* assays. Ellagic acid and Chlorogenic acid showed efficient inhibitory activity against CT as evidenced by a higher binding inhibition percentage of CT to GM1 receptor and reduction in cellular cAMP levels. These two phenolic acids when tested *in vivo* against CT, significantly reduced fluid accumulation and histopathological changes in ligated-ileal loops. Interestingly these phenolic acids showed higher inhibitory activity against CT compared to the standard Gallic acid. Our study validated the traditional use of these

plants against CT-induced diarrhea and identified the bioactive compounds responsible for the activity.

LIMITATIONS AND PROSPECTIVE

This study for the first time used cell-free culture filtrate (CFCF) of clinical isolates of *V. cholerae* in which CT was quantified using GM1 ELISA. Non-membrane damaging cytotoxin (NMDCY) was also quantified as 100% tissue culture infective dose ($TCID_{100}$) using cell-based assays. Along with anti-CT activity, the selected six plants were also evaluated for their activity against NMDCY using CFCF.

Crude hydro-alcoholic extracts of selected six plants were used for evaluating their activity against CT and NMDCY. From the selected six, *C. arborea, P. granatum* and *P. guajava* were observed to act efficiently against CT and NMDCY from our *in vitro* studies. Further fractionation of these crude extracts into polyphenols and alkaloids can give us the leads about the group of phytocompounds acting against CT and NMDCY which is the prospective of present findings. Clinical studies with *C. arborea, P. granatum,* and *P. guajava* along with their bio-active compounds Ellagic acid and Chlorogenic acid will approve their use against CT-induced diarrhea minimizing the use of antibiotics which is a rising concern now.

BIBLIOGRAPHY

1. Salcedo CM. Modification of the treatment protocol as a strategy in the control of the cholera epidemic in Haiti 2016-2017. Modification of the treatment protocol as a strategy in the control of the cholera epidemic in Haiti 2016–2017. 2018 Sep 25.

2. Finkelstein RA. Cholera, *Vibrio cholerae* O1 and O139, and other pathogenic vibrios. Medical Microbiology. 4th edition. 1996.

3. Pang H, Le PU, Nabi IR. Ganglioside GM1 levels are a determinant of the extent of caveolae/raft-dependent endocytosis of cholera toxin to the Golgi apparatus. Journal of cell science. 2004; 117(8):1421-30.

4. Hazes B, Read RJ. Accumulating evidence suggests that several AB-toxins subvert the endoplasmic reticulum-associated protein degradation pathway to enter target cells. Biochemistry. 1997;36(37):11051-4.

5. Cassel D, Pfeuffer T. Mechanism of cholera toxin action: covalent modification of the guanyl nucleotide-binding protein of the adenylate cyclase system. Proceedings of national academy of sciences of the United States of America. 1978;*75*:2669–2673.

6. Dengo-Baloi LC, Semá-Baltazar CA, Manhique LV, Chitio JE, Inguane DL, Langa JP. Antibiotics resistance in El Tor *Vibrio cholerae* 01 isolated during cholera outbreaks in Mozambique from 2012 to 2015. PloS one. 2017;12(8):e0181496.

7. Brijesh S, Daswani P, Tetali P, Antia N, Birdi T. Studies on the antidiarrheal activity of *Aegle marmelos* unripe fruit: Validating its traditional usage. BMC complementary and alternative medicine. 2009;9(1):1-2.

8. Birdi T, Daswani P, Brijesh S, Tetali P, Natu A, Antia N. Newer insights into the mechanism of action of *Psidium guajava* L. leaves in infectious diarrhea. BMC complementary and alternative medicine. 2010;10(1):1-1.

9. Sharma DK, Gupta VK, Kumar S, Joshi V, Mandal RS, Prakash AB, Singh M. Evaluation of antidiarrheal activity of ethanolic extract of *Holarrhena antidysenterica* seeds in rats. Veterinary world. 2015;8(12):1392

10. Qnais EY, Elokda AS, Abu Ghalyun YY, Abdulla FA. Antidiarrheal Activity of the Aqueous extract of *Punica granatum* (Pomegranate) peels. Pharmaceutical biology. 2007;45(9):715-20

11. Rahman MT, Khan OF, Saha S, Alimuzzaman M. Antidiarrhoeal activity of the bark extract of *Careya arborea* Roxb. Fitoterapia. 2003;74(1-2):116-8.

12. Taqvi SI, Shah AJ, Gilani AH. Insight into the possible mechanism of antidiarrheal and antispasmodic activities of piperine. Pharmaceutical biology. 2009;47(8):660-4.

13. Ugboko HU, Nwinyi OC, Oranusi SU, Oyewale JO. Childhood diarrheal diseases in developing countries. Heliyon. 2020;6(4):e03690.

14. Platts-Mills JA, Babji S, Bodhidatta L, Gratz J, Haque R, Havt A, McCormick BJ, McGrath M, Olortegui MP, Samie A, Shakoor S. Pathogen-specific burdens of community diarrhea in developing countries: a multisite birth cohort study (MAL-ED). The lancet global health. 2015;3(9):e564-75.

15. Bhattacharya A, Das SK. Water, sanitation and hygiene: the unfinished agenda in the World Health Organization South-East Asia Region. WHO south-east Asia journal of public health. 2017;6(2):22-6.
16. Nemeth, Valerie, Nicholas Pfleghaar. "Diarrhea." 2017.
17. Hodges K, Gill R. Infectious diarrhea: cellular and molecular mechanisms. Gut microbes. 2010;1(1):4-21.
18. Navaneethan U, Giannella RA. Mechanisms of infectious diarrhea. Nature clinical practice gastroenterology & hepatology. 2008;5(11):637-47.
19. Gore JI, Surawicz C. Severe acute diarrhea. Gastroenterology clinics. 2003;32(4):1249-67.
20. Pawlowski SW, Warren CA, Guerrant R. Diagnosis and treatment of acute or persistent diarrhea. Gastroenterology. 2009;136(6):1874-86.
21. Cholera Annual Report 2019, Weekly Epidemiological Record 31 September 2020, Vol 95, 38 (441-448).
22. Ng QX, De Deyn ML, Loke W, Yeo WS. Yemen's cholera epidemic is a one health issue. Journal of preventive medicine and public health. 2020;53(4):289.
23. Bryce J, Boschi-Pinto C, Shibuya K, Black RE, WHO Child Health Epidemiology Reference Group. WHO estimates of the causes of death in children. The lancet. 2005;365(9465):1147-52.
24. Faruque SM, Albert MJ, Mekalanos JJ. Epidemiology, genetics, and ecology of toxigenic *Vibrio cholerae*. Microbiology and molecular biology reviews. 1998;62(4):1301-14.
25. Chatterjee SN, Chaudhuri K. Lipopolysaccharides of *Vibrio cholerae*: I. Physical and chemical characterization. Biochimica et biophysica acta (BBA) - Molecular basis of disease. 2003;1639(2):65-79.

26. Morris Jr JG, Acheson D. Cholera and other types of vibriosis: a story of human pandemics and oysters on the half shell. Clinical infectious diseases. 2003;37(2):272-80.

27. Longini Jr IM, Yunus M, Zaman K, Siddique AK, Sack RB, Nizam A. Epidemic and endemic cholera trends over a 33-year period in Bangladesh. The Journal of infectious diseases. 2002;186(2):246-51.

28. Nair GB, Safa A, Bhuiyan NA, Nusrin S, Murphy D, Nicol C, Valcanis M, Iddings S, Kubuabola I, Vally H. Isolation of *Vibrio cholerae* O1 strains similar to pre-seventh pandemic El Tor strains during an outbreak of gastrointestinal disease in an island resort in Fiji. Journal of medical microbiology. 2006;55(11):1559-62.

29. Nair GB, Qadri F, Holmgren J, Svennerholm AM, Safa A, Bhuiyan NA, Ahmad QS, Faruque SM, Faruque AS, Takeda Y, Sack DA. Cholera due to altered El Tor strains of *Vibrio cholerae* O1 in Bangladesh. Journal of clinical microbiology. 2006;44(11):4211-3.

30. Lam C, Octavia S, Reeves P, Wang L, Lan R. Evolution of seventh cholera pandemic and origin of 1991 epidemic, Latin America. Emerging infectious diseases. 2010;16(7):1130.

31. Comstock LE, Maneval Jr D, Panigrahi P, Joseph A, Levine MM, Kaper JB, Morris Jr JG, Johnson JA. The capsule and O antigen in *Vibrio cholerae* O139 Bengal are associated with a genetic region not present in *Vibrio cholerae* O1. Infection and immunity. 1995;63(1):317-23.

32. Dutta D, Chowdhury G, Pazhani GP, Guin S, Dutta S, Ghosh S, Rajendran K, Nandy RK, Mukhopadhyay AK, Bhattacharya MK, Mitra U. *Vibrio cholerae*

non-O1, non-O139 serogroups and cholera-like diarrhea, Kolkata, India. Emerging infectious diseases. 2013;19(3):464.

33. Crowe SJ, Newton AE, Gould LH, Parsons MB, Stroika S, Bopp CA, Freeman M, Greene K, Mahon BE. Vibriosis, not cholera: toxigenic *Vibrio cholerae* non-O1, non-O139 infections in the United States, 1984–2014. Epidemiology & infection. 2016;144(15):3335-41.

34. Colwell RR. Global climate and infectious disease: the cholera paradigm. Science. 1996;274(5295):2025-31.

35. Mutreja A, Kim DW, Thomson NR, Connor TR, Lee JH, Kariuki S, Croucher NJ, Choi SY, Harris SR, Lebens M, Niyogi SK. Evidence for several waves of global transmission in the seventh cholera pandemic. Nature. 2011;477(7365):462.

36. Khan AI, Chowdhury F, Harris JB, Larocque RC, Faruque AS, Ryan ET, Calderwood SB, Qadri F. Comparison of clinical features and immunological parameters of patients with dehydrating diarrhea infected with Inaba or Ogawa serotypes of *Vibrio cholerae* O1. Scandinavian journal of infectious diseases. 2010;42(1):48-56.

37. Espinosa E, Barre FX, Galli E. Coordination between replication, segregation and cell division in multi-chromosomal bacteria: lessons from *Vibrio cholerae*. International microbiology. 2017;20(3):121-9.

38. Waldor MK, Rubin EJ, Pearson GD, Kimsey H, Mekalanos JJ. Regulation, replication, and integration functions of the *Vibrio cholerae* CTXΦ are encoded by region RS2. Molecular microbiology. 1997;24(5):917-26.

39. Kirn TJ, Bose N, Taylor RK. Secretion of a soluble colonization factor by the TCP type 4 pilus biogenesis pathway in *Vibrio cholerae*. Molecular microbiology. 2003;49(1):81-92.

40. Herrington DA, Hall RH, Losonsky GE, Mekalanos JJ, Taylor RK, Levine MM. Toxin, toxin-coregulated pili, and the toxR regulon are essential for *Vibrio cholerae* pathogenesis in humans. Journal of experimental medicine. 1988;168(4):1487-92.

41. Karaolis DK, Johnson JA, Bailey CC, Boedeker EC, Kaper JB, Reeves PR. A *Vibrio cholerae* pathogenicity island associated with epidemic and pandemic strains. Proceedings of the national academy of sciences. 1998;95(6):3134-9.

42. Yu RR, DiRita VJ. Regulation of gene expression in *Vibrio cholerae* by ToxT involves both antirepression and RNA polymerase stimulation. Molecular microbiology. 2002;43(1):119-34.

43. Miller VL, Taylor RK, Mekalanos JJ. Cholera toxin transcriptional activator ToxR is a transmembrane DNA binding protein. cell. 1987;48(2):271-9.

44. Snow J. On the Mode of Communication of Cholera (2nd edn.) John Churchill.

45. Siddique AK, Cash R. Cholera outbreaks in the classical biotype era. Cholera Outbreaks. 2013;1-6.

46. Koch R. An address on cholera and its bacillus. British medical journal. 1884;2(1236):453.

47. Cvjetanovic B, Barua D. The seventh pandemic of cholera. Nature. 1972;239(5368):137-8.

48. Glass RI, Huq I, Alim AR, Yunus M. Emergence of multiply antibiotic-resistant *Vibrio cholerae* in Bangladesh. Journal of infectious diseases. 1980;142(6):939-42.

49. Glass RI, Huq MI, Lee JV, Threlfall EJ, Khan MR, Alim AR, Rowe B, Gross RJ. Plasmid-borne multiple drug resistance in *Vibrio cholerae* serogroup O1, biotype El Tor: evidence for a point-source outbreak in Bangladesh. Journal of infectious diseases. 1983;147(2):204-9.

50. Aoun J, Hayashi M, Sheikh IA, Sarkar P, Saha T, Ghosh P, Bhowmick R, Ghosh D, Chatterjee T, Chakrabarti P, Chakrabarti MK. Anoctamin 6 contributes to Cl− secretion in accessory cholera enterotoxin (Ace)-stimulated diarrhea: An essential role for phosphatidylinositol 4, 5-bisphosphate (PIP2) signaling in cholera. Journal of biological chemistry. 2016;291(52):26816-36.

51. Uzzau S, Lu R, Wang W, Fiore C, Fasano A. Purification and preliminary characterization of the zonula occludens toxin receptor from human (CaCo2) and murine (IEC6) intestinal cell lines. FEMS microbiology letters. 2001;194(1):1-5.

52. Al-Majali AM, Asem EK, Lamar CH, Robinson JP, Freeman MJ, Saeed AM. Studies on the mechanism of diarrhea induced by *Escherichia coli* heat-stable enterotoxin (STa) in newborn calves. Veterinary research communications. 2000;24(5):327-38.

53. Awasthi SP, Asakura M, Chowdhury N, Neogi SB, Hinenoya A, Golbar HM, Yamate J, Arakawa E, Tada T, Ramamurthy T, Yamasaki S. Novel cholix toxin variants, ADP-ribosylating toxins in *Vibrio cholerae* non-O1/non-O139 strains, and their pathogenicity. Infection and immunity. 2013;81(2):531-41.

54. Cordero CL, Kudryashov DS, Reisler E, Satchell KJ. The actin cross-linking domain of the V*ibrio cholerae* RTX toxin directly catalyzes the covalent cross-linking of actin. Journal of biological chemistry. 2006;281(43):32366-74.

55. Wu Z, Nybom P, Magnusson KE. Distinct effects of *Vibrio cholerae* haemagglutinin/protease on the structure and localization of the tight junction-associated proteins occludin and ZO-1. Cellular microbiology. 2000;2(1):11-7.

56. Moschioni M, Tombola F, Bernard MD, Coelho A, Zitzer A, Zoratti M, Montecucco C. The *Vibrio cholerae* haemolysin anion channel is required for cell vacuolation and death. Cellular microbiology. 2002;4(7):397-409.

57. Yamamoto K, Al-Omani M, Honda T, Takeda Y, Miwatani T. Non-O1 *Vibrio cholerae* hemolysin: purification, partial characterization, and immunological relatedness to El Tor hemolysin. Infection and immunity. 1984;45(1):192-6.

58. McCardell BA, Madden JM, Shah DB. Isolation and characterization of a cytolysin produced by *Vibrio cholerae* serogroup non-O1. Canadian journal of microbiology. 1985;31(8):711-20.

59. Ichinose YO, Yamamoto K, Nakasone N, Tanabe MJ, Takeda T, Miwatani T, Iwanaga M. Enterotoxicity of El Tor-like hemolysin of non-O1 *Vibrio cholerae*. Infection and immunity. 1987;55(5):1090-3.

60. Mitra R, Saha PK, Basu I, Venkataraman A, Ramakrishna BS, Albert MJ, Takeda Y, Nair GB. Characterization of non-membrane-damaging cytotoxin of non-toxigenic *Vibrio cholerae* O1 and its relevance to disease. FEMS microbiology letters. 1998;169(2):331-9.

61. Pang H, Le PU, Nabi IR. Ganglioside GM1 levels are a determinant of the extent of caveolae/raft-dependent endocytosis of cholera toxin to the Golgi apparatus. Journal of cell science. 2004;117(8):1421-30.

62. Hazes B, Read RJ. Accumulating evidence suggests that several AB-toxins subvert the endoplasmic reticulum-associated protein degradation pathway to enter target cells. Biochemistry. 1997;36(37):11051-4.

63. Gill DM, Meren R. ADP-ribosylation of membrane proteins catalyzed by cholera toxin: basis of the activation of adenylate cyclase. Proceedings of national academy of sciences of the United States of the America.1978;75:3050–3054.

64. Cassel D, Pfeuffer T. Mechanism of cholera toxin action: covalent modification of the guanyl nucleotide-binding protein of the adenylate cyclase system. Proceedings of national academy of sciences of the United States of the America. 1978; 75:2669–2673.

65. Deeks ED, Cook JP, Day PJ, Smith DC, Roberts LM, Lord JM. The low lysine content of ricin A chain reduces the risk of proteolytic degradation after translocation from the endoplasmic reticulum to the cytosol. Biochemistry. 2002;41(10):3405-13.

66. Lopez AL, Gonzales ML, Aldaba JG, Nair GB. Killed oral cholera vaccines: history, development and implementation challenges. Therapeutic advances in vaccines. 2014;2(5):123-36.

67. Song KR, Lim JK, Park SE, Saluja T, Cho SI, Wartel TA, Lynch J. Oral cholera vaccine efficacy and effectiveness. Vaccines. 2021;9(12):1482.

68. Musekiwa A, Volmink J. Oral rehydration salt solution for treating cholera:≤ 270 mOsm/L solutions vs≥ 310 mOsm/L solutions. Cochrane database of systematic reviews. 2011;(12).

69. Bajait C, Thawani V. Role of zinc in pediatric diarrhea. Indian journal of pharmacology. 2011;43(3):232.

70. Leibovici-Weissman YA, Neuberger A, Bitterman R, Sinclair D, Salam MA, Paul M. Antimicrobial drugs for treating cholera. Cochrane database of systematic reviews. 2014;(6).

71. Williams PC, Berkley JA. Guidelines for the management of paediatric cholera infection: a systematic review of the evidence. Paediatrics and international child health. 2018;38(sup1):S16-31.

72. Martínez JL. Antibiotics and antibiotic resistance genes in natural environments. Science. 2008;321(5887):365-7.

73. Bhattacharya D, Sayi DS, Thamizhmani R, Bhattacharjee H, Bharadwaj AP, Roy A, Sugunan AP. Emergence of multidrug-resistant *Vibrio cholerae* O1 biotype El Tor in Port Blair, India. The American journal of tropical medicine and hygiene. 2012;86(6):1015.

74. Bag S, Ghosh TS, Banerjee S, Mehta O, Verma J, Dayal M, Desigamani A, Kumar P, Saha B, Kedia S, Ahuja V. Molecular insights into antimicrobial resistance traits of commensal human gut microbiota. Microbial ecology. 2019;77:546-57.

75. Verma J, Bag S, Saha B, Kumar P, Ghosh TS, Dayal M, Senapati T, Mehra S, Dey P, Desigamani A, Kumar D. Genomic plasticity associated with antimicrobial resistance in *Vibrio cholerae*. Proceedings of the National Academy of Sciences. 2019;116(13):6226-31.

76. Mhalu FS, Mmari PW, Ijumba J. Rapid emergence of El Tor *Vibrio cholerae* resistant to antimicrobial agents during first six months of fourth cholera epidemic in Tanzania. The Lancet. 1979;313(8112):345-7.

77. Ghosh A, Ramamurthy TJ. Antimicrobials & cholera: are we stranded?. The Indian journal of medical research. 2011;133(2):225.

78. McArthur AG, Waglechner N, Nizam F, Yan A, Azad MA, Baylay AJ, Bhullar K, Canova MJ, De Pascale G, Ejim L, Kalan L. The comprehensive antibiotic resistance database. Antimicrobial agents and chemotherapy. 2013;57(7):3348-57.

79. Njume C, Goduka NI. Treatment of diarrhea in rural African communities: an overview of measures to maximise the medicinal potentials of indigenous plants. International journal of environmental research and public health. 2012;9(11):3911-33.

80. Ashish M, Vinit S, Kritika H, Kumar MS. Plants used for treatment of diarrhea: an ayurvedic prospective.

81. Brijesh S, Daswani P, Tetali P, Antia N, Birdi T. Studies on the antidiarrheal activity of *Aegle marmelos* unripe fruit: Validating its traditional usage. BMC complementary and alternative medicine. 2009;9(1):47.

82. Shamkuwar PB, Sahi SR, Pawar DP. Efficacy of *Aegle marmelos* L. Corr.(Rutaceae) in Ayurvedic antidiarrheal formulation. European journal of experimental biology. 2012;2:194-8.

83. Joshi PV, Patil RH, Maheshwari VL. *In vitro* antidiarrheal activity and toxicity profile of *Aegle marmelos* Correa ex Roxb. dried fruit pulp.

84. Dhuley JN. Investigation on the gastroprotective and antidiarrheal properties of *Aegle marmelos* unripe fruit extract. Hindustan antibiotics bulletin. 2003;45(1-4):41-6.

85. Mazumder R, Bhattacharya S, Mazumder A, Pattnaik AK, Tiwary PM, Chaudhary S. Antidiarrheal evaluation of *Aegle marmelos* (Correa) Linn. root extract. Phytotherapy research. 2006;20(1):82-4.

86. Vinita Bisht N, Johar V. Bael (*Aegle marmelos*) Extraordinary species of India: a review. International journal of current microbiology and applied sciences. 2017;6:1870-87.

87. Rahman S, Parvin R. Therapeutic potential of *Aegle marmelos* (L.)-An overview. Asian Pacific journal of tropical disease. 2014;4(1):71-7.

88. Katram N, Garlapati PK, Yadavalli C, Methal RE, Rajappa SB, Raghavan AK. *Aegle marmelos* extract rich in marmelosin exacted ameliorative effect against chromium-induced oxidative stress and apoptosis through regulation of Gadd45 in HepG2 cell line. Journal of food biochemistry. 2021;45(4):e13704.

89. Mishra A, Seth A, Maurya SK. Therapeutic significance and pharmacological activities of antidiarrheal medicinal plants mention in Ayurveda: A review. *J*ournal of intercultural ethnopharmacology. 2016;5(3):290.

90. Rahman MT, Khan OF, Saha S, Alimuzzaman M. Antidiarrheal activity of the bark extract of *Careya arborea* Roxb. Fitoterapia. 2003;74(1-2):116-8.

91. Satish KB, Vrushabendra SB, Kamal KG, Mohan BG. Review on *Careya arborea* Roxb. International journal of research in ayurveda and pharmacy. 2010;1(2):306-15.

92. Sambath Kumar R. Hepatoprotective and *in vivo* antioxidant effects of *Careya arborea* against carbon tetrachloride induced liver damage in rats. International journal of molecular medicine and advanced sciences. 2005;1:418-24.

93. Senthilkumar N, Badami S, Cherian MM, Hariharapura RC. Potent *in vitro* cytotoxic and antioxidant activity of *Careya arborea* bark extracts. Phytotherapy research. 2007;21(5):492-5.

94. Kumar RS, Sundram RS, Sivakumar P, Nethaji R, Senthil V, Murthy NV, Kanagasabi R. CNS activity of the methanol extracts of *Careya arborea* in

experimental animal model. Bangladesh journal of pharmacology. 2008;3(1):36-43.

95. Kumar K, Mruthunjaya K, Kumar S, Mythreyi R. Anti ulcer activity of ethanol extract of the stem bark of *Careya arborea* Roxb. International current pharmaceutical journal. 2013;2(3):78-82.
96. Jeevan Ram A, Venkata Raju RR. Certain potential crude drugs used by tribals of Nallamalais, Andhra Pradesh for skin diseases. Ethnobotany. 2001;13(1):110-5.
97. Jamadagni PS, Pawar SD, Jamadagni SB, Chougule S, Gaidhani SN, Murthy SN. Review of *Holarrhena antidysenterica* (L.) Wall. ex A. DC: Pharmacognostic, pharmacological, and toxicological perspective. Pharmacognosy reviews. 2017;11(22):141.
98. Sharma DK, Gupta VK, Kumar S, Joshi V, Mandal RS, Prakash AB, Singh M. Evaluation of antidiarrheal activity of ethanolic extract of *Holarrhena antidysenterica* seeds in rats. Veterinary world. 2015;8(12):1392.
99. Ballal M, Srujan D, Bhat KK, Shirwaikar A, Shivananda PG. Antibacterial activity of *Holarrhena antidysenterica* [Kurchi] against the enteric pathogens. Indian journal of Pharmacology. 2000;32(6):392.
100. Somanadhan B, Varughese G, Palpu P, Sreedharan R, Gudiksen L, Smitt UW, Nyman U. An ethnopharmacological survey for potential angiotensin converting enzyme inhibitors from Indian medicinal plants. Journal of ethnopharmacology. 1999;65(2):103-12.
101. Kavitha, D, P. N. Shilpa, S. Niranjali Devaraj. Antibacterial and antidiarrheal effects of alkaloids of *Holarrhena antidysenterica* WALL. 2004.

102. Raman MS, Sultana NA, Anwar MN. *In vitro* antimicrobial activity of Holarrifine 24-ol isolated from the stem bark of *Holarrhena antidysenterica*. International journal of agricuture and biology. 2004;6(4):698-700.

103. Begum S, Usmani SB, Siddiqui BS, Siddiqui S. Alkaloidal constituents of the bark of *Holarrhena antidysenterica*. Heterocycles (Sendai). 1993;36(4):717-23.

104. Das AK, Mandal SC, Banerjee SK, Sinha S, Das J, Saha BP, Pal M. Studies on antidiarrheal activity of *Punica granatum* seed extract in rats. Journal of ethnopharmacology. 1999;68(1-3):205-8.

105. Qnais EY, Elokda AS, Abu Ghalyun YY, Abdulla FA. Antidiarrheal Activity of the Aqueous extract of *Punica granatum* (Pomegranate) peels. Pharmaceutical biology. 2007;45(9):715-20.

106. Shamkuwar PB, Pawar DP. Evaluation of antidiarrheal potential of *Punica granatum* L.(Punicaceae) in Ayurvedic formulation. Journal of chemical and pharmaceutical research. 2012;4:1489-92.

107. Derakhshan Z, Ferrante M, Tadi M, Ansari F, Heydari A, Hosseini MS, Conti GO, Sadrabad EK. Antioxidant activity and total phenolic content of ethanolic extract of pomegranate peels, juice and seeds. Food and chemical toxicology. 2018;114:108-11.

108. Tomás-Barberán FA, Garcia-Villalba R, Gonzalez-Sarrias A, Selma MV, Espin JC. Ellagic acid metabolism by human gut microbiota: consistent observation of three urolithin phenotypes in intervention trials, independent of food source, age, and health status. Journal of agricultural and food chemistry. 2014;62(28):6535-8.

109. Kumar S, Kamboj J, Sharma S. Overview for various aspects of the health benefits of *Piper longum* linn. fruit. Journal of acupuncture and meridian studie*s*. 2011;4(2):134-40.

110. Bajad S, Bedi KL, Singla AK, Johri RK. Antidiarrheal activity of piperine in mice. Planta medica. 2001;67(03):284-7.

111. Bajad S, Bedi KL, Singla AK, Johri RK. Piperine inhibits gastric emptying and gastrointestinal transit in rats and mice. Planta medica. 2001;67(02):176-9.

112. Taqvi SI, Shah AJ, Gilani AH. Insight into the possible mechanism of antidiarrheal and antispasmodic activities of piperine. Pharmaceutical biology. 2009;47(8):660-4.

113. Kaushik D, Rani R, Kaushik P, Sacher D, Yadav J. *In vivo* and *in vitro* antiasthmatic studies of plant *Piper longum* Linn. International journal of pharmacology. 2012;8(3):192-7.

114. Lu C, Zhang B, Xu T, Zhang W, Bai B, Xiao Z, Wu L, Liang G, Zhang Y, Dai Y. Piperlongumine reduces ovalbumin-induced asthma and airway inflammation by regulating nuclear factor-κB activation. International journal of molecular medicine. 2019;44(5):1855-65.

115. Koul IB, Kapil A. Evaluation of the liver protective potential of piperine, an active principle of black and long peppers. Planta medica. 1993;59(05):413-7.

116. Ojewole JA. Antiinflammatory and analgesic effects of *Psidium guajava* Linn.(Myrtaceae) leaf aqueous extract in rats and mice. Methods and findings in experimental and clinical pharmacology. 2006;28(7):441-6.

117. Jaiarj P, Khoohaswan P, Wongkrajang Y, Peungvicha P, Suriyawong P, Saraya MS, Ruangsomboon O. Anticough and antimicrobial activities of *Psidium guajava* Linn. leaf extract. Journal of ethnopharmacology. 1999;67(2):203-12.

118. Biswas B, Rogers K, McLaughlin F, Daniels D, Yadav A. Antimicrobial activities of leaf extracts of guava (*Psidium guajava* L.) on two gram-negative and gram-positive bacteria. International journal of microbiology. 2013

119. Jassal K, Kaushal S. Phytochemical and antioxidant screening of guava (*Psidium guajava*) leaf essential oil. Agricultural research journal. 2019;56:528.

120. Ashraf A, Sarfraz RA, Rashid MA, Mahmood A, Shahid M, Noor N. Chemical composition, antioxidant, antitumor, anticancer and cytotoxic effects of *Psidium guajava* leaf extracts. Pharmaceutical biology. 2016;54(10):1971-81.

121. Tang SM, Deng XT, Zhou J, Li QP, Ge XX, Miao L. Pharmacological basis and new insights of quercetin action in respect to its anti-cancer effects. Biomedicine & pharmacotherapy. 2020;121:109604.

122. Díaz-de-Cerio E, Gómez-Caravaca AM, Verardo V, Fernández-Gutiérrez A, Segura-Carretero A. Determination of guava (*Psidium guajava* L.) leaf phenolic compounds using HPLC-DAD-QTOF-MS. Journal of functional foods. 2016;22:376-88.

123. Ćujić N, Šavikin K, Janković T, Pljevljakušić D, Zdunić G, Ibrić S. Optimization of polyphenols extraction from dried chokeberry using maceration as traditional technique. Food chemistry. 2016;194: 135-142.

124. Cherubin P, Garcia M.C, Curtis D, Britt C.B, Craft Jr J.W, Burress H, Berndt C, Reddy S, Guyette J, Zheng T, Huo Q. Inhibition of cholera toxin and other AB toxins by polyphenolic compounds. PloS one. 2016;11(11): 0166477.

125. Singleton V.L, Orthofer R, Lamuela-Raventós R.M. Analysis of total phenols and other oxidation substrates and antioxidants by means of folin-ciocalteu reagent. Methods in enzymology. 1999; 299:152-178.

126. Zhishen J, Mengcheng T, Jianming W. The determination of flavonoid contents in mulberry and their scavenging effects on superoxide radicals. Food chemistry. 1999;64(4):555-559.

127. Dey S, Parande M.V, Parande A.M, Lakkannavar S.L, Rathore P.K, Mantur B.G, Kholkute S.D, Roy S. Twin outbreak of cholera in rural North Karnataka, India. Indian journal of medical research. 2014;140(3): 420.

128. Roy S, Parande M.V, Mantur B.G, Bhat S, Shinde R, Parande A.M, Meti R.S, Chandrasekhar M.R, Kholkute S.D, Saini A, Joshi M. Multidrug-resistant *Vibrio cholerae* O1 in Belgaum, south India. Journal of medical microbiology. 2012;61(11):1574-1579.

129. McCormack WM, DeWitt WE, Bailey PE, Morris GK, Soeharjono P, Gangarosa EJ. Evaluation of thiosulfate-citrate-bile salts-sucrose agar, a selective medium for the isolation of *Vibrio cholerae* and other pathogenic vibrios. Journal of infectious diseases. 1974;129(5):497-500.

130. Wright MH, Adelskov J, Greene AC. Bacterial DNA extraction using individual enzymes and phenol/chloroform separation. Journal of microbiology & biology education. 2017;18(2):18-2.

131. Naha A, Pazhani GP, Ganguly M, Ghosh S, Ramamurthy T, Nandy RK, Nair GB, Takeda Y, Mukhopadhyay AK. Development and evaluation of a PCR assay for tracking the emergence and dissemination of Haitian variant ctxB in *Vibrio cholerae* O1 strains isolated from Kolkata, India. Journal of clinical microbiology. 2012;50(5):1733-6.

132. Iwanaga M, Yamamoto K, Higa N, Ichinose Y, Nakasone N, Tanabe M. Culture conditions for stimulating cholera toxin production by *Vibrio cholerae* O1 El Tor. Microbiology and immunology. 1986;30(11):1075-1083.

133. Kanjilal S, Citorik R, LaRocque R.C, Ramon, M.F, Calderwood S.B. A systems biology approach to modeling *Vibrio cholerae* gene expression under virulence-inducing conditions. Journal of bacteriology. 2010;192(17): 4300-4310.

134. Guerrant RL, Fang GD, Thielman NM, Fonteles MC. Role of platelet activating factor in the intestinal epithelial secretory and Chinese hamster ovary cell cytoskeletal responses to cholera toxin. Proceedings of the national academy of sciences. 1994;91(20):9655-8.

135. Svennerholm A.M, Wiklund G. Rapid GM1-enzyme-linked immunosorbent assay with visual reading for identification of *Escherichia coli* heat-labile enterotoxin. Journal of clinical microbiology. 1983;17(4): 596-600.

136. Dawson, R.M. Characterization of the binding of cholera toxin to ganglioside GM1 immobilized onto microtitre plates. Journal of applied toxicology. 2005;25(1): 30-38.

137. Plumb J.A, Milroy R, Kaye S.B. Effects of the pH dependence of 3-(4, 5-dimethylthiazol-2-yl)-2, 5-diphenyltetrazolium bromide-formazan absorption on chemosensitivity determined by a novel tetrazolium-based assay. Cancer research. 1989;49(16):4435-4440.

138. Saha P, Das B, Chaudhuri K. Role of 6-gingerol in reduction of cholera toxin activity *in vitro* and *in vivo.* Antimicrobial agents and chemotherapy. 2013;57(9):4373-80.

139. Allen WJ, Balius TE, Mukherjee S, Brozell SR, Moustakas DT, Lang PT, Case DA, Kuntz ID, Rizzo R. DOCK 6: Impact of new features and current docking performance. Journal of computational chemistry. 2015;36(15):132-56.

140. Merritt EA, Sarfaty S, Akker FV, L'Hoir C, Martial JA, Hol WG. Crystal structure of cholera toxin B-pentamer bound to receptor GM1 pentasaccharide. Protein science. 1994;3 (2):166-75.

141. Xiong G, Wu Z, Yi J, Fu L, Yang Z, Hsieh C, Yin M, Zeng X, Wu C, Lu A, Chen X. ADMETlab 2.0: an integrated online platform for accurate and comprehensive predictions of ADMET properties. Nucleic acids research. 2021;49 (W1):W5-14.

142. Abraham MJ, Murtola T, Schulz R, Pá ll S, Smith JC, Hess B. GROMACS: High performance molecular simulations through multi-level parallelism from laptops to supercomputers. SoftwareX. 2015;2 :19–25.

143. Bhandare VV, Ramaswamy A. The proteinopathy of D169G and K263E mutants at the RNA Recognition Motif (RRM) domain of tar DNA-binding protein (tdp43) causing neurological disorders: A computational study. Journal of biomolecular structure and dynamics. 2018;36(4):1075-93.

144. Gangopadhyay A, Chakraborty HJ, Datta A. Employing virtual screening and molecular dynamics simulations for identifying hits against the active cholera toxin. Toxicon. 2019;170:1-9.

145. Dwivedi PS, Patil VS, Khanal P, Bhandare VV, Gurav S, Harish DR, Patil BM, Roy S. System biology-based investigation of Silymarin to trace hepatoprotective effect. Computers in biology and medicine. 2022; 105223.

146. Kumari R, Kumar R. g_mmpbsa A GROMACS tool for high-throughput MM-PBSA calculations. Journal of chemical information and modeling. 2014;54(7) :1951-62.

147. Visualizer BD. Dassault Systemes; San Diego, CA, USA: 2021. Version v21. 2021;1:20298.

148. Pai SR, Joshi RK. Optimized Densitometric Analysis for Determination of Triterpenoid Isomers in *Vitex negundo* L. Leaf. National academy science letters. 2018;41(5):323-7.

149. Pai S, Upadhya V, Hegde H, Joshi R, Kholkute S. New report of triterpenoid betulinic acid along with oleanolic acid from Achyranthes aspera by reversed-phase-ultra flow liquid chromatographic analysis and confirmation using high-performance thin-layer chromatographic and fourier transform-infrared spectroscopic technique. *Journal of planar chromatography-Modern TLC*. 2014;27(1):38-41.

150. Sawasvirojwong S, Srimanote P, Chatsudthipong V, Muanprasat C. An Adult Mouse Model of *Vibrio cholerae*-induced Diarrhea for Studying Pathogenesis and Potential Therapy of Cholera, PLoS neglected trophical diseases. 2013;7(6):e2293.

151. Basu I, Mitra R, Saha P.K, Ghosh A.N, Bhattacharya J, Chakrabarti M.K, Takeda Y, Nair G.B. Morphological and cytoskeletal changes caused by non-membrane damaging cytotoxin of *Vibrio cholerae* on Int 407 and HeLa cells. FEMS microbiology letters. 1999;179(2): 255-263.

152. Saha P.K, Nair G.B. 1997. Production of monoclonal antibodies to the non-membrane-damaging cytotoxin (NMDCY) purified from *Vibrio cholerae* O26 and distribution of NMDCY among strains of *Vibrio cholerae* and other enteric bacteria determined by monoclonal-polyclonal sandwich enzyme-linked immunosorbent assay. Infection and immunity. 1997;65(2): 801-805.

153. Sharma C, Thungapathra M, Ghosh A, Mukhopadhyay A.K, Basu A, Mitra R, Basu I, Bhattacharya S.K, Shimada T, Ramamurthy T, Takeda T. Molecular analysis of non-O1, non-O139 *Vibrio cholerae* associated with an unusual

upsurge in the incidence of cholera-like disease in Calcutta, India. Journal of clinical microbiology. 1998; 36(3):756-763.

154. Saha P.K, Koley H, Nair G.B. Purification and characterization of an extracellular secretogenic non-membrane-damaging cytotoxin produced by clinical strains of *Vibrio cholerae* non-O1. Infection and Immunity. 1996;64(8):3101-3108.
155. Baek Y, Lee D, Lee J, Yoon Y, Nair GB, Kim DW, Kim EJ. 2020. Cholera toxin production in *Vibrio cholerae* O1 El tor biotype strains in single-phase culture. Frontiers in microbiology. 2020; 11:825.
156. Jobling M.G, Yang Z, Kam W.R, Lencer W.I, Holmes R.K. 2012. A single native ganglioside GM1-binding site is sufficient for cholera toxin to bind to cells and complete the intoxication pathway. American society for microbiology. 2012; 3(6):00401-12.
157. Thiagarajah J.R, Verkman A.S. CFTR pharmacology and its role in intestinal fluid secretion. Current opinion in pharmacology. 2003;3(6):594-599.
158. Usta C, Ozdemir S, Schiariti M, Puddu PE. The pharmacological use of ellagic acid-rich pomegranate fruit. International journal of food sciences and nutrition. 2013;64(7):907-13.
159. Han DH, Lee MJ, Kim JH. Antioxidant and apoptosis-inducing activities of ellagic acid. Anticancer research. 2006;26(5A):3601-6.
160. Losso JN, Bansode RR, Trappey II A, Bawadi HA, Truax R. *In vitro* anti-proliferative activities of ellagic acid. The journal of nutritional biochemistry. 2004;15(11):672-8.

161. Farah A, Monteiro M, Donangelo CM, Lafay S. Chlorogenic acids from green coffee extract are highly bioavailable in humans. The journal of nutrition. 2008;138(12):2309-15.

162. Sato Y, Itagaki S, Kurokawa T, Ogura J, Kobayashi M, Hirano T, Sugawara M, Iseki K. *In vitro* and *in vivo* antioxidant properties of chlorogenic acid and caffeic acid. International journal of pharmaceutics. 2011;403(1-2):136-8.

163. Wang L, Du H, Chen P. Chlorogenic acid inhibits the proliferation of human lung cancer A549 cell lines by targeting annexin A2 *in vitro* and *in vivo*. Biomedicine & pharmacotherapy. 2020;131:110673.

164. Guyette J, Cherubin P, Serrano A, Taylor M, Abedin F, O'Donnell M, Burress H, Tatulian SA, Teter K. Quercetin-3-rutinoside blocks the disassembly of cholera toxin by protein disulfide isomerase. Toxins. 2019;11(8):458.

165. Iwaz J, Lafont S, Revillard JP. Elevation of cyclic 3′ 5′ adenosine monophosphate levels by cholera toxin inhibits the generation of interleukin 2 activity. Cellular immunology. 1986;103(2):455-61.

166. Toda M, Okubo S, Ikigai H, Suzuki T, Suzuki Y, Hara Y, Shimamura T. The protective activity of tea catechins against experimental infection by *Vibrio cholerae* O1. Microbiology and immunology. 1992;36(9):999-1001.

167. Saito T, Miyake M, Toba M, Okamatsu H, Shimizu S, Noda M. Inhibition by apple polyphenols of ADP-ribosyltransferase activity of cholera toxin and toxin-induced fluid accumulation in mice. Microbiology and immunology. 2002;46(4):249-55.

ANNEXURES

ANNEXURE - A

- **Certificates of plants authentication**

Unriped fully matured fruits of *A. marmelos*, bark of *C. arborea* and *H. antidysenterica*; young leaves of *P. guajava*; fruits of *P. granatum* and *P. longum* were collected from Belagavi district, Karnataka, India and certified by a plant taxonomist at ICMR-NITM, Belagavi.

राष्ट्रीय पारम्परिक चिकित्साविज्ञान संस्थान
ICMR-NATIONAL INSTITUTE OF TRADITIONAL MEDICINE
(भूतपूर्व क्षेत्रीय आयुर्विज्ञान अनुसंधान केन्द्र Formerly Regional Medical Research Centre)
Nehru Nagar, Belagavi-590 010

भारतीय आयुर्विज्ञान अनुसंधान परिषद
INDIAN COUNCIL OF MEDICAL RESEARCH
स्वास्थ्य अनुसंधान विभाग, स्वास्थ्य और परिवार कल्याण मंत्रालय, भारत सरकार
Department of Health Research,
Ministry of Health & Family Welfare, Govt. of India

Dr. Harsha Hegde
Scientist-E
harshah@icmr.gov.in

Date: 22-04-2022

AUTHENTICATION

This is to authenticate that the plant materials submitted by Ms. Rajitha Charla, ICMR-SRF, ICMR-NITM, Belagavi are identified as ***Punica granatum* L. (Lythraceae)** and ***Piper longum* L. (Piperaceae)**. The herbarium specimens of the same have been deposited in our herbaria with accession numbers RMRC-1690 and RMRC-1691 respectively.

Harsha Hegde

राष्ट्रीय पारम्परिक चिकित्साविज्ञान संस्थान
ICMR-NATIONAL INSTITUTE OF TRADITIONAL MEDICINE
(भूतपूर्व क्षेत्रीय आयुर्विज्ञान अनुसंधान केन्द्र Formerly Regional Medical Research Centre)
Nehru Nagar, Belagavi-590 010

भारतीय आयुर्विज्ञान अनुसंधान परिषद
INDIAN COUNCIL OF MEDICAL RESEARCH
स्वास्थ्य अनुसंधान विभाग, स्वास्थ्य और परिवार कल्याण मंत्रालय, भारत सरकार
Department of Health Research,
Ministry of Health & Family Welfare, Govt. of India

Dr. Harsha Hegde
Scientist-E
harshah@icmr.gov.in

Date: 28-07-2020

AUTHENTICATION

This is to authenticate that the plant materials brought by Ms. Rajitha Charla, ICMR-SRF, ICMR-NITM, Belagavi are identified as:

***Aegle marmelos* Correa** (Rutaceae)
Voucher No. RMRC-1588

***Psidium guajava* L.** (Myrtaceae)
Voucher No. RMRC-1589

***Careya arborea* Roxb.** (Lecythidaceae)
Voucher No. RMRC-1590

***Holarrhena antidysenterica* (L.) Wall. ex DC.** (Apocynaceae)
Voucher No. RMRC-1591

Harsha Hegde
Scientist-E

ANNEXURE - B

Animal Ethical Approval certificate

- **Ethical approval for animal studies**

This animal experiments were performed in the present study after receiving the ethical clearance from Institutional Animal Ethics Committee (IAEC) of ICMR-NITM Belagavi; resolution number IAEC/ICMR-NTM BGM/2018/2, Reg. No. (Reg no:1388/GO/Re/S/10/CPCSEA) dated 21-07-2018.

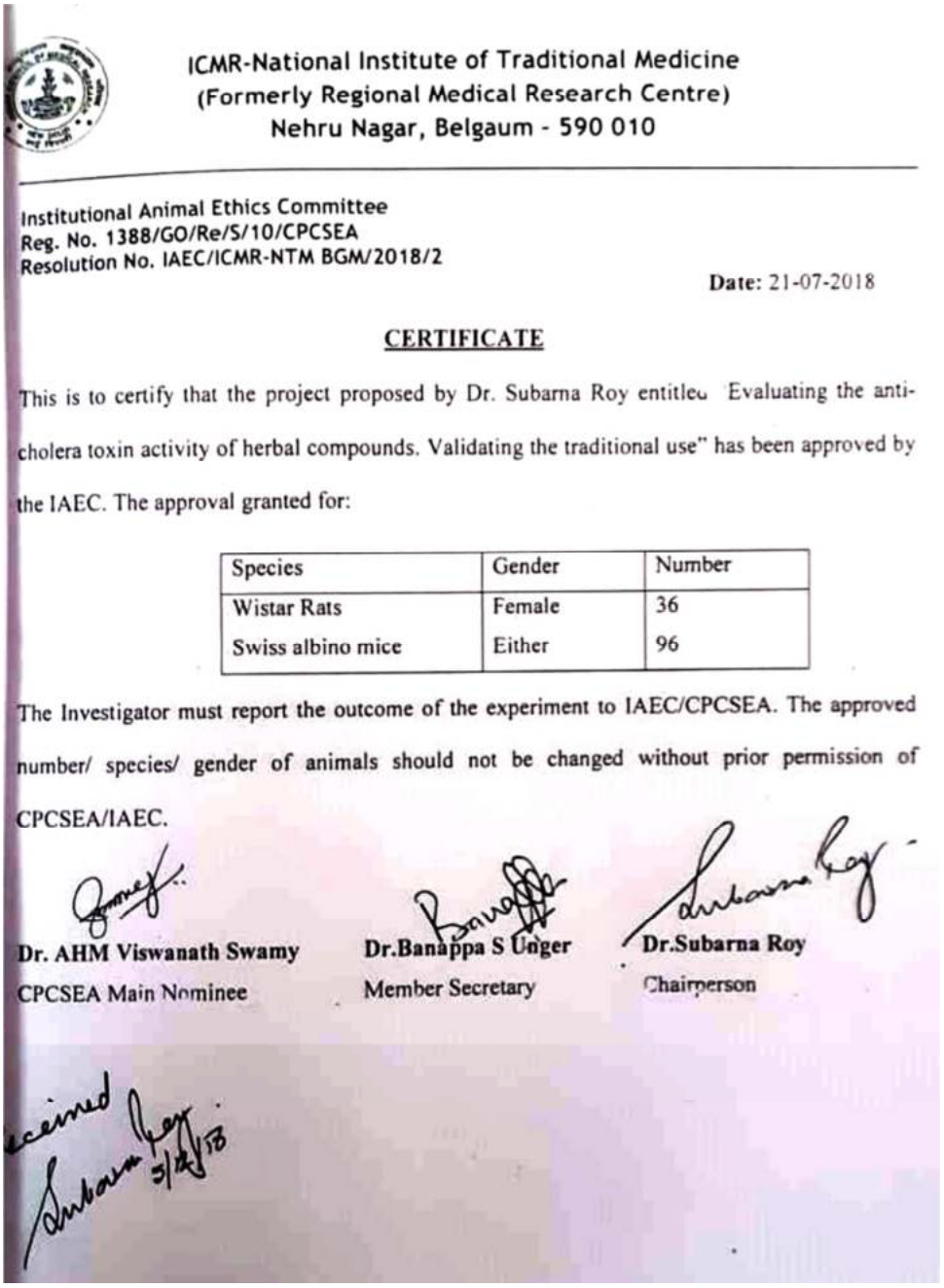

ICMR-National Institute of Traditional Medicine
(Formerly Regional Medical Research Centre)
Nehru Nagar, Belgaum - 590 010

Institutional Animal Ethics Committee
Reg. No. 1388/GO/Re/S/10/CPCSEA
Resolution No. IAEC/ICMR-NTM BGM/2018/2

Date: 21-07-2018

CERTIFICATE

This is to certify that the project proposed by Dr. Subarna Roy entitled Evaluating the anti-cholera toxin activity of herbal compounds. Validating the traditional use" has been approved by the IAEC. The approval granted for:

Species	Gender	Number
Wistar Rats	Female	36
Swiss albino mice	Either	96

The Investigator must report the outcome of the experiment to IAEC/CPCSEA. The approved number/ species/ gender of animals should not be changed without prior permission of CPCSEA/IAEC.

Dr. AHM Viswanath Swamy
CPCSEA Main Nominee

Dr.Banappa S Unger
Member Secretary

Dr.Subarna Roy
Chairperson

Received 5/12/18

ANNEXURE - C

- **List of Publications**

1. **Charla R**, Patil PP, Bhatkande AA, Khode NR, Balaganur V, Hegde HV, Harish DR, Roy S. In Vitro and In Vivo Inhibitory Activities of Selected Traditional Medicinal Plants against Toxin-Induced Cyto-and Entero-Toxicities in Cholera. Toxins. 2022 Sep 20;14(10):649.

Impact factor: 5.075

2. **Charla R**, Patil PP, Patil VS, Bhandare VV, Karoshi V, Balaganur V, Joshi RK, Harish DR, Roy S. Anti-Cholera toxin activity of selected polyphenols from *Careya arborea*, *Punica granatum,* and *Psidium guajava*. Frontiers in Cellular and Infection Microbiology. 2023 Apr 11;13:260.

Impact factor: 6.073

Note: The above mentioned impact factor of the journal are based on the Web of Science and Scopus data respectively during the year of thesis submission (2023).

toxins

MDPI

Article

In Vitro and In Vivo Inhibitory Activities of Selected Traditional Medicinal Plants against Toxin-Induced Cyto- and Entero- Toxicities in Cholera

Rajitha Charla [1,2], Priyanka P. Patil [1,2], Arati A. Bhatkande [1], Nisha R. Khode [1], Venkanna Balaganur [3], Harsha V. Hegde [1], Darasaguppe R. Harish [1,*] and Subarna Roy [1,*]

[1] Indian Council of Medical Research—National Institute of Traditional Medicine, Belagavi 590010, India
[2] KLE College of Pharmacy Belagavi, KLE Academy of Higher Education and Research (KAHER), Belagavi 590010, India
[3] Indian Council of Agricultural Research—Krishi Vigyan Kendra, University of Agricultural Sciences, Bagalkot 587101, India
* Correspondence: harish.dr@icmr.gov.in (D.R.H.); roys@icmr.gov.in (S.R.)

Abstract: *Careya arborea*, *Punica granatum*, *Psidium guajava*, *Holarrhena antidysenterica*, *Aegle marmelos*, and *Piper longum* are commonly used traditional medicines against diarrhoeal diseases in India. This study investigated the inhibitory activity of these plants against cytotoxicity and enterotoxicity induced by toxins secreted by *Vibrio cholerae*. Cholera toxin (CT) and non-membrane damaging cytotoxin (NMDCY) in cell free culture filtrate (CFCF) of *V. cholerae* were quantified using GM1 ELISA and cell-based assays, respectively. Hydro-alcoholic extracts of these plants and lyophilized juice of *P. granatum* were tested against CT-induced elevation of cAMP levels in CHO cell line, binding of CT to ganglioside GM1 receptor and NMDCY-induced cytotoxicity. Significant reduction of cAMP levels in CFCF treated CHO cell line was observed for all extracts except *P. longum*. *C. arborea*, *P. granatum*, *H. antidysenterica* and *A. marmelos* showed >50% binding inhibition of CT to GM1 receptor. *C. arborea*, *P. granatum*, and *P. guajava* effectively decreased cytotoxicity and morphological alterations caused by NMDCY in CHO cell line. Further, the efficacy of these three plants against CFCF-induced enterotoxicity was seen in adult mice ligated-ileal loop model as evidenced by decrease in volume of fluid accumulation, cAMP levels in ligated-ileal tissues, and histopathological changes in intestinal mucosa. Therefore, these plants can be further validated for their clinical use against cholera.

Keywords: cholera toxin; cytotoxicity; GM1 ELISA; morphological alterations; non-membrane damaging cytotoxin; cell free culture filtrate

Key Contribution: Cell free culture filtrate of clinical isolate of *V. cholerae* containing CT and NMDCY toxins was utilised in the present study and the inhibitory efficacy of six traditionally used anti-diarrhoeal plants against these toxins were investigated by in vitro and in vivo methods.

check for updates

Citation: Charla, R.; Patil, P.P.; Bhatkande, A.A.; Khode, N.R.; Balaganur, V.; Hegde, H.V.; Harish, D.R.; Roy, S. In Vitro and In Vivo Inhibitory Activities of Selected Traditional Medicinal Plants against Toxin-Induced Cyto- and Entero-Toxicities in Cholera. *Toxins* **2022**, *14*, 649. https://doi.org/10.3390/toxins14100649

Received: 4 August 2022
Accepted: 9 September 2022
Published: 20 September 2022

Publisher's Note: MDPI stays neutral with regard to jurisdictional claims in published maps and institutional affiliations.

1. Introduction

V. cholerae, the causative agent of cholera is a facultative anaerobic gram negative, motile, non-spore forming curved rod-shaped bacteria that contains both toxigenic and non-toxigenic strains that differ in their virulence gene contents and polysaccharide surface antigens [1]. The production of Cholera toxin (CT), an 84Kd oligomeric protein efficiently secreted into the culture supernatant by the bacteria's type 2 secretion system, is a defining feature of epidemic *V. cholerae* strains. CT is a traditional A-B toxin with a larger A subunit (CTA, catalytic domain) and five B subunits (CTB, binding domain). Its intoxication is caused by a series of events that begin with CTB binding to the GM1 receptor on intestinal epithelial cells and end with constitutive activation of adenylate cyclase, which continuously stimulates cAMP production [2]. This causes an electrolytic imbalance in

frontiers | Frontiers in Cellular and Infection Microbiology

TYPE Original Research
PUBLISHED 11 April 2023
DOI 10.3389/fcimb.2023.1106293

OPEN ACCESS

EDITED BY
Ibrahim Bitar,
Charles University, Czechia

REVIEWED BY
Jorge Alberto Giron,
University of Puebla, Mexico
Tooba Mahboob,
University of Malaya, Malaysia

*CORRESPONDENCE
Darasaguppe R. Harish
harish.dr@icmr.gov.in
Subarna Roy
roys@icmr.gov.in

SPECIALTY SECTION
This article was submitted to Antibiotic Resistance and New Antimicrobial drugs, a section of the journal Frontiers in Cellular and Infection Microbiology

RECEIVED 23 November 2022
ACCEPTED 28 February 2023
PUBLISHED 11 April 2023

CITATION
Charla R, Patil PP, Patil VS, Bhandare VV, Karoshi V, Balaganur V, Joshi RK, Harish DR and Roy S (2023) Anti-Cholera toxin activity of selected polyphenols from *Careya arborea*, *Punica granatum*, and *Psidium guajava*. *Front. Cell. Infect. Microbiol.* 13:1106293. doi: 10.3389/fcimb.2023.1106293

Anti-Cholera toxin activity of selected polyphenols from *Careya arborea*, *Punica granatum*, and *Psidium guajava*

Rajitha Charla[1,2], Priyanka P. Patil[1,2], Vishal S. Patil[1,2], Vishwambhar V. Bhandare[1,3], Veeresh Karoshi[1], Venkanna Balaganur[4,5], Rajesh K. Joshi[1], Darasaguppe R. Harish[1]* and Subarna Roy[1]*

[1]Indian Council of Medical Research - National Institute of Traditional Medicine, Belagavi, Karnataka, India, [2]KLE Academy of Higher Education and Research (KAHER), Belagavi, India, [3]Department of Microbiology, Shivaji University, Kolhapur, India, [4]Indian Council of Agricultural Research – Krishi Vigyan Kendra, Bagalkot, Karnataka, India, [5]University of Agricultural Sciences, Dharwad, Karnataka, India

Introduction: *Careya arborea*, *Punica granatum*, and *Psidium guajava* are traditionally used to treat diarrheal diseases in India and were reported to show anti-Cholera toxin activity from our earlier studies. As polyphenols are reported to neutralize Cholera toxin (CT), the present study investigated the inhibitory activity of selected polyphenols from these plants against CTB binding to GM1 receptor using *in silico*, *in vitro*, and *in vivo* approaches.

Methods: Molecular modelling approach was used to investigate the intermolecular interactions of selected 20 polyphenolic compounds from three plants with CT using DOCK6. Based on intermolecular interactions, two phenolic acids, Ellagic acid (EA) and Chlorogenic acid (CHL); two flavonoids, Rutin (RTN) and Phloridzin (PHD) were selected along with their respective standards, Gallic acid (GA) and Quercetrin (QRTN). The stability of docked complexes was corroborated using molecular dynamics simulation. Furthermore, in vitro inhibitory activity of six compounds against CT was assessed using GM1 ELISA and cAMP assay. EA and CHL that showed prominent activity against CT in *in vitro* assays were investigated for their neutralizing activity against CT-induced fluid accumulation and histopathological changes in adult mouse.

Results and discussion: The molecular modelling study revealed significant structural stability of the CT-EA, CT-CHL, and CT-PHD complexes compared to their respective controls. All the selected six compounds significantly reduced CT-induced cAMP levels, whereas EA, CHL, and PHD exhibited > 50% binding inhibition of CT to GM1. The EA and CHL that showed prominent neutralization activity against CT from *in vitro* studies, also significantly decreased CT-induced fluid accumulation and histopathological changes in adult mouse. Our study identified bioactive compounds from these three plants against CT-induced diarrhea.

KEYWORDS

cell free culture filtrate, Cholera toxin, cytotoxicity, docking, GM1 ELISA, molecular dynamics simulations

ANNEXURE - D

- **List of Presentations**

1. Poster on " *In silico* and *in vitro* studies of selected polyphenols from *C. arborea*, *P. guajava* and *P. granatum* against Cholera toxin at International Conference On Current Technologies And Opportunities In Bio-Sciences; Mar 2023 (Secured first prize for this poster presentation)
2. Poster on "Investigating the inhibitory efficacy of selected traditional medicinal plants against Cholera toxin and Non-membrane damaging cytotoxin of *V. cholerae*" at International Conference On Drug Discovery; Nov 2022.
3. Poster on "Pre-Clinical Studies on hydro-alcoholic extracts of *C. arborea*, *P. guajava* and *P. granatum* against Cholera toxin" at National Conference On Advances In Analytical Techniques For Materials And Bio-medical Application; Dec 2022.

(***Certificates are attached***)

DSIR
DEPARTMENT OF SCIENTIFIC AND INDUSTRIAL RESEARCH

UNIVERSITY OF AGRICULTURAL SCIENCES, BANGALORE

COLLEGE OF AGRICULTURE, HASSAN & COMBETT INSTITUTE, BANGALORE

INTERNATIONAL CONFERENCE ON CURRENT TECHNOLOGIES AND OPPORTUNITIES IN BIO-SCIENCE

CERTIFICATE

This is to certify that RAJITHA CHARLA, PRUTHVIRAJ CHAVAN

has secured **First** / ~~**Second**~~ / ~~**Third**~~ **Prize in** ~~**Oral**~~ / **Poster Presentation** in the International Conference on **"Current Technologies and Opportunities in Bio-Science"** jointly organized by College of Agriculture, Hassan, UAS (B) and COMBETT Institute, Bangalore at College of Agriculture, Hassan, Karnataka from 27th to 29th March, 2023.

V.R.S

Co-Chairman

Chairman
Organizing Committee

International Conference on Drug Discovery

Nov. 10th & 11th 2022, BITS Pilani, K K Birla Goa Campus

Certificate

ICDD 2022

This is to certify that

Rajitha Chala

has successfully participated in International Conference on Drug Discovery held at BITS-Pilani K K Birla Goa Campus on 10th & 11th Nov. 2022 and presented a poster.

R. Raghu
Vice President

Suman Kundu

Prof. Suman Kundu
Director, BITS Pilani,
K.K. Birla Goa Campus

Schrödinger | BITS Pilani
K K Birla Goa Campus

NATIONAL CONFERENCE ON

ADVANCES IN ANALYTICAL TECHNIQUES FOR MATERIALS AND BIO-MEDICAL APPLICATION

(AATMABIMAN - 2022)

Organized by

In Association with

Dept. of CHEMISTRY
RANI CHANNAMMA UNIVERSITY

Dept. of APPLIED SCIENCES
VISHVESVARAYA TECHNOLOGICAL UNIVERSITY

Indian Society of Analytical Scientists (ISAS)
Belagavi Chapter

CERTIFICATE

This is to certify that Prof./Dr./Mr./Ms. Rajitha Charla

~~participated~~ / presented a paper (~~Oral~~/Poster) titled Pre-clinical studies on Hydro-alcoholic extracts of C. arborea, P. granatum & P. guajava against Cholera toxin. at the National Conference on

ADVANCES IN ANALYTICAL TECHNIQUES FOR MATERIALS AND BIO-MEDICAL APPLICATION (AATMABIMAN - 2022)

held during 15-16 December 2022 at Rani Channamma University, Belagavi-591156, Karnataka, INDIA.

Prof. J. Manjanna
Organizing Chair

Dr. PP Chandrachoodan
President, ISAS

Dr. Prasanna D. Shivaramu
Organising Secretary